Synthesis and development of Activated Carbon supported Iron (Fe) catalyst for Fischer Tropsch Synthesis

By

Saleem Munir

Reg. No. 00000119840

Session 2015-17

Supervised by

Dr. Naseem Iqbal

U.S. - Pakistan Center for Advance Studies in Energy

National University of Sciences and Technology

H-12, Islamabad 44000, Pakistan

July 2018

Synthesis and development of Activated Carbon supported Iron (Fe) catalyst for Fischer Tropsch Synthesis

By
Saleem Munir
Reg. No. 00000119840
Session 2015-17

Supervised by
Dr. Naseem Iqbal

A Thesis Submitted to the
U.S. - Pakistan Center for Advance Studies in Energy in partial fulfillment of the requirements for the degree of
MASTERS of SCIENCE in
ENERGY SYSTEMS ENGINEERING

U.S. - Pakistan Center for Advance Studies in Energy
(USPCASE) National University of Sciences and Technology (NUST)
H-12, Islamabad 44000, Pakistan

July 2018

THESIS ACCEPTANCE CERTIFICATE

Certified that final copy of MS/MPhil thesis written by Mr. Saleem Munir ,(Registration No. 00000119840), of USPCAS-E has been vetted by undersigned, found complete in all respects as per NUST Statues/Regulations, is free of plagiarism, errors, and mistakes and is accepted as partial fulfillment for award of MS/MPhil degree. It is further certified that necessary amendments as pointed out by GEC members of the scholar have also been incorporated in the said thesis.

Signature: _____

Name of Supervisor Dr. Naseem Iqbal

Date: _____

Signature (HoD): _____

Date: _____

Signature (Dean/Principal): _____

Date: _____

Certificate

This is to certify that work in this thesis has been carried out by **Mr. Saleem Munir** and completed under my supervision in Fossil Fuel Lab, U.S. - Pakistan Centre for Advance Studies in Energy (USPCAS-E), National University of Sciences and Technology (NUST), H-12, Islamabad, Pakistan.

Supervisor: _____

Dr. Naseem Iqbal
USPCAS-E
NUST, Islamabad

GEC member # 1: _____

Dr. M. Bilal Khan
USPCAS-E
NUST, Islamabad

GEC member # 2: _____

Dr. Rabia Liaquat
USPCAS-E
NUST, Islamabad

GEC member # 3: _____

Dr. M. Bilal Sajid
USPCAS-E
NUST, Islamabad

HoD - ESE _____

Dr. Naseem Iqbal
USPCAS-E
NUST, Islamabad

Principal/ Dean _____

Dr. Zuhair S. Khan
USPCAS-E
NUST, Islamabad

Dedication

I dedicate this work to my parents, family, teachers and especially my brother Mr. Jamil Ahmad for their love, motivation and inspiration.

Abstract

Energy consumption is increasing day by day placing a lot of load on fossil fuels which in turns cause various threats to environment. Among other forms of energy, liquid fuels are most commonly and intensively used in daily life. To match the demand of liquid fuels scientists are working to find new sources to generate relatively clean liquid fuels that poses minimum environmental threat. Fischer Tropsch Synthesis is one of such efforts that generate synthetic hydrocarbons from various sources like coal, biomass, natural gas and environmental carbon dioxide. The Fischer Tropsch Synthesis uses syngas (mixture of carbon monoxide and hydrogen) to generate liquid hydrocarbons at high temperatures of 200 to 350 ^{o}C in the presence of a catalyst at high pressures (up to 20 bars). This study focuses on developing a carbon based iron catalyst for Fischer Tropsch Synthesis (FTS) process and to check the effect of promoters on the activity of the prepared catalyst. Potassium promoter is used in this study. Carbon supported iron catalyst is prepared by co-precipitation method and the promoter is added by wetness impregnation method. The qualitative and quantitative analyses of all the prepared samples are done using various characterization techniques. XRD and SEM were performed to gather information about the structure and morphology of the catalyst. EDS was used for elemental analysis of the samples. BET and TGA are two techniques that give information about the properties of catalyst like surface area and thermal stability. The samples were tested for FTS process in a micro reactor especially to check the C_{5+} selectivity. The product obtained from FTS reactor was analyzed by using GC-MS. The results showed very high C5+ selectivity for promoted catalyst as compared to unprompted catalyst.

Key Words: Fischer Tropsch Synthesis; Activated Carbon; Iron Catalyst; Potassium Promoter.

Table of Contents

List of Figures

List of Tables

List of Abbreviations

GHG	Green House Gasses
CTL	Coal to Liquid
DCL	Direct Coal Liquefaction
ICL	Indirect Coal Liquefaction
DMF	Dimethylformamide
BLT	Biomass to Liquid Technology
GTL	Gas to Liquid Technologies
FTS	Fischer Tropsch Synthesis
BPD	Barrels per Day
FBR	Fixed Fluidized Bed Reactor
MOF	Metal Organic Framework
SEM	Scanning Electron Microscopy
XRD	X-Ray Diffraction
TGA	Thermo Gravimetric Analysis
GCMS	Gas Chromatography and mass spectroscopy
HTFT	High Temperature Fischer Tropsch
LTFT	Low Temperature Fischer Tropsch
PBSi	Phosphorus, Boron and Silicon

List of Publications

I. **Saleem Munir**, Muhammad Amin, Naseem Iqbal, Jamil Ahmad, "*Synthesis and Characterization of Activated Carbon from Pongamia Pinnata tree by H_3PO_4 chemical activation"*, 2nd International Conference on Impact of Nano Science on Energy technologies (NanoSET-2017), 25-27 October 2017 in Comsat Lahore, Pakistan. (Presented)

II. Muhammad Amin, **Saleem Munir**, Naseem Iqbal, *"Development of MOF derived iron catalyst for a Fischer Tropsch synthesis"*, International Conference on Recent Innovations in Science, Engineering, Technology and Management (ASAR-ICRISETM-2017), 15 July 2017 in Bengaluru, India. (Presented)

III. Muhammad Amin, **Saleem Munir**, Naseem Iqbal, *"Synthesis and characterization of Activated Carbon from olive tree by H_3PO_4 chemical activation"*, International Conference on Phosphorous, Boron and Silicon (PBSi-2017), 03-05 July 2017 in Paris France. (Presented)

*** Annex I**

*** Annex II**

*** Annex III**

Chapter 1

1.1 Introduction

Energy growth is directly linked to well-being and abundance across the globe. One of the important challenge that mankind will have to face in future is lessening of fossil fuel .Among fossil fuels oil hold the utmost importance due to its extensive use in motor vehicles and energy generation. The utilizing of oil at 20^{th} century is at peak level and natural resources of oil are going to depleted [1]. The combustion of fossil fuels is producing worldwide environmental issues like global warming, climate change and harmful emission of gases (NOx, SOx and Particulate matters). Moreover biomass, coal and natural gas are best option to meet the requirement of oil share in energy and transportation sector. Coal and biomass resources can be utilized without effecting environmental issues like burning coal and biomass in control method to produce hydrogen and carbon monoxide (syngas). One of the main objectives is to make inexpensive and highly selective catalyst for Fischer Tropsch Synthesis.

Following are the main objectives covered in this thesis;

- Synthesis of catalyst using different synthesis techniques and using different precipitating agents
- Comparison of catalysts prepared using different techniques and different precipitating agents
- Application of synthesized catalyst in Fischer Tropsch Synthesis
- Different catalysts tested with different temperature condition in Fischer Tropsch Synthesis

A process of gas to liquid fuel production with no emission to environment is Fischer Tropsch Synthesis. In FTS by using well known and reputable catalytic chemical process to produce liquid hydrocarbon fuels from syngas [2]. A German scientist who invented the Fischer-Tropsch process where synthesis of hydrocarbons from syngas is performed (a mixture of H_2 and CO). The Fischer Tropsch Synthesis uses hydrogen and carbon monoxide to generate a mixture of hydrocarbon at high temperature and high pressure with a suitable catalyst. The Fischer Tropsch synthesis process gives clean production of hydrocarbons from syngas. Moreover the product obtained fron Ficher Tropsch is free from sulfur. There are four active material used for

Fischer Tropsch Synthesis like nickel, ruthenium, cobalt and iron. Iron and cobalt are mostly used for gasoline and diesel like products respectively. At that time different process industries such like SASOL and Shell are working on this field and they are producing a large variety of hydrocarbons in a large scale from syngas.

The Fischer-Tropsch synthesis reaction is

$$CO+ (1+n/2) H2 \rightarrow CH_n + H_2O$$

Here 'n' is present the average ratio (H/CO) of hydrocarbons which are being produced. Different kind of promoters and binders are commonly used in iron catalyst for increasing the selectivity of hydrocarbons. Iron catalysts are classified into a supported and bulk catalyst both one is prepared by wet impregnation method. In a supported iron catalyst requires an addition of metal support in order to prevent the particle accumulation. They have also ability to exhibit a higher mechanical strength as compared to bulk iron catalyst [3].

1.2 Background of Fischer Tropsch Synthesis

Fischer-Tropsch synthesis is the significant GTL technology (gas-to-liquids) which converts syngas, obtained from natural gas, coal and biomass, to liquid hydrocarbon fuels and other petrochemicals in the presence of a catalyst under certain conditions. More than seventy years old method to produce synthetic fuel from fischer tropsch reaction. Franz Fischer was well aware of industrial organic chemistry when the gases of CO and H_2 enter into the reactor with the presence of heterogeneous catalyst and that vision takes might importance when the reserves of oil and gas are being consumed in very short time and the demand of hydrocarbons are increased [4]. In1902, when Sabatier and Sendersen report the formation of methane from carbon monoxide and hydrogen by using a Ni and Co based catalysts. After few years in 1908, Orlov finds the ethene with the use of Ni-pd catalysts. In 1913 the B. Anilin und S. Fabrik (BASF) of Ludwigshafen, Germany, discovered that combination of oxygenated compounds and higher hydrocarbons could be manufactured catalytically from syngas under high temperatures and high pressures [5]. In 1924 Fischer and Tropsch report that liquid product of hydrocarbons over a Fe catalyst. In 1936 commercialization of FT process are started and produced 200,000 t/year capacities. Fischer Tropsch Synthesis was first introduced by Germany around WWII. In 1955, Sasol I starts the production with the combine effect of fixed and fluid bed reactors.

1.3 Industrialization of Fischer Tropsch Process

The first plant of FT synthesis was operated by Ruhrchemie AG in Oberhausen, Germany, in 1936 after acquiring patent rights to the FT process in 1934. This small-scale plant had 52 reactors operated at atmospheric pressure, and it had a production capacity of 70,000 tonnes per annum [6]. In South Africa the Sasol plant used a synfuel technology for the production of liquids products. . Sasol has improved its Arge reactor in order to increase the higher molecular weight hydrocarbons and also operates slurry phase distillate process. Slurry phase distillate process produce more olefinic and straight chain paraffin's than the other types of reactors. Sasol Slurry Phase Distillate plants are converting 100 MMscfd of natural gas into 10,000 barrels per day of liquid hydrocarbons with capital cost of US$250 million. In recent era Sasol has increased the production unit of alumina spheres plant in Brunsbüttel to 4,000 tonnes per annum [7].

In Norway the Statoil plant that are working on development of catalyst and designing the reactor to produce liquid fuel products from natural gas. The catalyst performance and synthesis is main challenge which that are going to face in the process [8]. Shell has made a plant in Bintulu a city of Malaysia for a capacity of 12 000 bbl/day in 1993 and they are producing a highly paraffinic which are free of nitrogen and sulfur. Within the duration of 10 years Shell has investing more than US$6 billion in a four plants for the production of liquid products [9].

Exxon has used natural gas as feedstock for the development of a commercial Fischer Tropsch process. A joint endeavor of Sasol and Qatar Petroleum named as Oryx GTL completed another gas-to-liquid plant association with Chevron in 2005. The plant has deliberately made in vicinity of large natural gas assets in the north of Qatar at the Ras Laffan industrial city complex. Sasol's slurry columns reactor was used in those plants and have a daily making capability of 34,000 barrels per day. The Syntroleum Corporation is a Fischer Tropsch plant located in USA which is being producing a diesel with the using of natural gas as a feedstock. The production capacity of synthetic crude is $20 per bbl [10]. Methanex plant located in a New Zealand, they are working on two different types of technology (i) methanol to gasoline and (ii) Mobil's methanol-to-gasoline. These processes are operated on the fluid bed reactor with a catalyst of ZSM-5 zeolite. This plant has producing up to 2.4 million tonnes methanol per annum.

Table 1: Currently operational Fischer Tropsch plants in Worldwide

Year	Plant/ Company	Production Level (bpd)	Country	City
1944	SHL	14,000	Germany	Ruhland
1955	Sasol-I	5600-8000	South Africa	Sasolburg
1980	Sasol II	$124 *10^3$	South Africa	Secunda
1983	Sasol III	$154*10^3$	South Africa	Secunda
1991	PetroSA	$22.5*10^3$	South Africa	Mossel Bay
1993	Bintulu GTL	14,700	Malaysia	Bintulu
1952	JSC Novocherkassk	50,000 t/y	Russia	Rostov
1985	ExxonMobil	14,500	New Zealand	New Plymouth
2002	Mossgas	1000	South Africa	Mossel-Bay
2004	SLH	400	USA	Ponca City
2006-2012	Qatar Petroleum/Sasol	$34*10^3$	Qatar	Oryx
2006	Qatar Petroleum/Shell	$140*10^3$	Qatar	Ras Laffan
2011	Exxan Mobile and Qatar Petroleum	154,000	Qatar	North East Doha

1.4 Fischer Tropsch Chemistry

1.4.1 Reactions

FTS has the polymerization reaction which produces numerous oligomers regularly circulated with carbon number range. In FTS the chemical reaction can be classified into main reaction, side reaction and reaction responsible for catalyst modification and shown in following

1.4.2 Main Reactions

Formation of Paraffin

$$(2n + 1)H_2 + nCO \rightarrow nH_2O + C_nH_{2n} + 2 \quad (1.1)$$

Formation of Olefin

$$2nH_2 + nCO \rightarrow nH_2O + C_nH_{2n} \quad (1.2)$$

Water-gas shift (WGS) reaction

$$H_2O + CO \leftrightarrow H_2 + CO_2 \quad (1.3)$$

1.4.3 Side Reactions

Alcohol production

$$2nH_2 + nCO \rightarrow (n - 1)H_2O + C_nH_{2n} + OH \quad (1.4)$$

Boudouard reaction

$$2CO \rightarrow C + CO_2 \quad (1.5)$$

1.4.4 Catalyst Modifications

Catalyst oxidation/ reduction

$$\text{a. } yCO + MxOy \leftrightarrow xM + yCO_2 \quad (1.6)$$

$$\text{b. } yH_2 + MxOy \leftrightarrow xM + yH_2O \quad (1.7)$$

Bulk carbide formation

$$xM + yC \leftrightarrow MxCy \quad (1.8)$$

Here ‘n’ represent the carbon number which depends on a number of factors, primarily the Hydrogen (H_2) to Carbon monoxide (CO) ratio of syngas and the nature of catalyst employed. The formation of Parrafins (eqn. 1.1) and formation of Olefins (eqn. 1.2) pre dominates the amalgamation. High Hydrogen (H_2) to Carbon monoxide (CO) ratio and catalysts having solid hydrogenating capabilities usually supports paraffins formation. Olefin formation is favored while using syngas having low Hydrogen to Carbon monoxide ratios and a catalyst with

weak hydrogenating capabilities. Water is also a crucial product from FTS apart from hydrocarbons. The existence of water is unwanted in Fischer-Tropsh synthesis since it affects conversion of syngas and chain selectivity. The properties of FTS fuel depend on the following process like synthetic gas adsorption on the catalyst, chain initiation, chain growth, methanation, hydrogenation to paraffin and dehydrogenation to olefins these are all the step to step process. The water-gas-shift reaction (eqn. 1.3) utilizes carbon monoxide and water, formed in the FTS reaction, and translates the reactants to carbon dioxide and hydrogen. Potassium-promoted iron catalysts promote the WGS reaction. Catalyst activation in FTS is complete by the reducing of catalysts with hydrogen (eqn. 1.6), carbon monoxide (eqn. 1.7) or synthetic gas. However, it has been reported [11] that the reducing atmosphere with hydrogen, carbon monoxide or synthetic gas often have major effects on catalytic selectivity and activity for Fe-based catalysts. For Iron catalyst, hydrogen reduced samples that show fewer activities for Fischer-Tropsch process than carbon monoxide and synthetic gas reduced samples. It is reported that reduction of Iron samples with hydrogen (H_2) follow to a metallic state (α-Fe), and Carbon monoxide or synthetic gas reduction follow to the metallic state and lesser amount of Iron carbides. It has been suggested that an active phase for Fischer-Tropsch reaction in iron catalysts having mixture of χ- and γ-iron carbides.

1.5 Fischer Tropsch synthesis Mechanism

Fischer Tropsch synthesis is continuously a topic of discussion since the first FTS mechanism was suggested by Fischer and Tropsch in the original paper [12]. The FTS mechanism can be classified into six step which are the following, reactant adsorption, chain initiation, chain growth, chain termination, product desorption and re-adsorption. Reaction path in Fischer Tropsch synthesis are clarify with the help of surface carbide mechanism, enol mechanism, CO addition mechanism and alkenyl mechanism.

1.5.1 Surface carbide mechanism

This mechanism was developed by Craxford and Rideal, in which the carbon monoxide is adsorbed on the surface and dissociates to forming water in the presence of hydrogen. The carbon is hydrogenated to form chemisorbed CH_2 which are ologimerizes to produce large carbon number hydrocarbons.

$$Co + CO \rightarrow Co–CO \quad (1.9)$$

$$Co–CO + H_2 \rightarrow Co–C + H_2O \quad (1.10)$$

$$Co–C + H_2 \rightarrow Co–CH_2 \rightarrow \rightarrow \text{higher hydrocarbons} \quad (1.11)$$

1.5.2 Surface Enol Mechanism

Surface Enol Mechanism consists of chain growth with the un-dissociative chemisorption of Carbon monoxide (CO) which reacts with adsorbed (H_2) to generate enolic (HCOH) components. The structure of product has increased by a combination of surface polymerization, condensation and elimination of water (H_2O).

1.5.3 CO Insertion Mechanism

CO-Insertion mechanism can be classified into few steps (i) adsorption of reactant and reactant consist of CO and H_2. (ii) Chain initiation (iii) chain propagation and finally chain termination step. In the below figure CO-Insertion mechanism is listed.

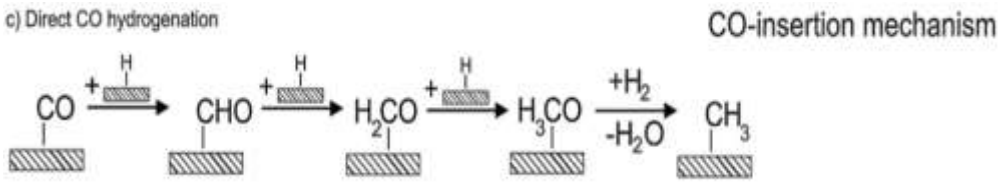

Figure 1: CO-Insertion mechanism

1.5.4 Alkenyl Mechanism

The alkenyl mechanism proposed by Maitlis and co-workers. This mechanism suggests polymer chain carriers are on the surface of alkenyl rather than alkyl. The CH_2 surface type is measured as the chain promulgation monomer. The surface vinyl species ($–CH=CH_2$), which is a chain starter, is generated by the reaction of a surface methyne ($\equiv CH$) and methylene ($=CH_2$) species. The chain growth occurs by coupling of sp2 (alkenyl) carbon with sp3 (methylene) carbon to form an allyl ($–CH_2CH=CH_2$). It has been shown in the literature that the pairing of sp2 with sp3 carbons in metal is a lesser energy process than Csp3 + Csp3 pairing reaction. The surface allyl species then isomerizes to the more reactive propenyl species ($–CH=CHCH_3$). Termination occurs by the reaction of surface (H_2) and the surface alkenyl giving predominantly α-olefins. This mechanism was tested by adding ethene-13C2 probes during FTS. Advantages of this mechanism include explaining; the formation of branched products (by allyl isomerization),

the little amount of C_2 products, and discharge of 1-alkenes as primary products (with a favorable hydrogenation reaction) [13]. However this mechanism is inadequate when explaining the formation of n-paraffin and the formation of oxygenates. Maitlis et al. proposed the main mechanism of allyl–vinyl isomerization, yet no experimental evidence for such a facile isomerization has been given.

1.6 Summary

The energy consumption of the planet earth is rising day by day. Fossil Fuels are very important to fulfill our present energy need. However, oil resources are going to depleted and rising environmental issues like greenhouse gases and climate change. Researchers have concern to produce clean and alternate source of green energy. There are several cleaner energy production techniques that are being used to produce synthetic liquid fuel like CLT, BLT, GLT and RCTL. The Fischer- Tropsch synthesis process provides the clean production of hydrocarbons from the mixture of hydrogen and carbon. It is a process which is used to generate liquid hydrocarbons from various sources like coal, biomass and natural gas. Iron based catalyst is largely used due to his water gas shift activity and low cost and received an immense attention of researchers. Moreover a number of promoters and binders can be used in iron base catalyst to increase the selectivity of hydrocarbons. There are several Fischer Tropsch synthesis plants which are currently producing liquid hydrocarbons all over the world to meet the human needs with a different proposed mechanism.

1.7 References

[1] H. Xiong, Y. Zhang, S. Wang, J. Li, Catalysis Communications, 2005, 6, 512.

[2] M Bing An, Kang Cheng, Cheng Wang, Ye Wang, and Wenbin Lin, Pyrolysis of metal organic frameworks to Fe3O4-Fe5C2 core shell nanoparticles for Fischer-Tropsch Synthesis, American Chemical Society, 1-35,2016

[3] Hans Schulz, Short history and present trends of Fischer-Tropsch synthesis, *Applied Catalysis*, 186, 3–12, 1999.

[4] F. Morales, B. M. Weckhuysen, Catalysis, 2006, 19, 1.

[5] X. Hao, G. Dong, Y. Xu, Y. Li, *Chemical* Engineering & Technology, 2007, 30, 1157-1165.

[6] Gas to Liquids, Historical Development and Future Prospects, Olga Glebova, Nov 2013, The Oxford institute for Energy studies.

[7] Uner, D. O. Ind. Eng. Chem. Res. 1998, 37, 2239.

[8] W. Ning, N. Koizumi, H. Chang, T. Mochizuki, T. Itoh, M. Yamada, Applied Catalysis *A*: General, 2006, 312, 35.

[9] Dalai, A. K.; Davis, B. H. *Appl.* Catal. A: Gen. 2008, 348, 1.

[10] Shroff, M. D.; Kalakkad, D. S.; Sault, A. G.; Datye, A. K. J. Catal. 1995, 156.

[11] Fischer, F.; Tropsch, H. Brennst. Chem. 1926, 7, 97.

[12] Calhorda, M. J.; Brown, M. J.; Cooley, N. A. Organometallics 1991, 10, 1431.

[13] Long, H. C.; Turner, M. L; Fornasiero, P.; M.P. J. Catal. 1997, 167, 172.

Chapter 2: Literature Review

2.1 Fischer-Tropsch Reactors

There are two FT operating regimes, FTS can be a high temperature Fischer Tropsch (HTFT) and low temperature Fischer Tropsch (LTFT) process and process which depend of required product [1, 2]. HTFT uses Iron based catalyst at high temperature ranging from 300 ^{o}C to 350 ^{o}C for the production of gasoline. LTFT operates on both cobalt and iron based catalysts at temperature ranging from 200 ^{o}C to 250 ^{o}C for the production of waxy and diesel [3]. The main advantage of HTFT process is that there is less liquid phase while in LTFT liquid phase is present.

2.2 Types of FT Reactors

FTS operation and reactor types are leading factors which control product distribution [4]. Low temperature FT reactors are classified into tubular fixed bed, micro channel and slurry bubble column reactors. Micro channel reactors show a superior productivity per reactor volume other than reactors. And their different characteristics and conversion per path are shown in a table below.

Table 2: Properties for different reactor for Low-Temperature Fischer Tropsch synthesis

Reactor	Conversion per path (%)	Capacity per reactor (bbl/day)	Characteristics
Tubular fixed-bed	30-35	≤6000	≤30,000 tubes with catalyst pellet or extradites
Slurry bubble column	55-65	≤25,000	Internal heat exchanger and optional product filter
Micro-Channel	65-75	≤1000	Metal block with < 2nm diameter channels

2.2.2 Fixed Bed Reactor

The fixed-bed reactor is the most competitive reactor technology and it holds an exceptional spot in FTS commercial practices, as demonstrated by the wide-ranging industrial

practices of Sasol and Shell [5]. Today the design of fixed bed reactors are based on a multi tubes heat exchangers due to control of heat effectively. That contains shells (evaporating water) and tubes (catalyst in the form of pellets is loaded into tubes). Main spot in a fixed bed reactor is that to avoid generating a hot spot because they cause sintering during the reaction. To remove the deactivation the following changing in tube diameter and size of catalyst is performed. Deactivation problem in a fixed bed reactor are solved be varying a partial pressure of reactant as well as a product and also size of catalyst within a tube length. Overall temperature in fixed bed reactor is slower than slurry bed reactor because the average composition of gases is richer than hydrogen. Within a reactor shell thousand ten of tubes are incorporated which can optimized the production and scale up the process and saving the timing. Loading and unloading of the tubes creates a problem in the catalyst process which are generally is fouling and these must be controlled during the reaction. The syngas entered above into the reactor and product are collected at the bottom of the reactor with a multiple tube are shown in below figure.

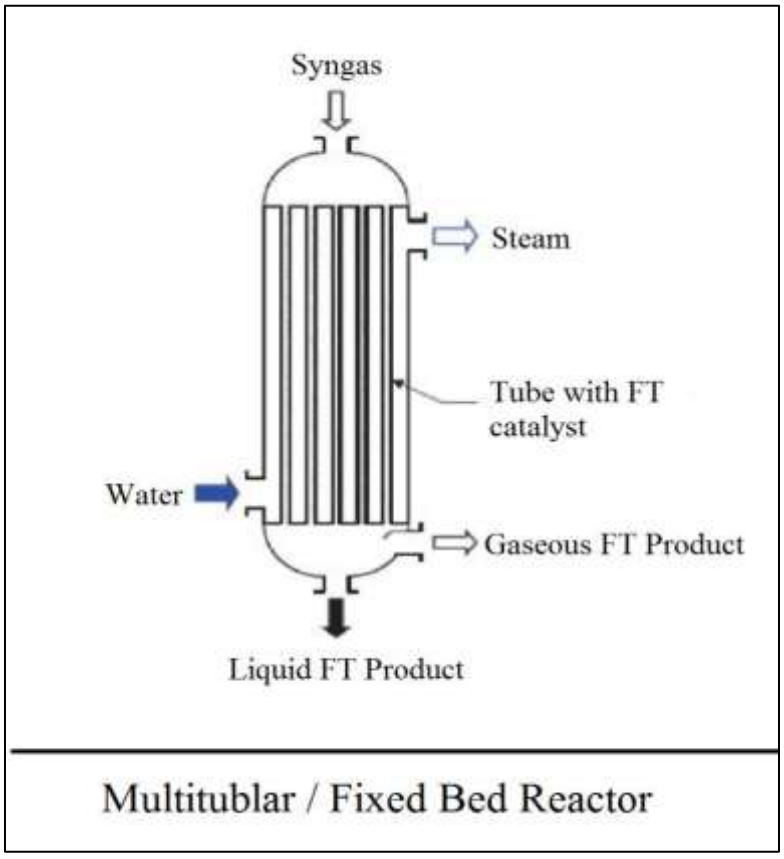

Figure 2: Schematic of Multitublar or Fixed Bed Reactor [5]

2.2.3 Fluidized Bed Reactor

In fluidized bed reactor the fuel particle is placed at bottom of the reactor and very quickly mixed with bed material and heat up the bed temperature. As a result, the fuel pyrolized very fast and mix with large amount of gases material. These types of reactor are operated at high temperature at the range of 350℃, 25 bar pressure and the quality of heat removal is high.

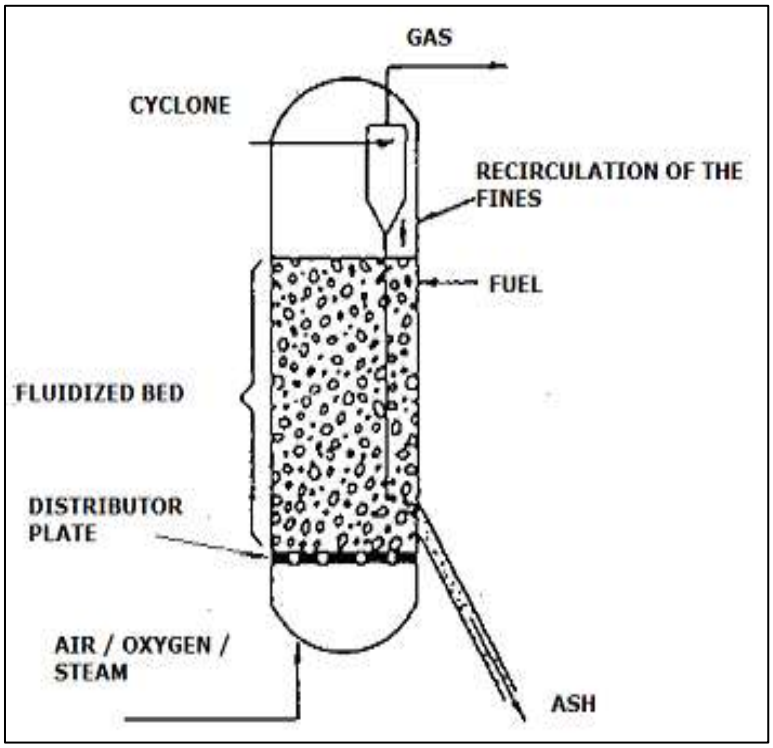

Figure 3: Schematic of Fluidized bed reactor [6]

2.2.4 Slurry Bubble Column Reactor

The idea of a slurry-bed reactor was firstly used from World War II till late 1970's by Kölbel and co-workers [7]. In this reactor the catalyst are suspended and reactant gases are bubbled through column. The concentration of the solid particles from bottom to top is diminishing which depends on the density of the catalyst particle, superficial gas velocity and their catalyst diameter. The liquid product is collected from center of the reactor and gases product from top of the reactor. The main factor which is controlled one is the overheating and other is settling of the catalyst both causes the deactivation. Slurry bubble column reactor have simple in construction, high heat transfer coefficient and high space time yield. To achieve high selectivity of hydrocarbons in slurry bubble column reactor there is a proper mixing of liquid and

gas that maintain the exit water concentration. The higher exit water concentration reduces the coke deposition during the process. Moreover to achieve a high CO conversion extensive amount of recycle syngas is required during the process.

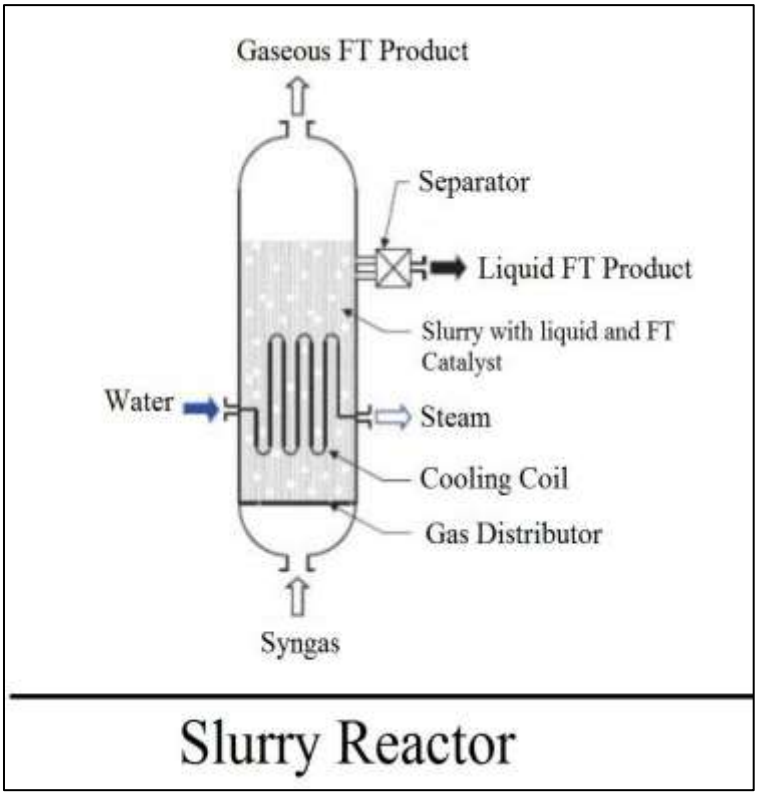

Figure 4: Schematics of Slurry Bubble Column Reactor [8]

2.2.5 Micro Channel Reactor

Micro channel reactor is well known due the heat and mass transfer rates. These types of reactor are loaded with highly active and stable catalysts. Selectivity's of hydrocarbons are highly achieved with a conversion rate of 90 %. Micro channel reactors are usually operated isothermally and pressure drop are relatively are generally low. Stability of catalyst to avoid the deactivation is done at high conversions.

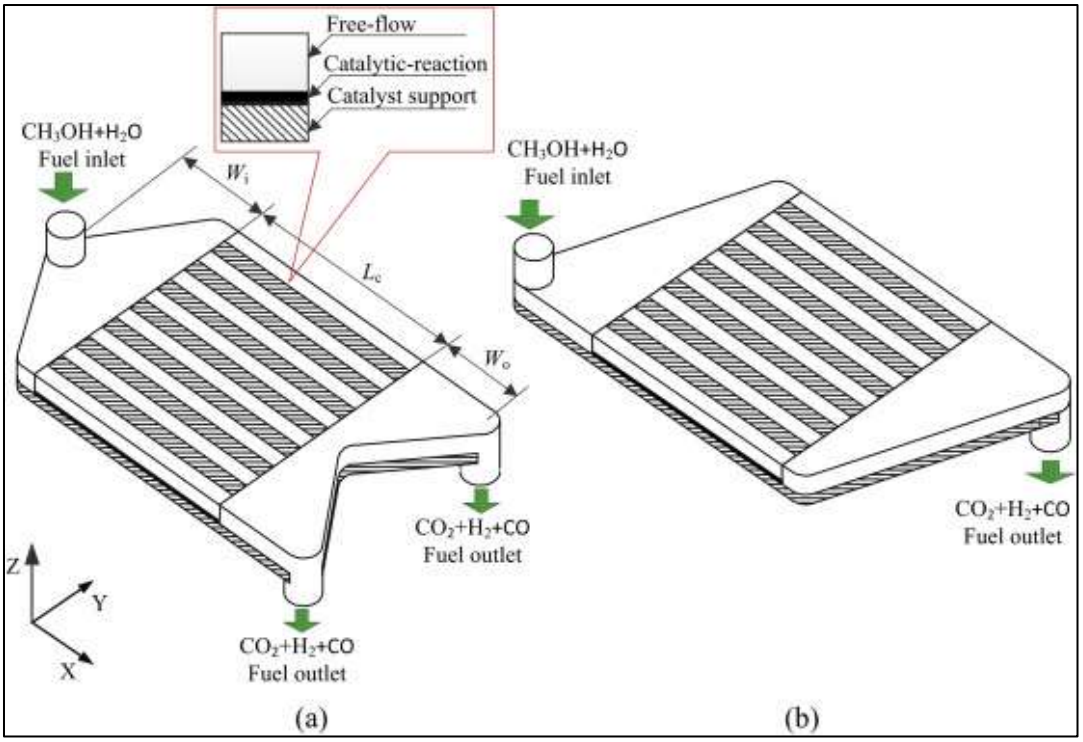

Figure 5: Schematic of Micro Channel Reactor [9]

2.3 Fischer Tropsch Synthesis Catalysts

2.3.1 Active Metals in FTS

The catalyst selection is very important in FTS because the end product depend on catalyst. There are three main properties of FT catalyst are catalyst activity, lifetime and selection of product [10, 11]. Four active materials are used as a catalyst like iron, cobalt, nickel and ruthenium. Mostly Iron and Cobalt are used as active material in FTS. Comparisons of the different characteristics for these metals are shown in Table . Nickel is not suitable for producing long chain hydrocarbons in FTS. Ruthenium is very costly and its international reserves are very scarce for large scale manufacturing, therefore Ni and Ru are not being used as FT catalyst. Iron and Cobalt based catalyst are used in FTS.

2.3.2 Iron

Iron is the catalyst of choice for many industries because it is inexpensive and gives good revenue with a wide product [12, 13]. Iron catalysts are commonly promoted with an alkali such as potassium and sodium to increase the olefinity of the hydrocarbons and encourage water gas shift reaction. When iron is used as the active metal it promotes the WGS reaction. This reaction

use CO and water made by the Fischer-Tropsch synthesis reaction to yield further H_2 as well as CO_2.

Iron stages that co-exist during and after activation include metallic and carbide and oxides. Surface carbidic iron is thought to be the active species in FTS [14]. Schulz et al [15] studied the behavior of a Fe-Al-Cu/K_2O catalyst and concluded that the FT activity was linked to the development of Hägg carbides (Fe_5C_2). The authors also reported that metallic iron is less active. Metallic iron is stated to be promptly transformed to these carbides (Fe_5C_2) upon mixing syngas if activation is performed using hydrogen [16]. High deactivation rates and the relatively short catalyst life-time are the major problems associated with iron based catalysts.

2.3.3 Cobalt

Cobalt catalysts are more costly than iron so they are only used industrially as supported catalysts. Cobalt-based (Co) catalysts have more hydrogenation activity, hereafter they incline to produce high molecular-weight paraffins and less oxygenates when matched with iron catalysts. Generally, cobalt catalysts are nearly three times more reactive than Iron catalysts in Fischer-Tropsch synthesis. Cobalt catalysts are nearly 250 times more costly than Iron Catalysts. The operating condition of catalyst are varying and normally in the range of (1-10 bar).

2.3.4 Ruthenium

Ruthenium has more active state and work at least reaction temperature. It yields the hydrocarbons of high molecular weight. High pressure and low temperature are suitable to produce high molecular mass waxes. Ru also used as a supported catalyst about 5 % and they produce light hydrocarbons.

2.3.5 Nickel

Nickel is not suitable for producing hydrogenation and long chain hydrocarbons in Fisher Tropsch synthesis. Nickel show a maximum level of activity when they adsorption of CO at moderate heat.

Table 3: Effect of Active Metal on the Nature of Product

Metal	Pressure (bars)	Temperature (^{o}C)	Nature of Product
Iron (Fe)	10-30	200-250	Alkanes, Alkenes, Oxygenates
Cobalt (Co)	5-30	170-250	Alkanes, Some Alkenes, Oxygenates
Ruthenium (Ru)	100-1000	150-250	Paraffin Waxes
Nickel (Ni)	10	170- 210	Alkanes, Some Alkenes

2.4 Flow Chart of Thesis

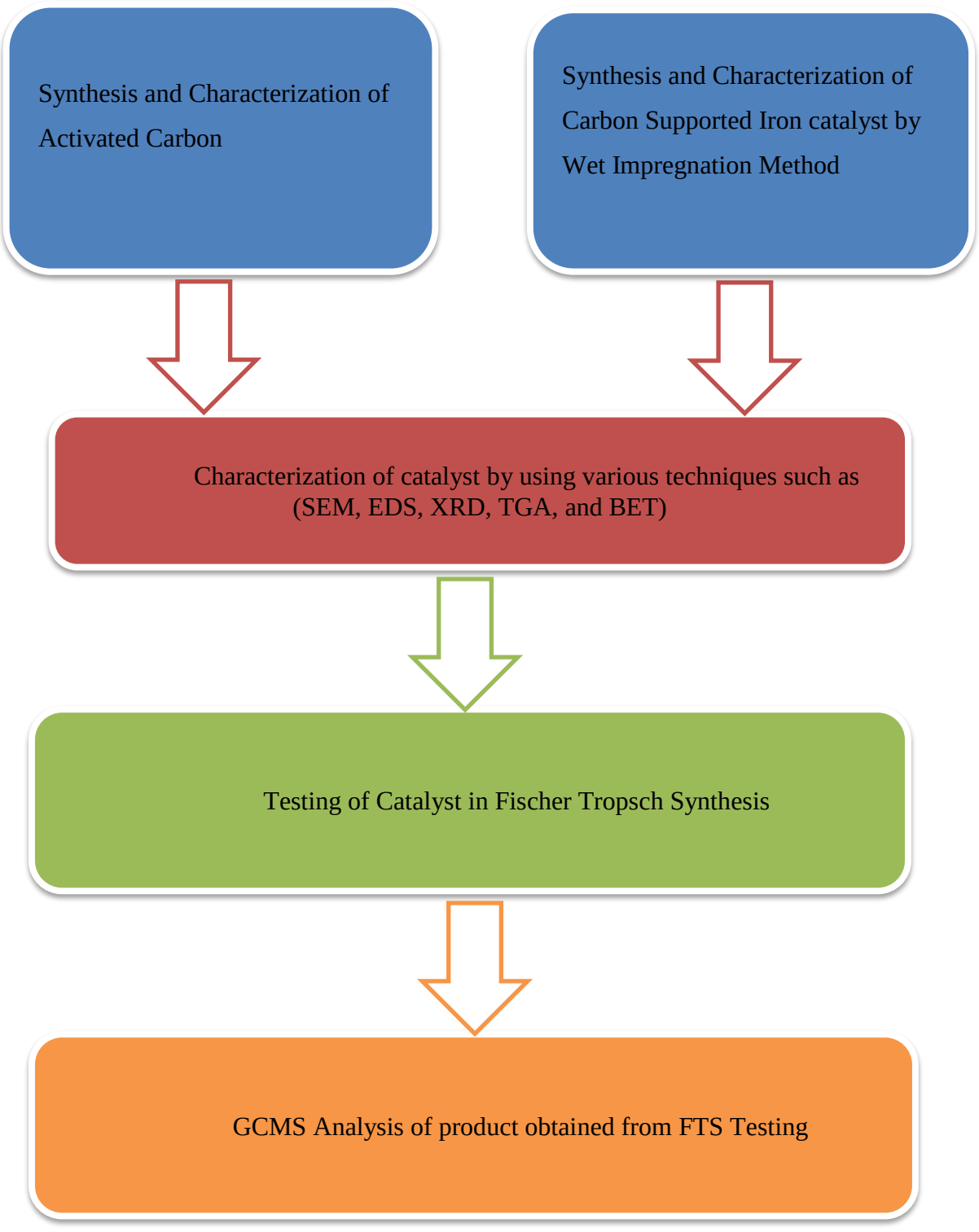

2.5 Summary

There are two main types of Fischer-Tropsch Synthesis (FTS) process; Low Temperature Fischer Tropsch Process and High Temperature Fischer Tropsch Process. The FTS process is carried out in a reactor that operates under certain conditions of temperature and pressure, in the presence of catalyst. There are four basic types of reactors that we use in FTS process: Fixed-bed reactor (FBR), Fluidized-bed reactor (FBR), Slurry Bubble Column Reactor (SBCR) and Micro Channel Reactor (MCR). The reaction conditions and nature of product required decides the catalyst that is used in FTS process. Among several other options the cobalt, iron, ruthenium, and nickel based catalyst are most commonly used in industry.

2.6 References

[1] Dry, Micheal. Entheny. Catalysis Today 2002, Vol: 71, 227-234.

[2] Esponoza, R. L.; Steynberg, A. P.; Jager, B.; Vosloo, A. C. Appl. Catal. A: Gen.1999, 186.

[3] Akhtar, A.; Pareek, V. K.; Tade, M. O. Chem. Prod. Process. Model. 2006, 1, 1.

[4] M. E. Dry, The Fischer-Tropsch synthesis, Springer-Verlag. New York, 1981.

[5] M. E. Dry, Applied Catalysis A: General, 1996, 138, 319.

[6] Kölbel, H.; Ralek, M. Catalyst Revolution Scientific Engineering. 1980, 221- 225.

[7] Fischer-Tropsch Technology edited by André Steynberg, Mark Dry p 69-74.

[8] D.Mei, L.Liang, M.Qian, Y.Feng A performance study of methanol steam reforming in an A-type microchannel reactor, 2014, 39, 17690-17701.

[9] Bukur, D. B.; Carreto-Vazquez, W. P. Topics Catal. 2005, 32, 135.

[10] Bartholomew, C. H. Appl. Catal. A: Gen. 2001, 212, 17.

[11] Ngantsoue-Hoc, W.; Zhang, Y.; O'Brien, R. J.; Luo, M.; Davis, B. H. Appl. Catal.

A: Gen. 2002, 236, 77.

[12] Li, S.; Krishnamoorthy, S.; Li, A.; Meitzner, G. D.; Iglesia, E. J. Catal. 2002, 206, 202.

[13] Luo, M.; Hamdeh, H.; Davis, B. H. Catal. Today 2009, 140, 127.

[14] Riedel, T.; Schulz, H.; Schaub, G.; Jun, K. W. S.; Lee, K. W. Top. Catal. 2003, 26, 41.

[15] Dry, M. E. The Fischer-Tropsch synthesis; Springer-Verlag: New York, 1981.

[16] Zimmerman, W. H.; Rossin, J. A.; Bukur, D. B. Ind. Eng. Chem. Res. 1989, 28, 406.

Chapter 3: Review on Different Characterization Techniques

Several characterization techniques are used for the qualitative analysis of prepared catalyst. XRD, SEM, EDS, BET, TGA and GC-MS tests have used in order to check the properties of catalyst. The basic working conditions and the principles of the techniques are mentioned below.

3.1 X-ray powder diffraction (XRD)

A German scientist "Wilhelm Conrad Rontgen" discovered the X-rays in 1895. X-ray powder diffraction (XRD) is used for identification of phase of crystalline material and information on unit cell dimensions. X-rays are electromagnetic waves of shorter wavelength having energy between 200 eV to 1 MeV [1]. XRD uses the method of constructive interference of crystalline sample with monochromatic X-rays. The main operating principle of XRD is determined by Bragg's law. The radiation having wavelength similar to atomic spacing of crystal is scattered by atoms of crystalline solid and experience constructive interference. Consider X-rays strikes on a crystalline solid having inter planar distance 'd'. Some of the X-rays got scattered from the crystal atoms. If the dispersed waves affect productively, they stay in phase as the variation between the path lengths of the two waves is equivalent to an integer multiple of the wavelength. The variation in the path length of two waves experiencing interference is given by $2d\sin\theta$ and θ is the scattering angle. The Bragg's law describes the relation of θ with wavelength and interplaner spacing 'd' for the constructive interference to be at its greatest by following equation

$$2d\mathrm{Sin}\theta = n\lambda$$

The material sample is finely pulverized and average bulk composition is defined using this technique. The high speed electrons are generated from filament, which strikes a metal plate (Cu) to give X-Rays. The generated x-rays are allowed to pass through a collimator which absorbs all X-rays except a narrow beam. Filters or crystal monochromators are used for monochromatization of X-rays. Moreover the X-rays fall on sample and the scattered X-rays are

recorded by a photographic film or counter methods. The result obtained from this technique is called diffractogram. The difractogram can be obtained in either intensity vs. transmittance or reflectivity format as shown in "figure 6". The apparatus used for analysis is "Bruker AXS Strahlenschutzbox (schmal) A25-A2".

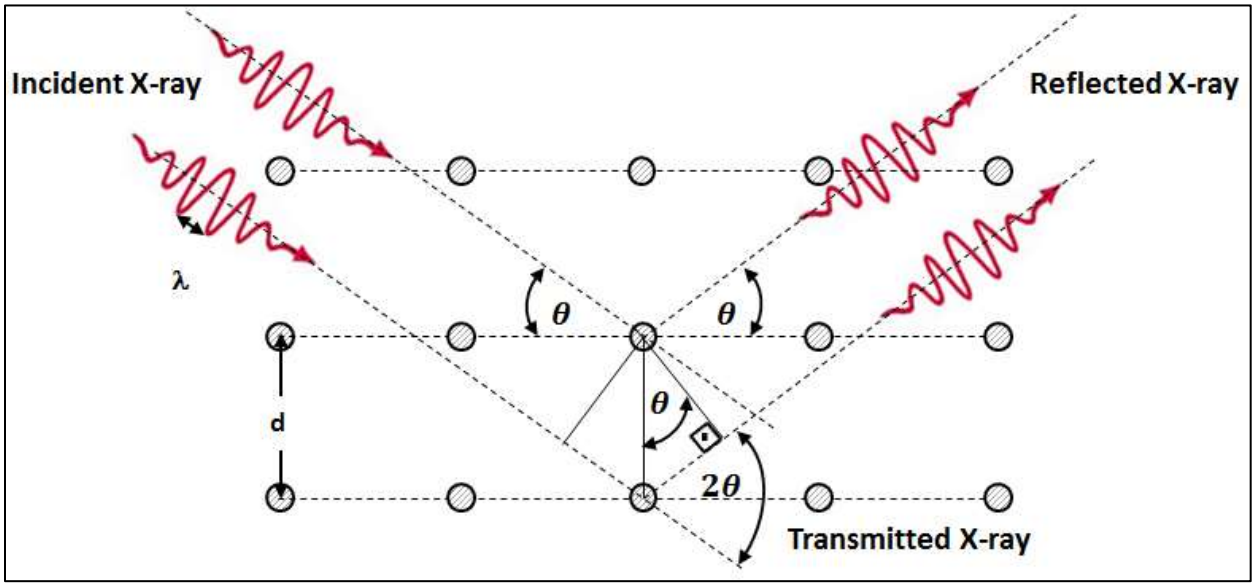

Figure 6 : Pictorial demonstration of Braggs Law

3.2 Scanning Electron Microscopy (SEM)

Scanning Electron Microscope is a technique that describes the structural properties of the material. There are two main component of SEM that is electronic console and electron column. Electronic console controls the knobs and switches are used to control the filament current, voltage, brightness and contrast. The function of electron column is generating electron beam with the help of vacuum pump, which is shown in "figure 7". Electromagnetic deflection coils are used to scan the sample image. The lower portion of the column is specimen chamber and second electron detector is present above the sample stage. Free electrons are produced from electron gun by thermionic emission from filament (tungsten) at temperature on 2700 K. the function of filament is to electrons generated from electron gun. Condenser lenses are used to converge the beam and pass through the focal point. The electrons column is used to find the aperture of sample image. These apertures reduce the extraneous electrons in the lenses. The size of the beam regulates with the using of final lens. Detailed specimen of SEM is in following [2].

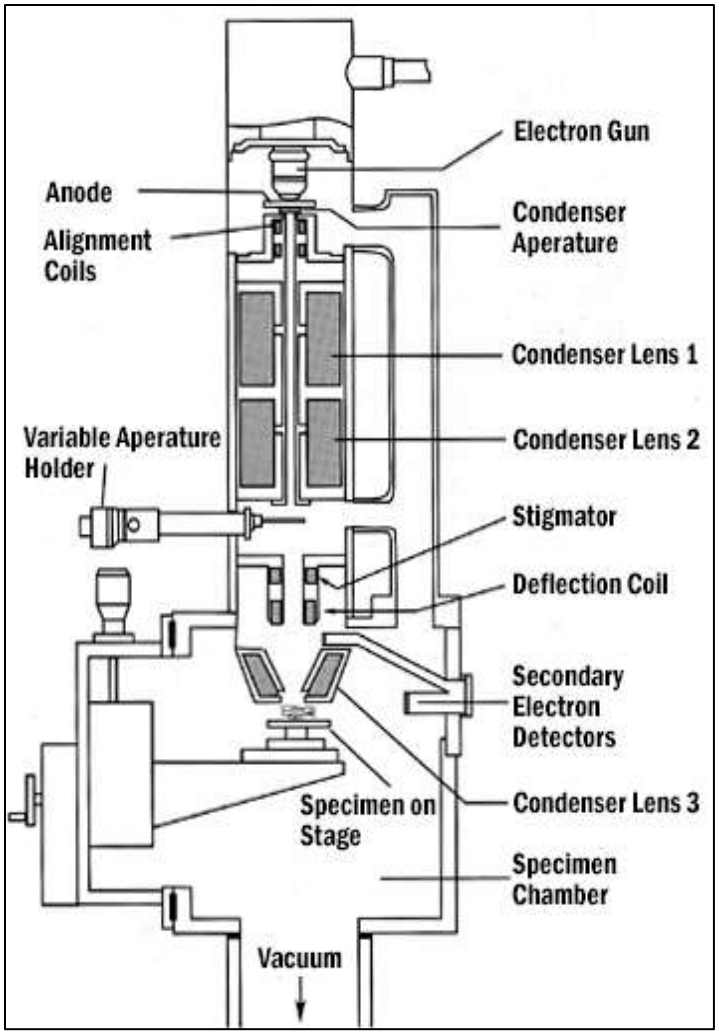

Figure 7: Scanning Electron Microscopy Instrumentation

Objective lens contains the deflection coils and images are normally formed by scanning with the restoring of electron beam. Sample chamber contains the sample stage and controls are located at the lower portion of the column. The morphology analysis is controlled by electron beam. A high pressure is required for the detail and good images ranging about $5*10^{-5}$torr [3]. The apparatus used for analysis is "TESCAN VEGA3 LMU".

3.3 Brunauer-Emmett-Teller Analyses (BET)

BET is named after the first names of its inventors Brunauer-Emmett-Teller. This technique is used for the external surface area evaluation and pore measurements yielding important information about the effects of porosity and particle size properties [4]. The

heterogeneous catalysts have individual or more group of pores whose size and volume are influenced by the method of preparation of catalyst.

The pores are differentiated in diverse classes reliant on their size.

- Micropores: Size < 2nm
- Mesopores: 2nm < Size < 50nm
- Macropores: Size > 50nm

Pores can further be divided in different categories depending upon their geometry. Pores can be cylindrical or slit shaped or more commonly irregular shaped. The irregular shaped pores can be bottleneck shaped or funnel shaped. Apart from that the pores can be divided into various categories depending upon their connectivity. Some pores are connected with each other to form a porous network whereas some pores are 'closed' which means they have no access from any sides. Some pores are 'through' which means they can be accessed from two or more sides where some pores are termed as 'open pores' because they can be accessed from only one side. These attributes of pores can greatly affect the catalytic behavior of the porous solid. Sometimes these pores can greatly enhance the activity of a catalyst whereas sometimes they limitations of coke deposition and diffusion can greatly hinder the catalytic activity of the catalyst as shown in "figure 8".

Nitrogen Adsorption at 77K is the best extensively used technique for surface area analysis and characterization of porous texture. This analysis method uses the nitrogen multilayer physical adsorption studied against change of pressure. First step is the determination of adsorption isotherm; nitrogen adsorbed volume against its relative pressure. The adsorption isotherm depends upon the porous texture of the solid. IUPAC suggests that there are six types of adsorption curves but only six are mentioned here because they are more commonly found in the catalysts used for FTS.

3.3.1 TYPE I (Microporous Solids)

There is strong contact among pore walls and the adsorbate because of which adsorption takes place at very low relative pressure. First the pores are filled at low relative pressures without capillary condensation. Once the pores got filled the adsorption is continued at external surface as in case of mesoporous solid.

3.3.2 TYPE II (Macroporous Solids)

At low pressure adsorption takes place due to formation of monolayer whereas at higher relative pressures multilayer adsorption takes pace. The monolayer and multilayer formation processes always overlaps.

3.3.3 TYPE IV (Meso porous Solid)

At low relative pressures monolayer formation takes place. At higher relative pressures multilayer formation occurs until a condensation pressure is achieved which gives a sharp rise in adsorbed volume.

3.3.4 TYPE VI (Ultra micro porous Solids)

The relative pressure at which adsorption occurs depends on the adsorbate-surface interaction. If the solid is energetically uniform the whole process takes place at a well-defined pressure. Whereas if the surface have energetically non uniform groups, a stepped isotherm is achieved. The apparatus used for analysis is Micromeritics Gemini VII surface and porosity 2390t.

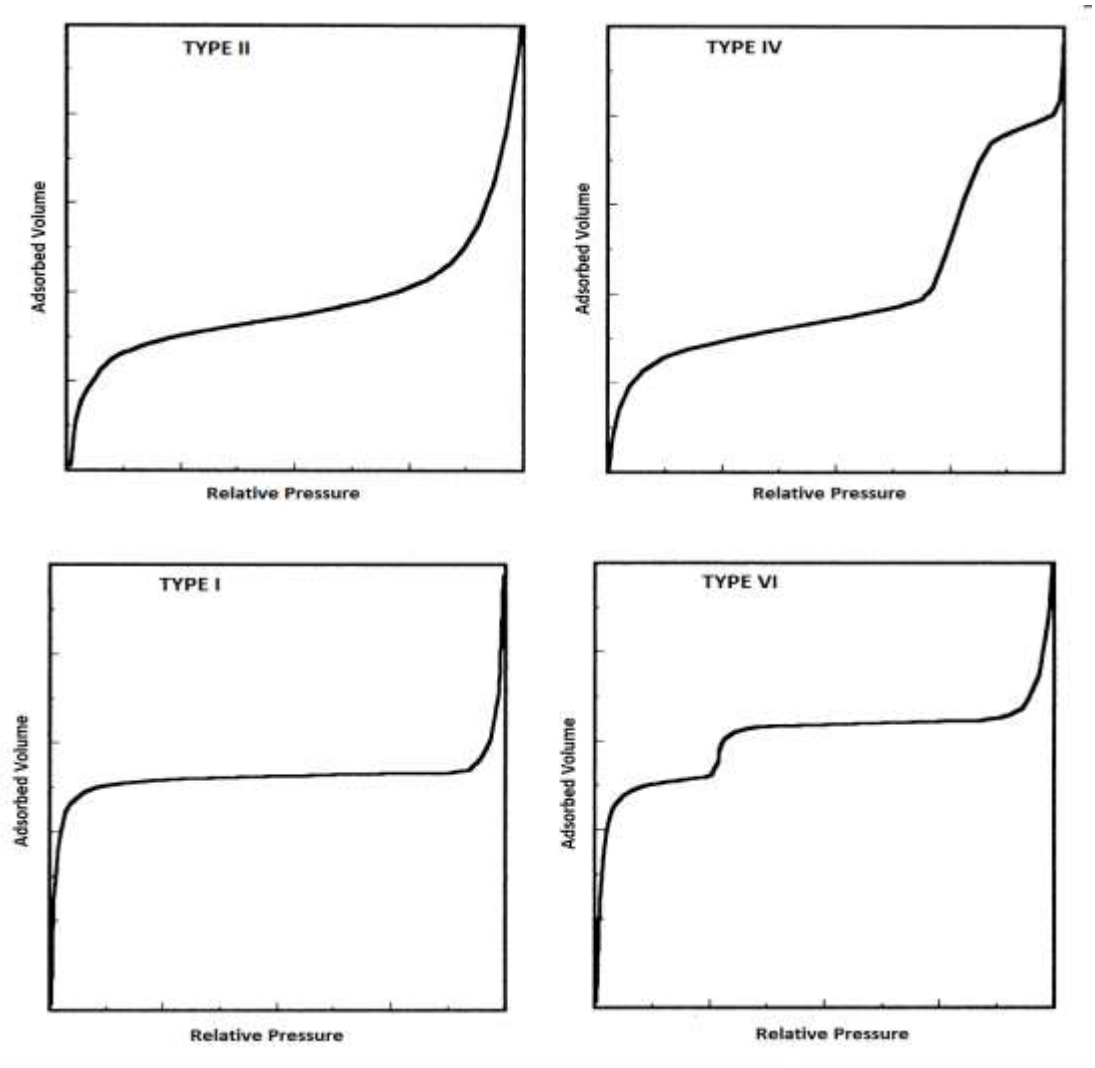

Figure 8 : Types of Adsorption Isotherms

3.4 Thermogravimetric analysis (TGA)

Thermal analysis is a technique used to study the changes in weight of a substance when subjected to the temperature change. When any material is subjected to heating under controlled environment it undergoes several changes due to reduction, oxidation, or decomposition. Such weight changes can be used to study the thermal stability and kinetics of any sample under temperature. The basic apparatus used for thermal analysis is mentioned in the 'Figure 9'.

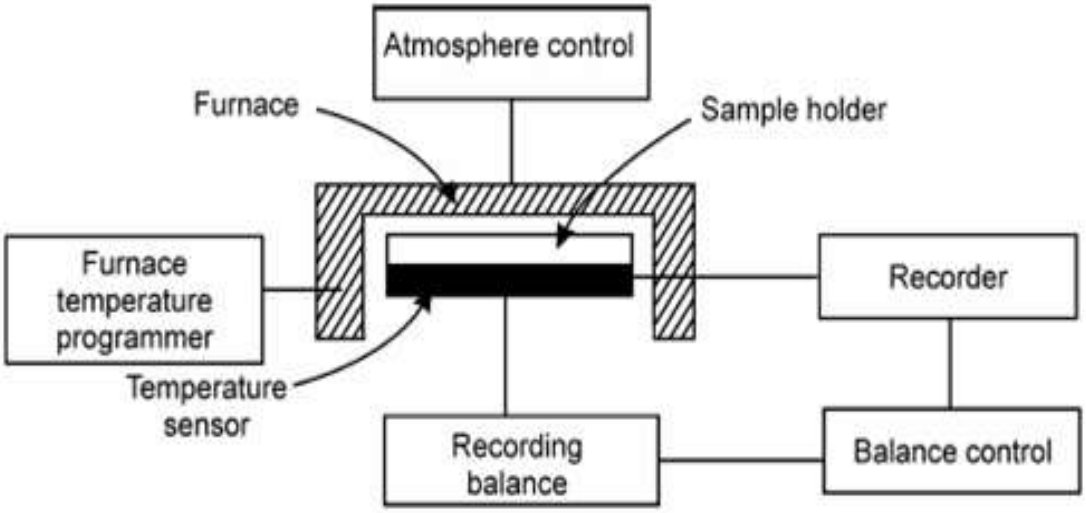

Figure 9: Thermal Gravimetric Analysis Apparatus

Thermo-gravimetric analysis also termed as thermal gravimetric analysis is a kind of thermal analysis. It is defined by International Confederation for Thermal Analysis and Calorimetric (ICTAC) as a method in which the variation in the mass of a sample is observed as it is subjected to a temperature controlled program. In this technique we observe the variations in physical or chemical properties of sample by with constant heating rate, or as a function of time (through constant temperature or constant mass loss). There are three types of thermal gravimetric analysis used as given below

3.4.1 Dynamic TGA

Weight change is examined while temperature rise is linear with time.

3.4.2 Static TGA

Weight change is recorded against time while providing constant temperature.

3.4.3 Quasistatic TGA

A series of temperature increase is provided and sample weight remains constant for each series.

The dynamic thermal gravimetric analysis is performed in this study. The constant rise in temperature is provided and the weight changes are studied. The apparatus used for analysis is "Shimadzu Simultaneous DTA-TG Analyzer (High Temperature Type) DTG-60 H 230 V".

3.5 Energy Dispersive X-ray Spectrometry (EDS)

EDS are attached with the scanning electron microscopy and solid sample are bombarded with the electron of focused beam to analyze the chemical composition. All the elements can be analyses from atomic number 4 (Be) to 92 (U). X-ray microanalysis can be done when high energy electron is bombarded with the sample in an electron microscopy. To separate the x-ray with the energy level so we use energy dispersive spectrometer. The basic diagram of apparatus is given in following figure.

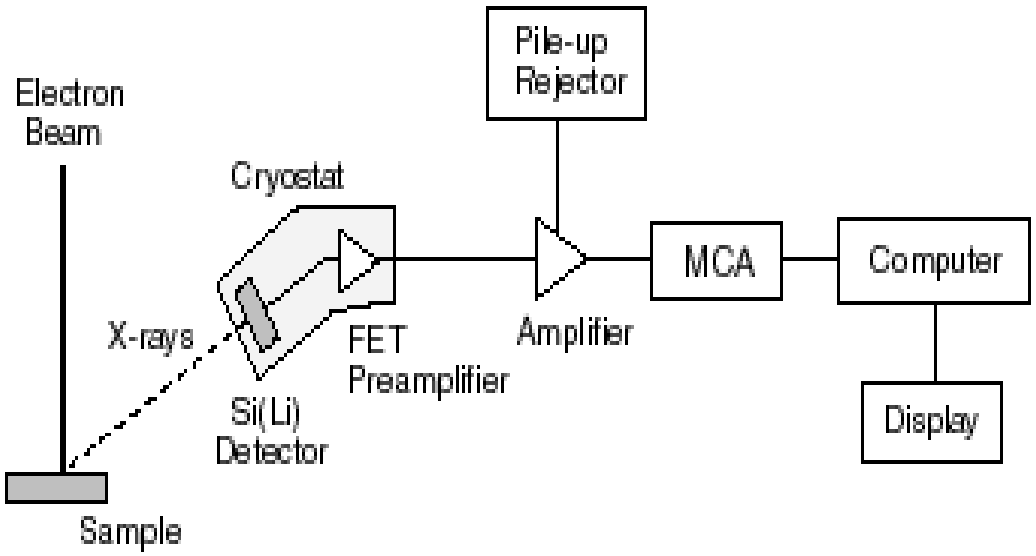

Figure 10: Energy Dispersive X-ray Spectrometry

3.6 Gas Chromatography - Mass Spectrometry (GC-MS)

GC-MS was performed to analyse the product obtained from FTS testing. GC-MS analysis as the name suggests, is a combination of two analysis techniques in sequence. Gas chromatography (GC) is used to separate multiple components of the sample whereas Mass spectrometer is used to analyze each component individually. GC separates the component of a sample based on their volatility. The sample is introduced into the GC injection port which is heated to around 300 ^{o}C to keep the sample in vaporized state. A carrier gas (usually helium) is used to move the sample in the chromatographic column. The column is 30 meter thin tube

having inner coating (stationary phase). The column is placed inside a specialized oven, which can operate at 40 to 400 ^{o}C temperature range. The sample moves across the column and the components of sample are separated due to their relative interaction with the coating of the column (stationary phase) and the carrier gas (mobile phase).

The sample exiting the GC column enters the ionization chamber of the MS. Two types of ionization techniques are used. In electron ionization (EI) electron beam is bombarded to the sample molecules to remove an electron, hence making it positively charged molecular ion or sometimes fragments of positively charged ions. Second method used for ionization is CI (chemical Ionization). CI ionizes methane first to generate a positive ion which further ionizes the sample molecule. The next part is (filter) mass analyzer which separates the charged ions based on various mass related properties. There are several types of analyzers that are being used commercially: quadrupoles, ion traps, time of flight to name a few.

After separation of charged species in filters, a detector is placed which counts the number of ions with specific mass. When single charged particle collides with the surface of detector it generates multiple electrons depending upon its mass. Each electron collides with secondary surface to create more electrons. Hence multiple electrons collisions with multiple surfaces give a cascade of electrons emitting the final surface. The output of the detector is amplified and sent to a computer to be displayed in the form of peaks called „mass spectrum". The height of the peak increases with number of counts detected with one particular mass. Figure 11 shows basic components of GC-MS analysis systems. The apparatus used for analysis is "Gas Chromatograph GC-2010 plus SHIMADZU."

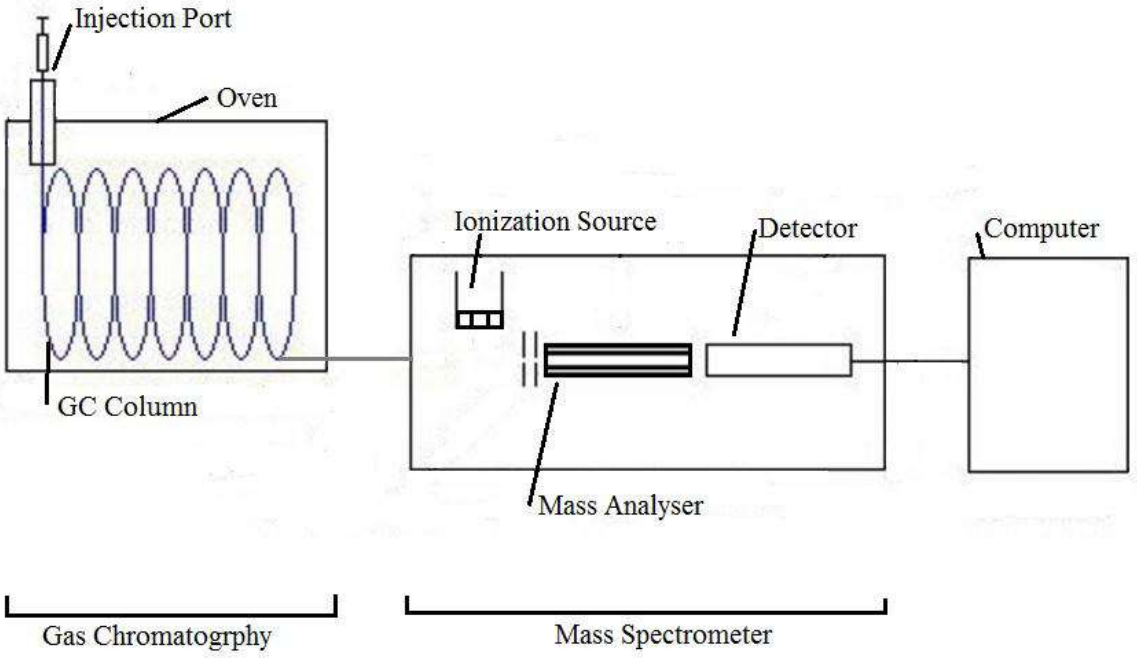

Figure 11 : Schematics of GC-MS Analysis System

3.7 Summary

For the testing of catalyst several characterization techniques like XRD, SEM, BET and TGA are used for the prepared catalyst. Scanning electron microscopy is a technique which can be used to find out the structural properties of the crystal. X-ray diffraction (XRD) is the technique to find out the phase of an unknown crystalline material and also the information about the crystal shape and size. EDS was used for the elemental analysis and TGA gives the information about the thermal degradation of the material. Then prepared catalyst is run into Fischer Tropsch synthesis reactor to find out the production of gasoline. The GCMS was done to analyze the composition of hydrocarbons.

3.8 References

[1] C. Suryanarayana, M. G. Norton, X-ray Diffraction: A Practical Approach, Plenum , New York, 1998.

[2] Brandon Cheney, Introduction to Scanning Electron Microscopy

[3] S. Lowell, J. E. Shields, M. A. Thomas, M. Thommes, Characterization of Porous Solids and Powders: Surface Area, Pore Size and Density, Kluwer Acadamic Publishers, London, 2009.

[4] P. Gabbott, Principles and Applications of Thermal Analysis, Blackwell Publications, UK, 2011.

Chapter 4: Methodology

There are three main steps in the preparation of catalyst. First one is development and synthesis of activated carbon then second is preparation of iron carbide catalyst by wet impregnation process and last one is promoter (potassium) loading on iron carbide with wet impregnation method. The prepared catalyst is characterized by using various analytical techniques to determine their properties. In the end the catalysts were tested in a fixed bed reactor for Fischer Tropsch Synthesis. The product collected from FTS was analyzed by using GC-MS. The detailed description of each step is mentioned below.

4.1 Catalyst preparation

4.1.1 Preparation of activated carbon

Fallen or dead leaves from "*Lantana*" are collected from garden, and dried in a sunlight atmosphere for 3-4 days and then oven dried at 105 ^{o}C for 5hr. Dried leaves are crushed and passed through a sieve of 250µm. phosphoric acid (H_3PO_4) is used as a activated agent that changed the thermal degradation of the "*Lantana*" tree leaves. H_3PO_4 are increasing the number of defects which anchoring site for metal particles and also increase the surface area. The absorption time of H_3PO_4 (wt. 50%) into leaves powder is 16hrs at room temperature with 3:1 ratio. Then the absorption material is calcined in a box resistance furnace at 500-600 ^{o}C for 2 hrs. The produce char is washed with distilled water to remove the excess H_3PO_4 until the neutral ph is achieved. Then dried in an oven at 105 ^{o}C for 1 hr. in order to obtain the activated carbon [1].

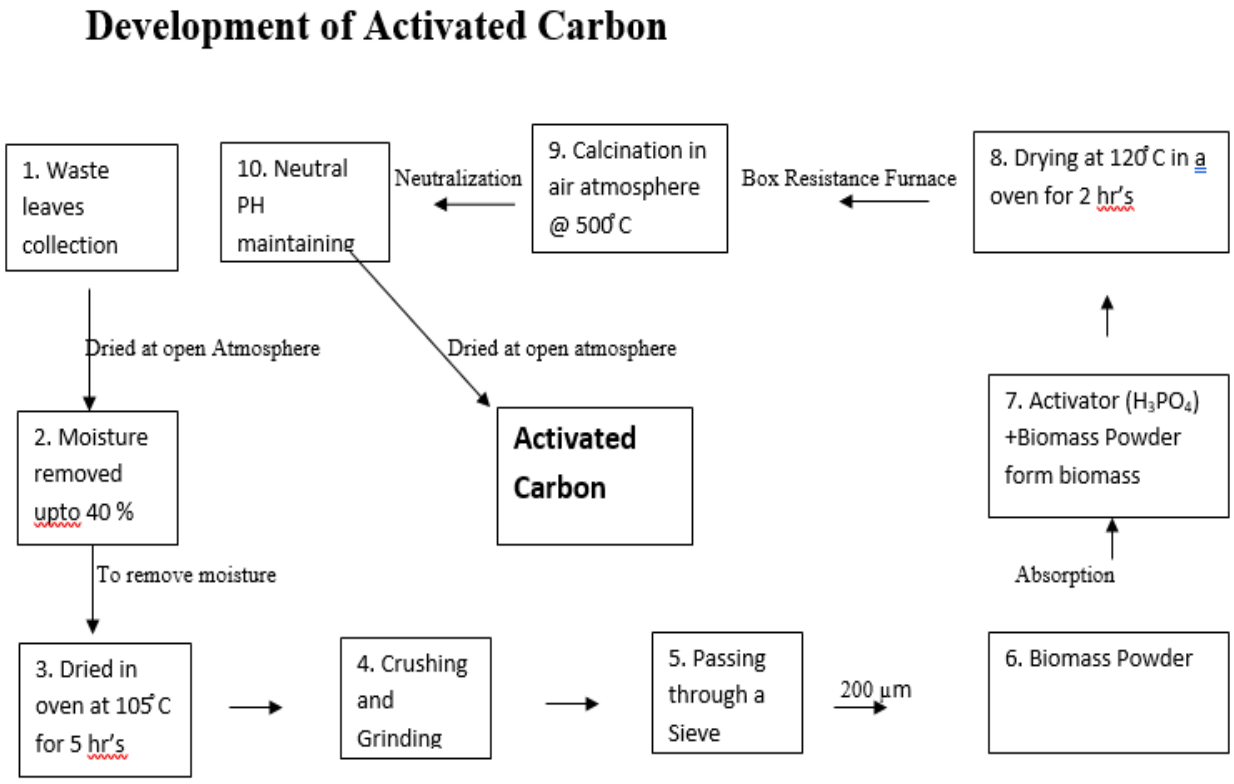

Figure 12 : Development of activated carbon

4.1.2 Preparation of catalyst

The catalyst was prepared by wet impregnation method in which the prepared 4 gram activated carbon from "*Lantana* ", are mixed with a 10% of iron nitrate ($Fe(NO_3)_3.9H_2O$) by adding drop wise 10 ml of deionized water. The sample was placed in a room (25 ^oC) for a 24 hrs. Finally the sample was calcined in a box resistance furnace at 350 ^oC for 3 hrs. and then dried at 120 ^oC for one hour [2].

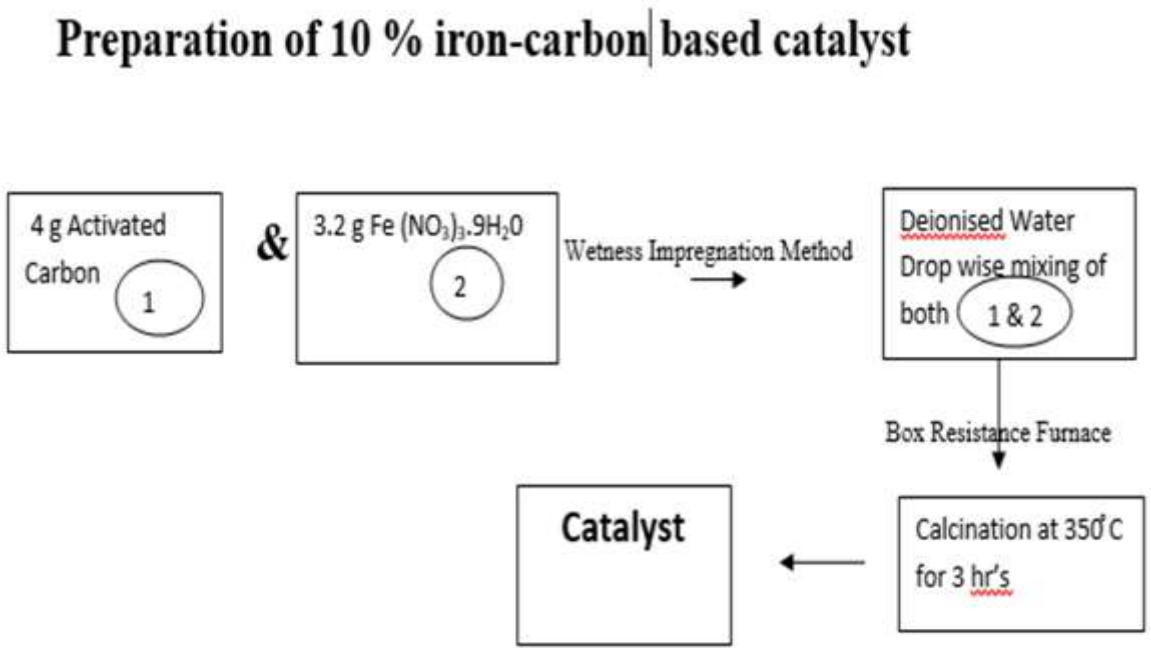

Figure 13: preparation of catalyst

4.1.3 Loading of promoter on catalyst

Potassium was used as a promoter in iron carbide catalyst. The promoter loading was done by wet impregnation method. In this method 3 % potassium was loaded on catalyst for this purposes potassium carbonate (k_2CO_3) dissolved in deionized water and drop wise mixed on prepared iron carbide catalyst. The sample was placed in room temperature for 24 hrs. At the end the sample was calcined in box resistance furnace at 400 ^oC for 2 hrs. and then dried at 100 ^oC for one hour in vacuum oven.

Table 4: List of prepared Catalyst

Name of Catalyst	Method of Preparation	Promoter
Fe-AC-K	Wet Impregnation	Potassium
Fe-AC	Wet Impregnation	Without Promoter

4.2 FTS Process

The catalyst was tested in a fixed bed micro reactor having length of 10 cm with a diameter of 3.3 cm. The nitrogen, carbon monoxide and hydrogen are provided to synthesize syngas artificially on lab scale. The flow of the gasses is controlled by flow controllers. The required composition of the syngas can be synthesized by controlling the flow through flow controllers. There is a pressure gauge that is used for the pressure measurements. A pressure safety valve is also installed for the safety purposes so that it releases excess pressure avoiding the reactor or the tubing to burst. After flow controllers the gasses passed down to reactor. An electric heater is placed around the reactor in spiral form to heat the reactor to desired temperatures.

The Fischer Tropsch reaction usually takes place at higher temperatures; therefore an insulation casing was installed to avoid heat losses. After the reactor the unreacted gasses passed to an escape pipe whereas the product is condensed in separators. Separator 1 is used for the collection of heavier products whereas the lighter products move down to separator 2, due to difference in their boiling point. After separators a back pressure valve is installed that ensures the high pressure between flow controllers and the back pressure valve. 1 grams of freshly prepared catalyst was mixed with 5gm of ceramic balls and loaded in the reactor. Glass wool plugs are inserted at the top and bottom of the reactor for packing purposes. The inert ceramic balls act a diluting material and have no effect on the selectivity and activity of catalyst [3].

4.2.1 FTS Reaction

After loading a catalyst into a reactor the reduction of catalyst was started with a hydrogen gas with flow rate of 30 sccm and nitrogen gas with 10 sccm, nitrogen gas used as a carrier. After reduction at 450 ^{o}C for 4 to 5 hrs then cooling down to 300 ^{o}C in order to promote the reaction at 20 bar under the presence of H_2/CO ratio 1:1.The product gases collected from separator are analyzed by chromatography and hydrocarbons on carbon basis [4]. In Fischer Tropsch process the reaction was started at 300 ^{o}C for a 10 hrs with 20 bar pressure. The flow rate of hydrogen and carbon monoxide was 30 sccm, and nitrogen was 10 sccm which act as an inert. The product is collected into a separator and sends into a distillation column for further purification of hydrocarbons.

4.2.2 The effect of Iron based catalyst on different temperature and pressure

The effect of temperature and pressure on the chain length is very complex. At low temperature (240ºC) an increase in pressure leads to increasing mass fractions of low molecular weight hydrocarbons, thus favoring the production of lighter fractions rather than waxy products. At high temperature (270 ºC) and low pressure favor an increase in liquid products of the range between C_{21} and C_{25}. An increase in pressure and temperature have allowed the production of waxy products with more than 35 carbons [5].

4.2.3 The effect of H_2/CO ratio in FTS

- By decreasing the H_2 / CO (0.7:1) ratio than less parrafins will produce and the number of oxygenates will also increase due to unsaturated hydrocarbons (Olefins).
- By increasing the H_2 / CO (2:1) ratio than less olefins will produce and number of oxygenates will decrease and also depend on pressure and temperature.

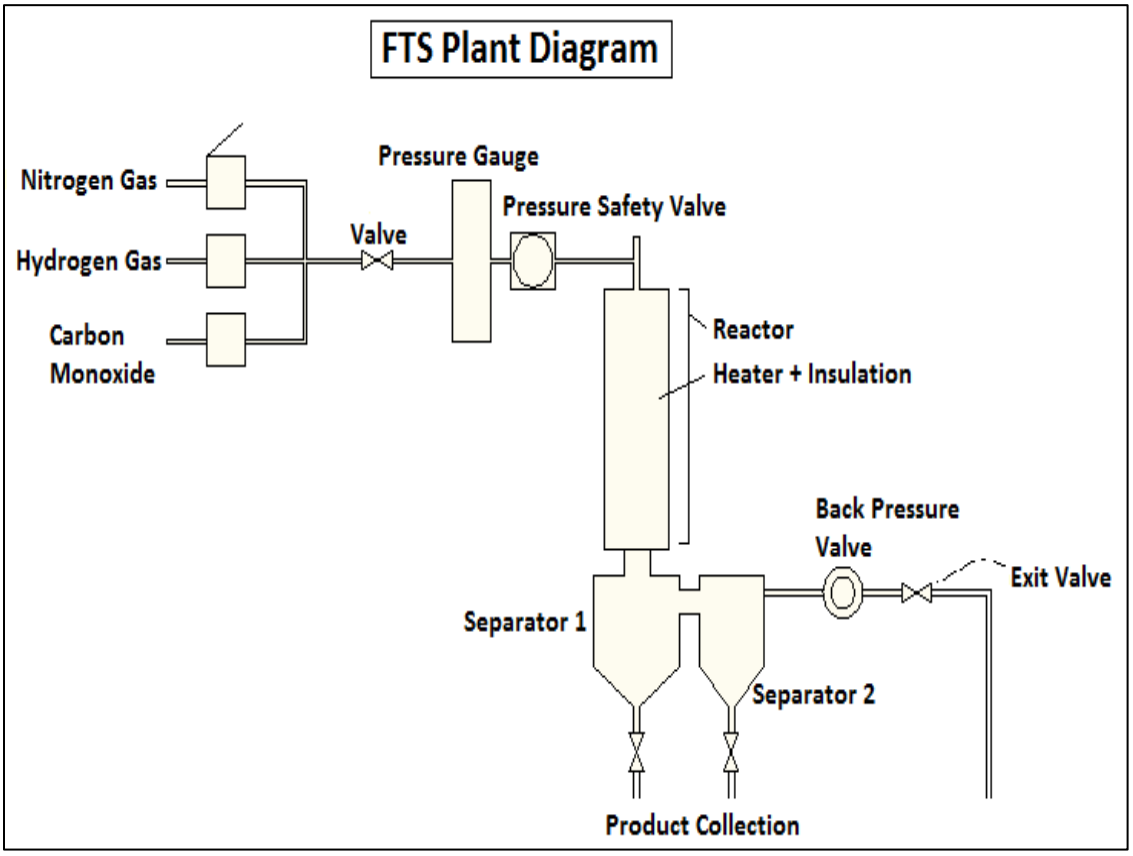

Figure 14: Lab scale FT Plant (NUST)

4.3 Summary

This study focused on the preparation of activated carbon and iron carbon catalyst. Two different catalysts were prepared by wet impregnation method. First catalyst was carbon supported iron catalyst using potassium as a promoter. Second catalyst was also carbon supported iron catalyst using without promoter effect. Both the catalyst was tested in fixed bed reactor at 300 ^{o}C and 20 bar pressure for 10 hrs.

4.4 References

[1] Chong Qin, Yao Chon, Jino-min Gao, Manufacture and characterization of activated carbon from marigold straw by H_3PO_4 chemical activation, Material letters,135,123-126, 2014

[2] YongweLu,QiangeYan,JnnKan,Baobao Cao, Jason Street,FeiYn, Fischer Tropsch Synthesis of olefin-rich liquid hydrocarbons from biomass-derived Syngas over carbon-encapsulated iron carbide\Iron nanoparticles Catalyst, Fuel,193,369-384,2017

[3] C. L. Bianchi, C. Pirola, and V. Ragaini, Catalysis Communications, 2006, 7, 669- 672

[4] Shin Wookkang, k. kim, D.Chum, J. Yang, H. Lao, H. Jung, J. Lim, S. Jang, C.Kim, C. Lae, S.Joo, J.Han, J. Park, High Performance Fe_5C_2@cmk-3 nanocatalyst for Selective and high yield Production of gasoline range hydrocarbons, Catalysis,349,66-74,2017

[5] F.E.M. Farias, F.R.C. Silva, S.J.M. Cartaxo, F.A.N. Fernandes, F.G. Sales, Effect of operating conditions on Fischer-Tropsch liquid products, Lat. Am. Appl. Res. 37 (2007) 283–287.

Chapter 5: Results and Discussion

5.1 Characterization Results

5.1.1 Scanning Electron Microscopy (SEM)

Scanning Electron Microscope is a technique that informs about the structural properties of the crystal. Scanning electron microscopy of activated carbon prepared from "*Lantana*" is shown in figure 15. The activated carbon is prepared by wet impregnation method. The micrograph images of prepared activated carbon are taken at different resolution. The high resolution image is marked as X10,000 which means that image is taken when subject is enlarged 10,000 times its original size and similarly other images are taken at X5,00 and.X2,000 resolutions. The figure 15 (a, b) shows that activated carbon is in tubular shape and figure (c) shows that the sample is porous due to the phosphoric acid is used as a activator agent.

The SEM images of carbon supported iron based catalyst are shown in figure 16. The images are taken at different resolutions X5, 000, X5, 500, X10, 000 and X20, 000 and all the images suggest the formation of needle like structures. At high magnification (11,700) the needles like and hexagonal structures are formed due to the increased in the Fe crystallite size.

The SEM images of carbon supported iron based catalyst with potassium promoter are shown in figure 17. The images are taken at different resolutions X2, 500, X20, 000, X40, 000 and X50, 000. In the images some of the potassium particles are agglomerates with carbon and iron particle. The SEM image also shows a layered and porous structure due to impregnation of potassium and iron carbide. The SEM of post processing carbon supported iron catalyst with potassium promoter is shown in figure 18. The images are taken at different resolutions X5, 000, X10, 000, X15, 000 and X20, 000. The results show that the needle and globular particles are deformed when they are process into the FT reactor at different conditions such like 300 ^{o}C for 10 hrs. at 20 bar pressure.

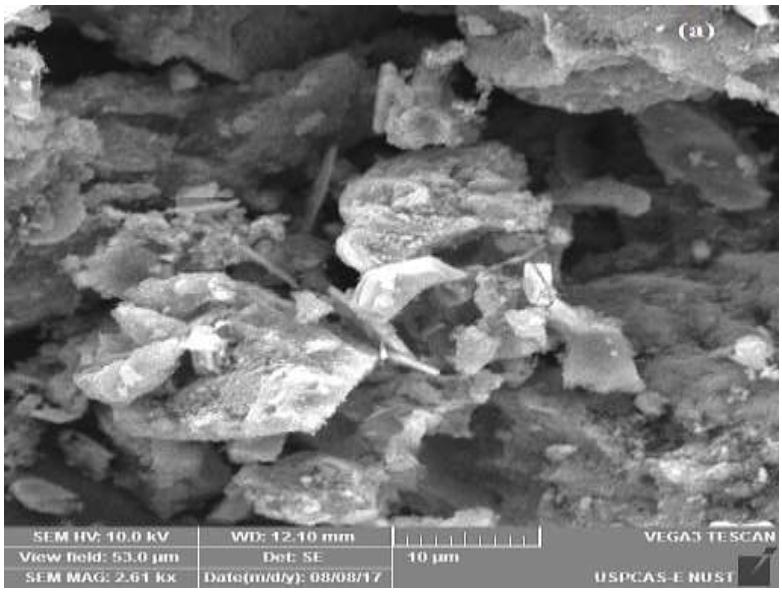
(a)
SEM HV: 10.0 kV
WD: 12.10 mm
VEGA3 TESCAN
View field: 53.0 µm
Det: SE
10 µm
SEM MAG: 2.61 kx
Date(m/d/y): 08/08/17
USPCAS-E NUST

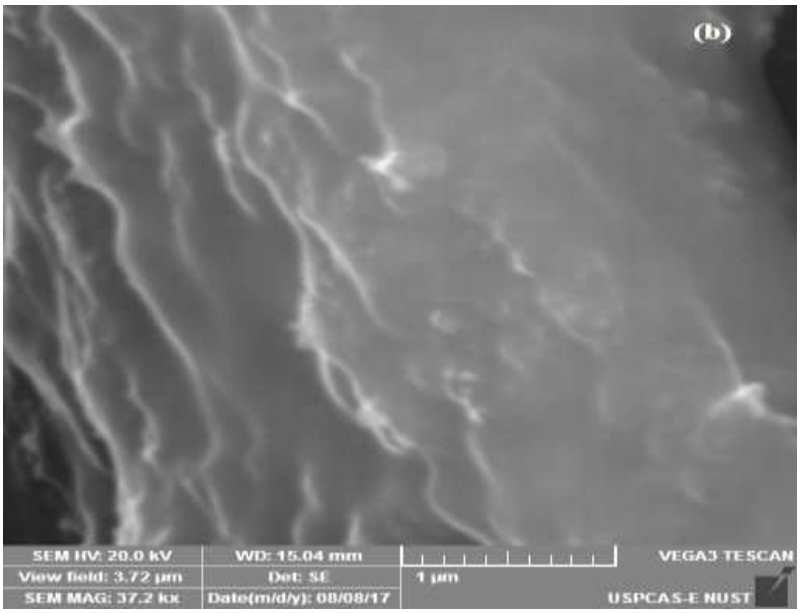
(b)
SEM HV: 20.0 kV
WD: 15.04 mm
VEGA3 TESCAN
View field: 3.72 µm
Det: SE
1 µm
SEM MAG: 37.2 kx
Date(m/d/y): 08/08/17
USPCAS-E NUST

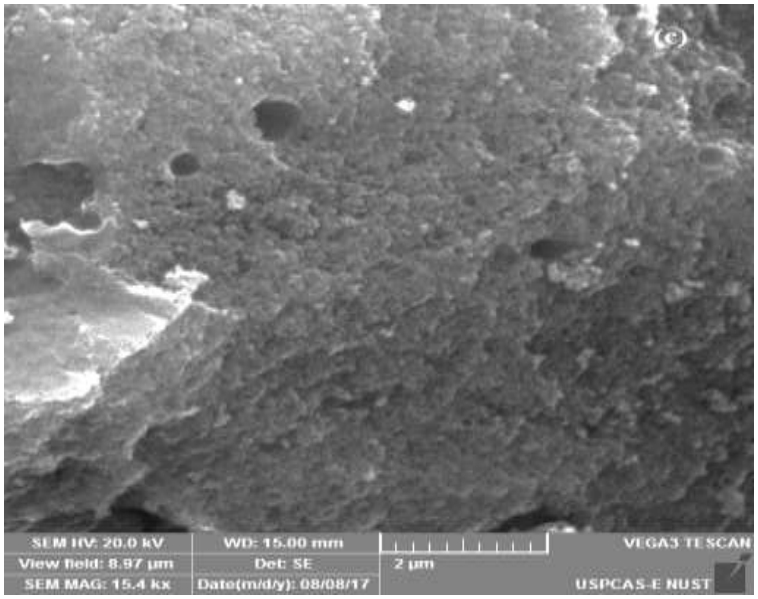

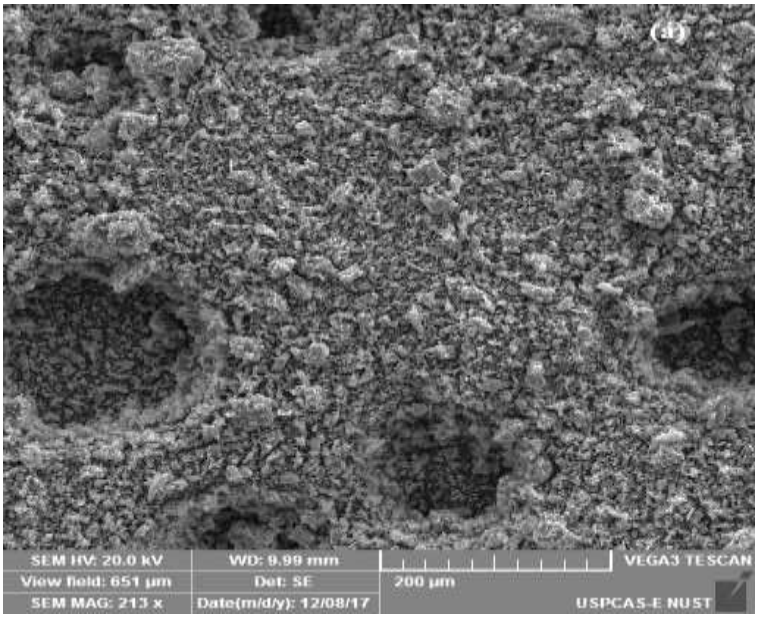

Figure 15: SEM image of Activated Carbon

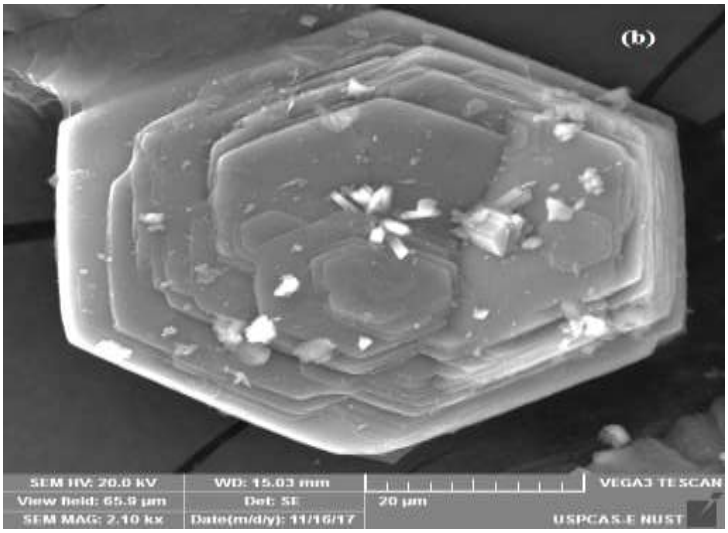

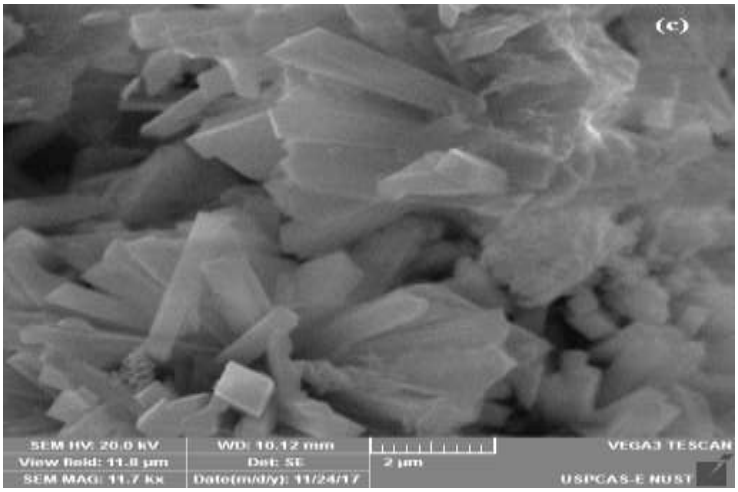

Figure 16: SEM image of Iron Carbide

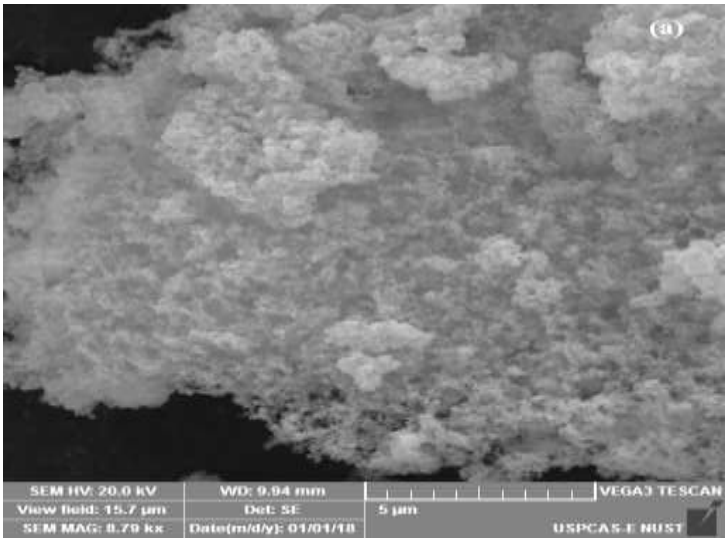

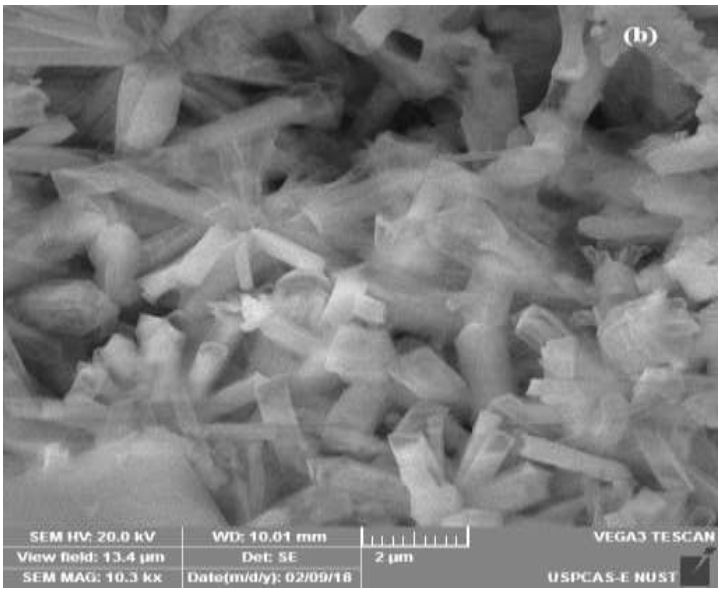

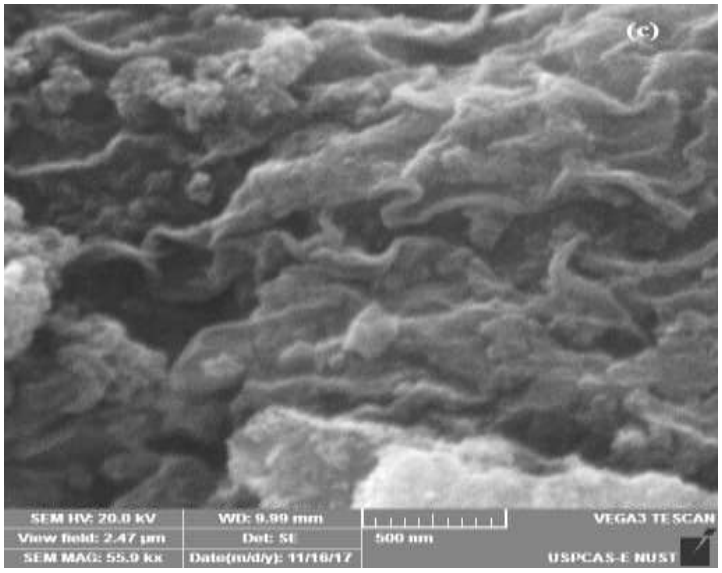

Figure 17: SEM image of iron carbide catalyst with potassium loading

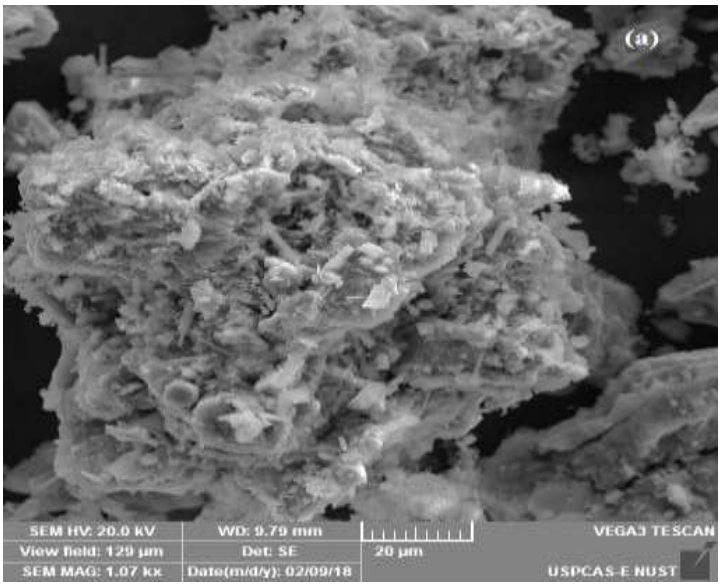
(a)
SEM HV: 20.0 kV
WD: 9.79 mm
VEGA3 TESCAN
View field: 129 µm
Det: SE
20 µm
SEM MAG: 1.07 kx
Date(m/d/y): 02/09/18
USPCAS-E NUST

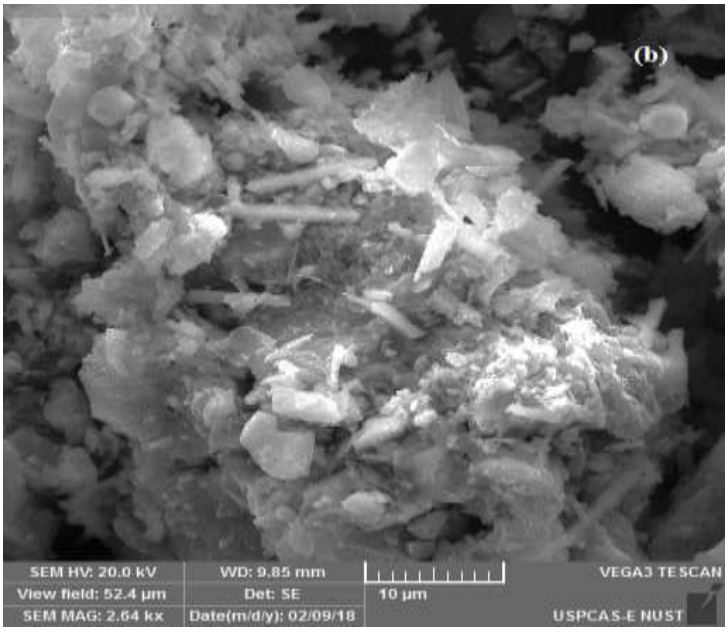
(b)
SEM HV: 20.0 kV
WD: 9.85 mm
VEGA3 TESCAN
View field: 52.4 µm
Det: SE
10 µm
SEM MAG: 2.64 kx
Date(m/d/y): 02/09/18
USPCAS-E NUST

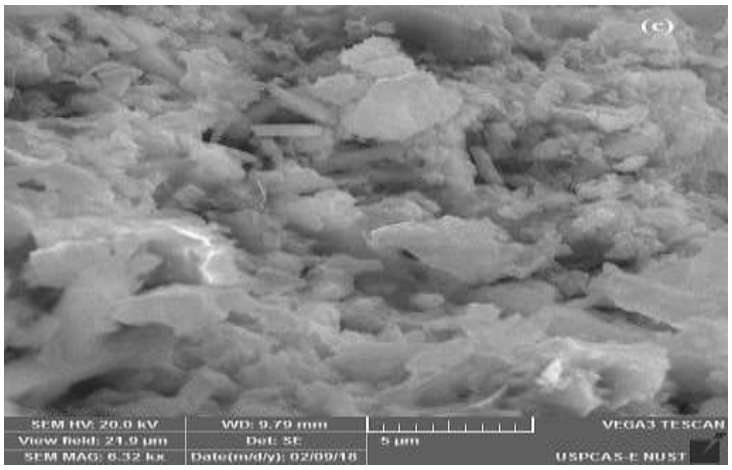

Figure 18: SEM image of iron carbide after FT test

5.1.2 Energy-dispersive X-ray Spectroscopy (EDS)

EDS data of prepared activated carbon, carbon supported iron catalyst with and without potassium promoter and catalyst used in FT plant after Fischer Tropsch synthesis (with potassium promoter) are shown in table 5. In the activated carbon the amount of phosphorus is present due to the H_3PO_4 which is used as the activator agent during the activated carbon preparation. In carbon iron supported catalyst (with & without promoter) the amount of oxygen are the confirmation of the oxide formation and these oxygen group are removed during the reduction process (water gas shift reaction). After the catalyst testing in FT plant (carbon supported iron catalyst with potassium promoter) a very small amount of calcium and magnesium are also present due the human error and does the effect the working of catalyst. The detailed analysis is given in following table.

Table 5: Elemental analysis from EDS

Sample ID	C (%)	P (%)	O (%)	Fe (%)	K (%)
AC "*Lantana*"	78.532	17.85	4.64	___	___
Fe-C	24.64	5.36	38.08	31.92	___
Fe-C-K	13.43	___	48.91	28.68	6.96
Fe-C-K (FT used)	21.74	___	42.57	24.46	4.05

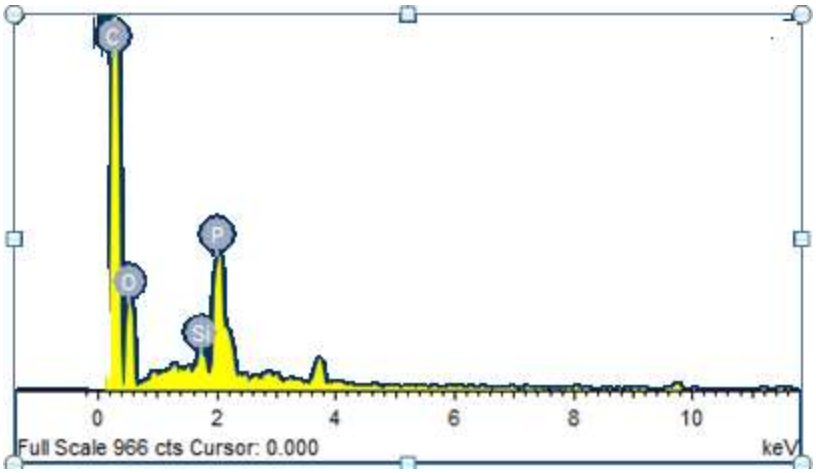

Figure 19: Activated carbon from "*Lantana*"

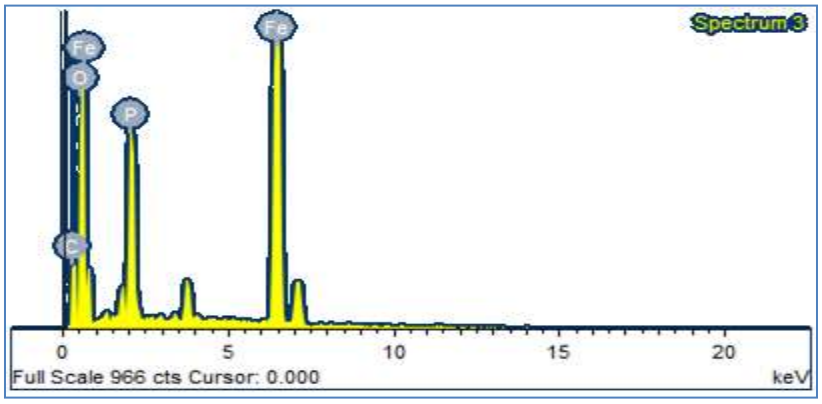

Figure 20: Carbon supported Iron catalyst

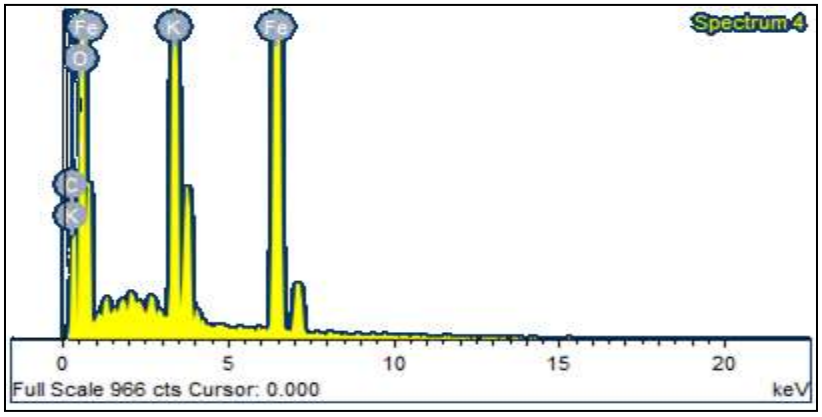

Figure 21: Carbon supported Iron catalyst with Potassium promoter

5.1.3 X-ray diffraction (XRD)

X-ray diffraction (XRD) is the technique to find out the phase of an unknown crystalline material and also the information about the crystal shape and size. XRD pattern of activated carbon prepared from "*Lantana*" are shown in the figure 23. XRD of activated carbon at angle 23.9^{o} with miller indices (201) having PDF # 22-1069. Small number of stacked layer are formed which is shown in the diffraction pattern with broad lines in the prepared activated carbon.

XRD of fresh Fe-C-K catalyst, is iron carbide (Fe_2C) at angle 43.2^{o} with miller indices (101) having PDF # 36-1249. At angle 29.7^{o} and 26.6^{o} with miller indices (111), (202) with PDF # 47-1409 and 16-0653 are respectively iron oxide (Fe_2O_3). At angle 24.8^{o} and 21.5^{o} with miller indices (203), (202) with PDF # 48-1206 are respectively amorphous carbon (C70).

XRD of used Fe-C-K catalyst, is iron carbide (Fe_3C) at angle 44.5^{o} with miller indices (220) having PDF # 35-0772. At angle 30.1^{o} with miller indices (110) with PDF # 40-1139 is iron oxide (Fe_2O_3). At angle 20.6^{o} and 23.9^{o} with miller indices (113) and (201) with PDF # 48-1449 and 22-1069 are respectively carbon.

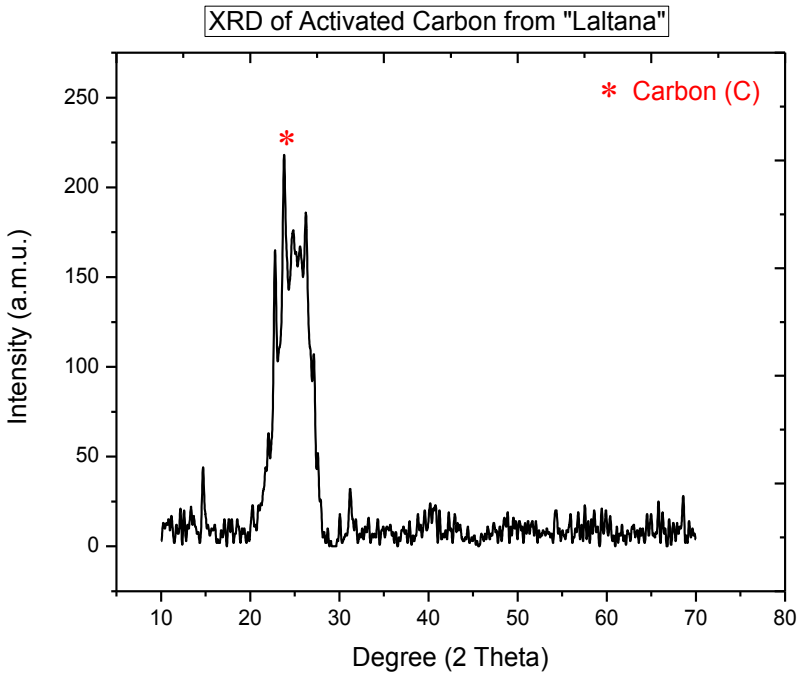

Figure 22: XRD of activated carbon

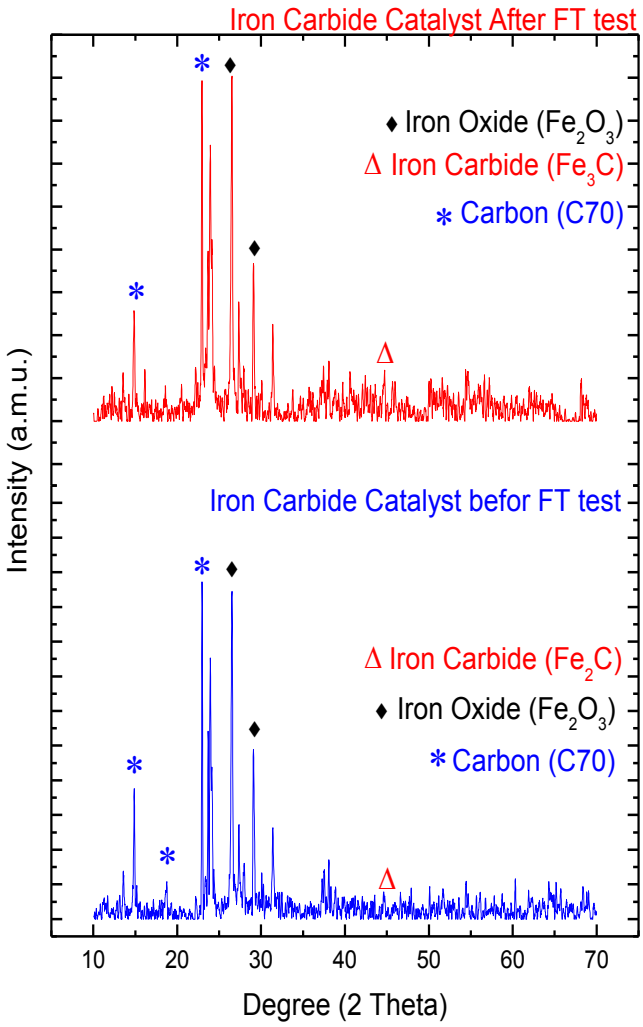

Figure 23: XRD of Fe-C-K catalyst before and after FT Test

5.1.4 Brunauer–Emmett–Teller (BET)

The surface area of the activated carbon and the carbon supported catalyst were determined by "Micromeritics Instrument Corp" company BET instrument. The surface area of activated is high as compared to the iron based catalyst. The isotherm gives us the information about the porous texture of the solids. The monolayer formation is the prevailing process at relative low pressure and multilayer absorption is take place when the relative pressure is

increased. The thickness of the adsorbate is increased gradually until the condensation point is achieved. The degassing condition of activated carbon 2 hrs at 100 ^{o}C but the condition of catalysts is 4 hrs degassing under nitrogen atmosphere at 350 ^{o}C. The surface area, pore volume, pore size and average particle size are shown in the below table.

Table 6: BET of Activated carbon and Fe-C catalyst

Sample	BET surface Area (m^2/g)	Pore Volume (cm^3/g)	Pore Size (nm)	Avg. Particle Size (nm)
AC "*Lantana*"	611.21	0.284	18.62	—
Fe-C	78.74	0.036	27.34	761.966

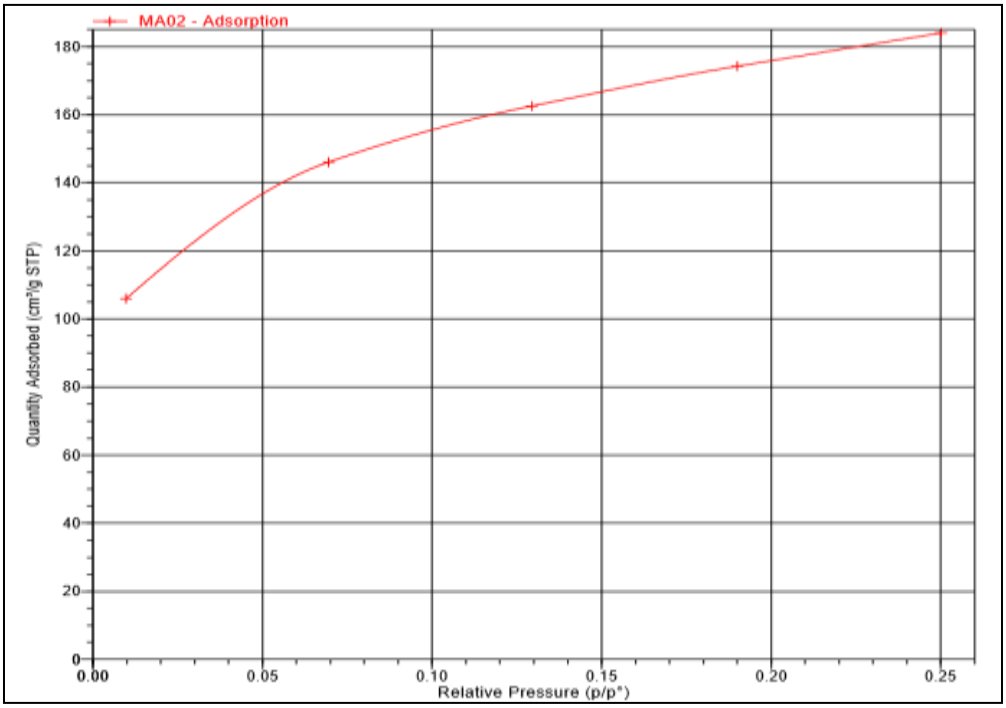

Figure 24: Adsorption isotherm of activated carbon

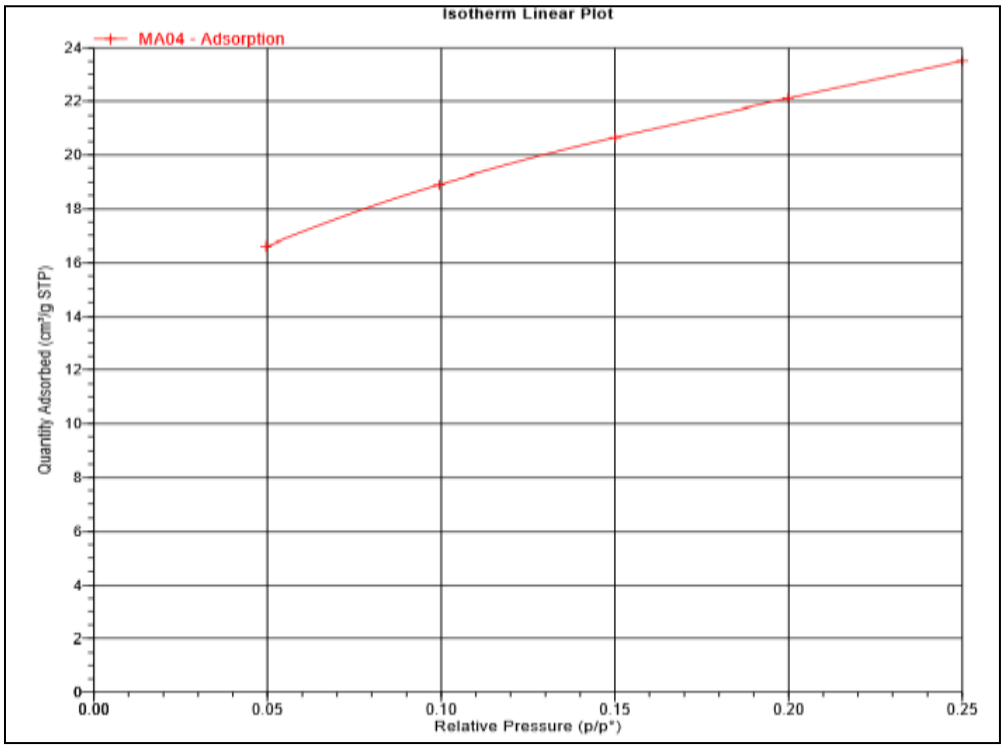

Figure 25: Adsorption isotherm of carbon supported iron based catalyst

5.1.5 Thermo-gravimetric Analysis (TGA)

Thermalgravitic analysis was done under nitrogen gas atmosphere. The activated carbon prepared from "*Lantana*" and all catalyst starts their weigt loss from 30-110 ^{o}C due to the water molecules in the interlayer space and sharply degarade at 450 ^{o}C and fully thermally degraded at above 600 ^{o}C. The carbon supported iron based catalyst thermally degarded at above 550 ^{o}C. The catalyst with potassium promoter shows his gradually decrease their weight and deompoise at about 600 ^{o}C. When the potassium promoter catalyst run into FT plant at certain condition then the behaviour of TGA analsis are changed and sharply degrade at 250 ^{o}C and full weight loss at below 500 ^{o}C.

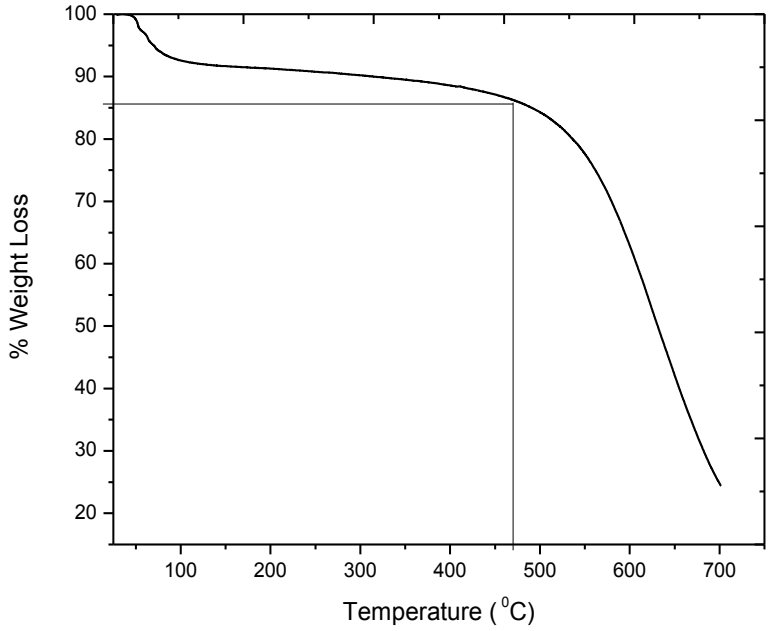

Figure 26: TGA of activated carbon

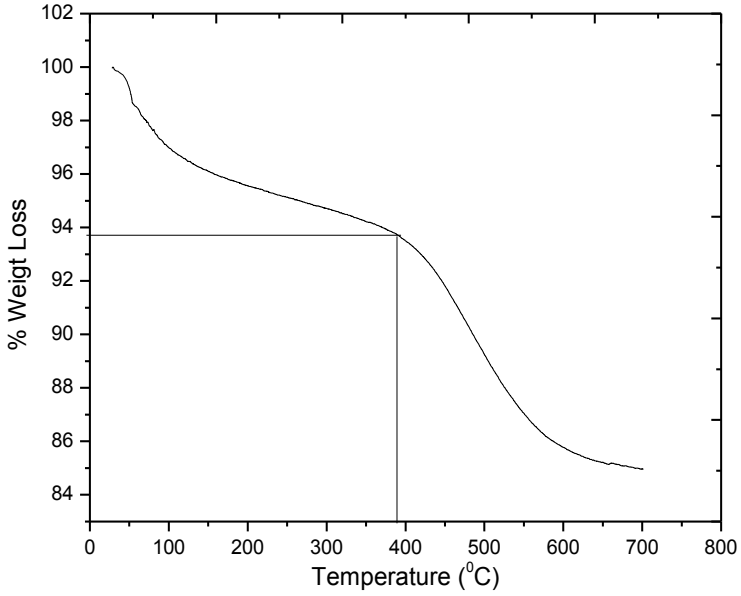

Figure 27: TGA of Fe-C-K Catalyst before FT Test

5.2 FTS Product Analysis

The Fischer Tropsch Synthesis was performed by using unprompted catalyst. The Iron Carbon catalyst was tested on 350 ^{o}C and at 20 bars. The product was collected form Separator 1 and Separator 2 in glass vials. The glass vials are sealed to avoid evaporation of any component of product. The Picture of collected samples in sealed glass vials are shown in "Figure 30". The "Shimadzu QP2010 Ultra" system is used for GC-MS analysis of product obtained from both separators. Injection temperature was set at 120 ^{o}C. Helium was used as carrier gas at pressure of 89.3 KPa and column flow rate of 1.44 mL/min. The total flow was 158.9 mL/min and total time of process is 25 minutes. The GCMS results shows almost 200 different peaks and following table shows the all possible compounds present in the product. The total percentage of different hydrocarbons (C_5-C_{11}) in the mixture is 45.63 % and (C_{12}-C_{22}) is 47.59 %.

In second experiment Iron Carbide catalyst was loaded with 3% potassium as a promoter and tested on 300 ^{o}C with 20 bar pressure. The product was collected form Separator 1 and Separator 2 in glass vials. The glass vials are sealed to avoid evaporation of any component of product. The total percentage of different hydrocarbons (C_5-C_{11}) in the mixture is 17.60 % and (C_{12}-C_{22}) is 80.22 %.

In third experiment Fe-C-K catalyst was reused and tested on 300 ^{o}C at 20 bars. The product was collected form Separator 1 and Separator 2 in glass vials. The glass vials are sealed to avoid evaporation of any component of product. The total percentage of different hydrocarbons (C_5-C_{11}) in the mixture is 33.20 % and (C_{12}-C_{22}) is 61.19 %.

Figure 28: FT Product collected from FT reactor

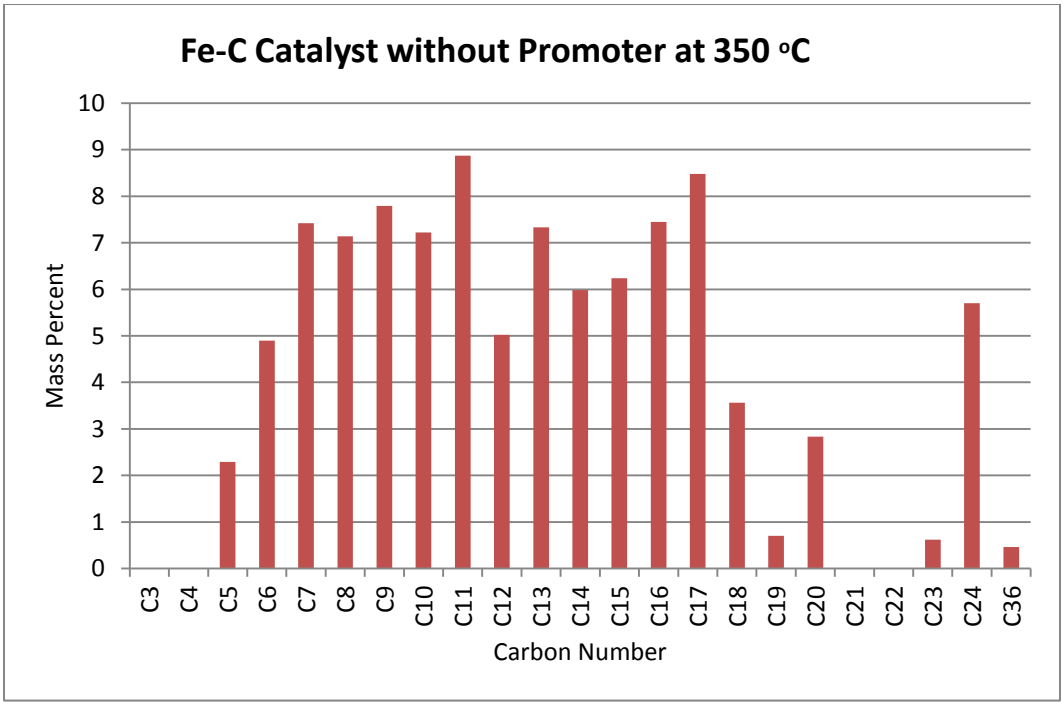

Figure 29: Chain Length Distribution of Carbon supported Iron Catalyst Results

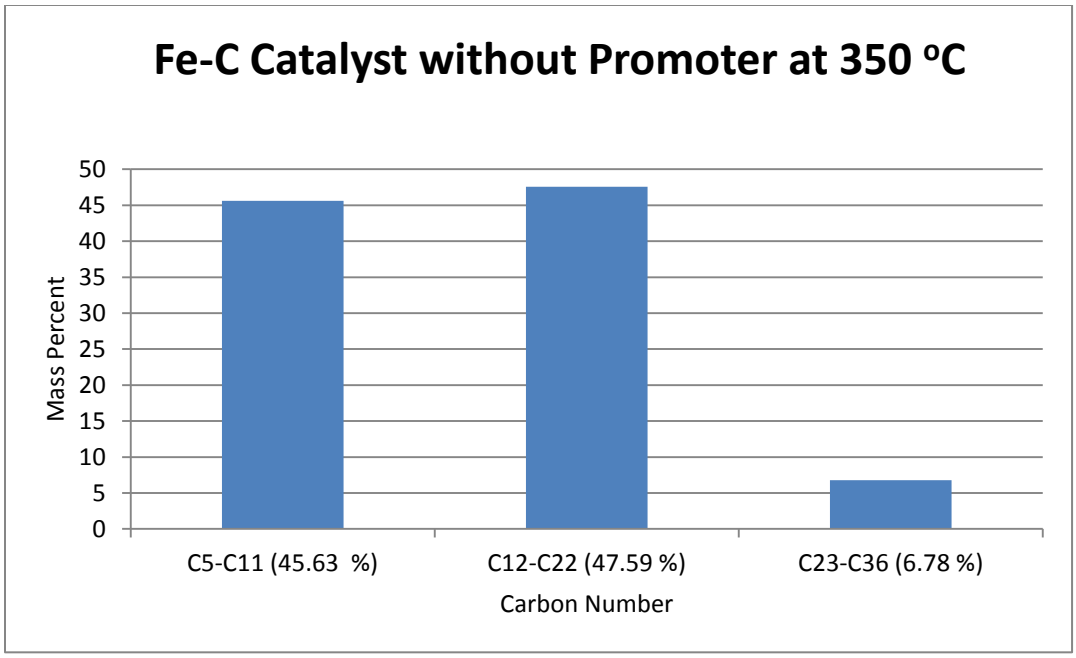

Figure 30: Chain Length Distribution of Carbon supported Iron Catalyst Results

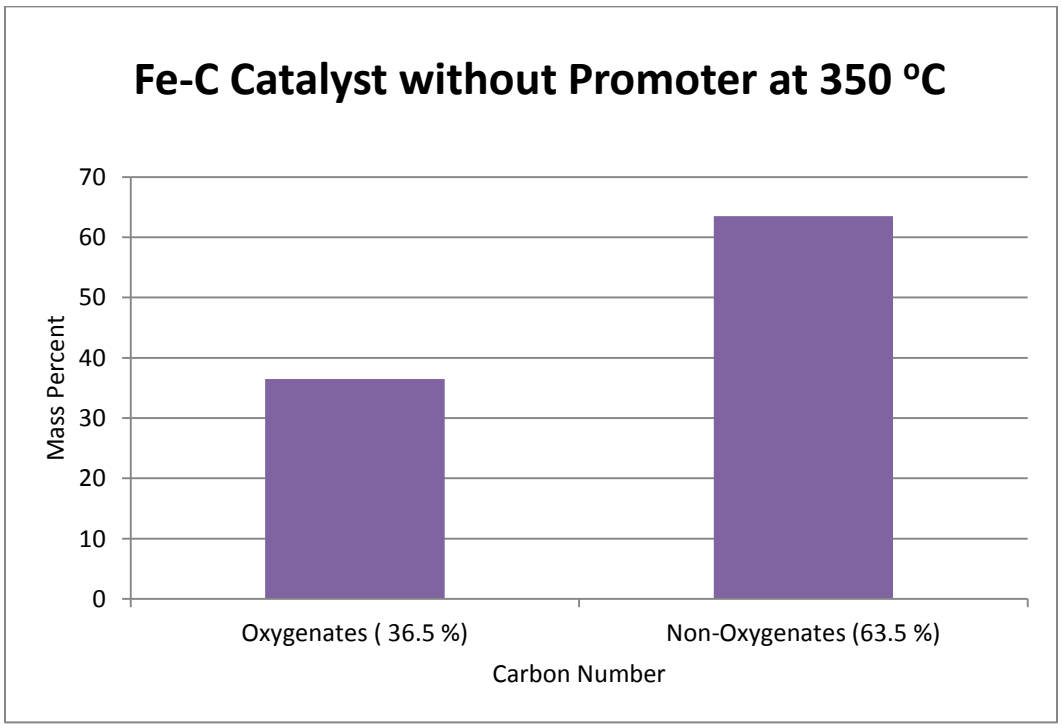

Figure 31: Comparison of Oxygenates and Non-Oxygenates

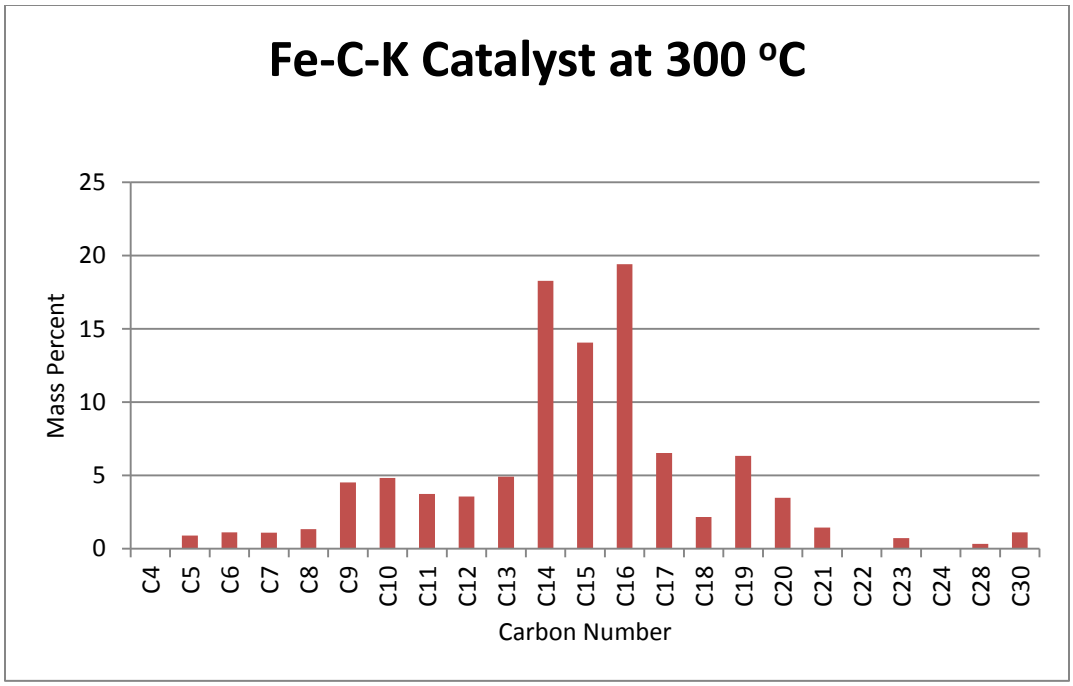

Figure 32: Chain Length Distribution of Iron Carbon Potassium Catalyst at 300 °C

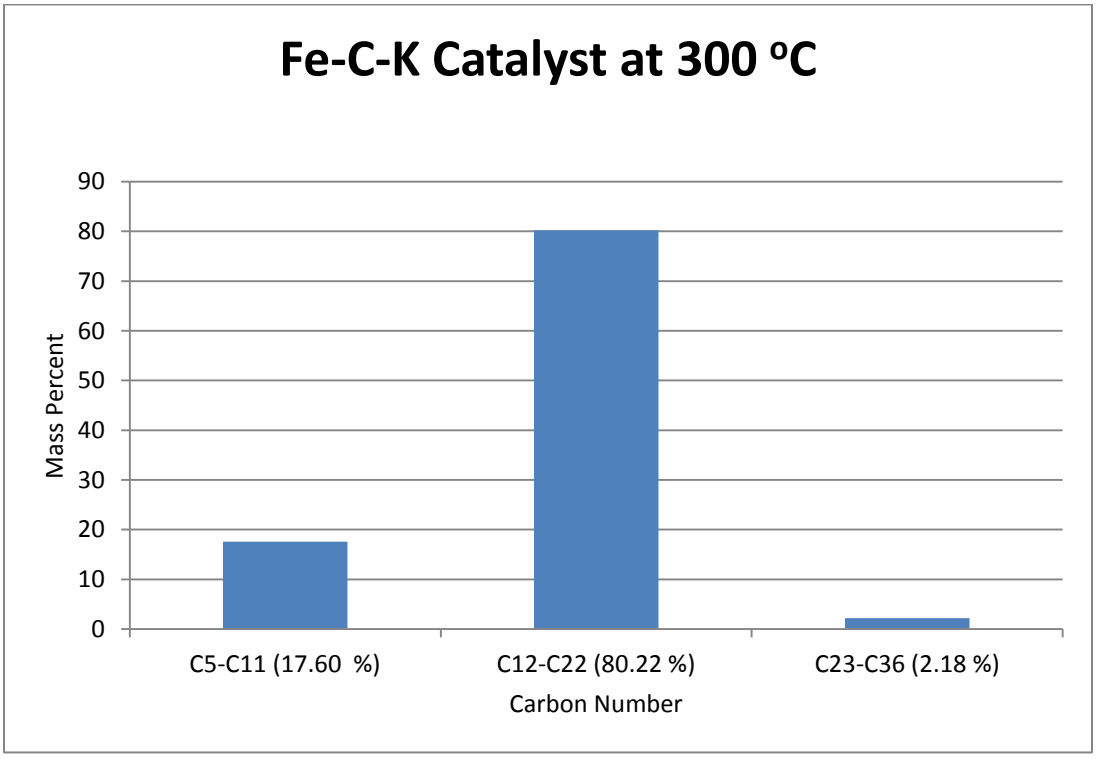

Figure 33: Chain Length Distribution of Iron Carbon Potassium Catalyst at 300 °C

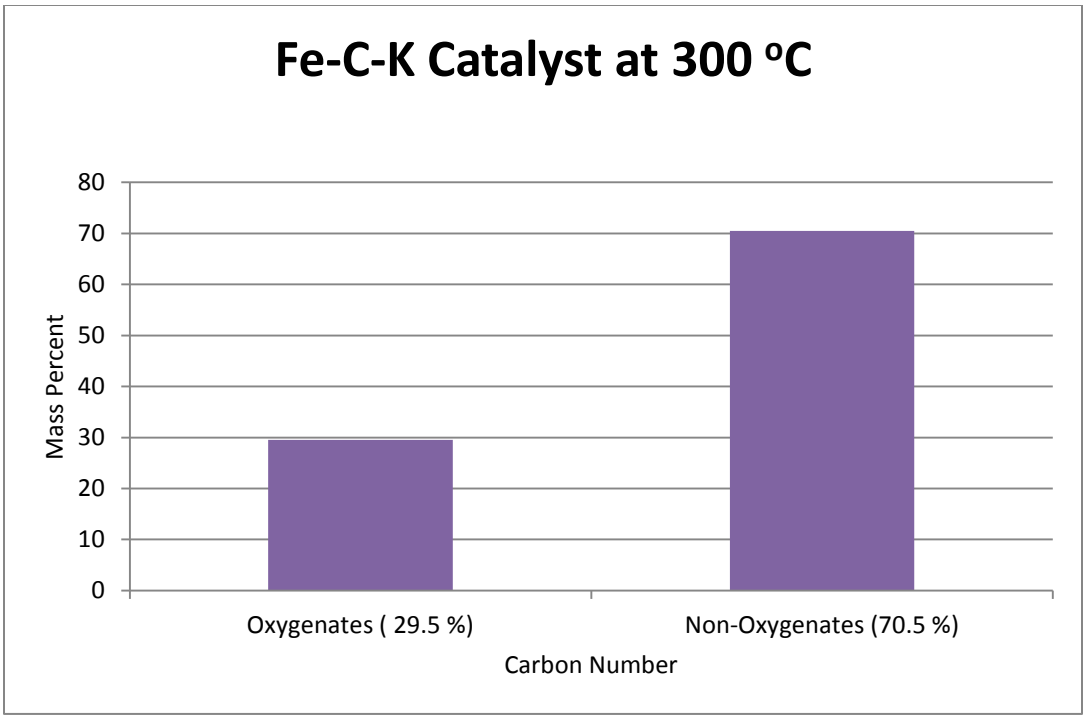

Figure 34: Comparison of Oxygenates and Non-Oxygenates at 300 °C

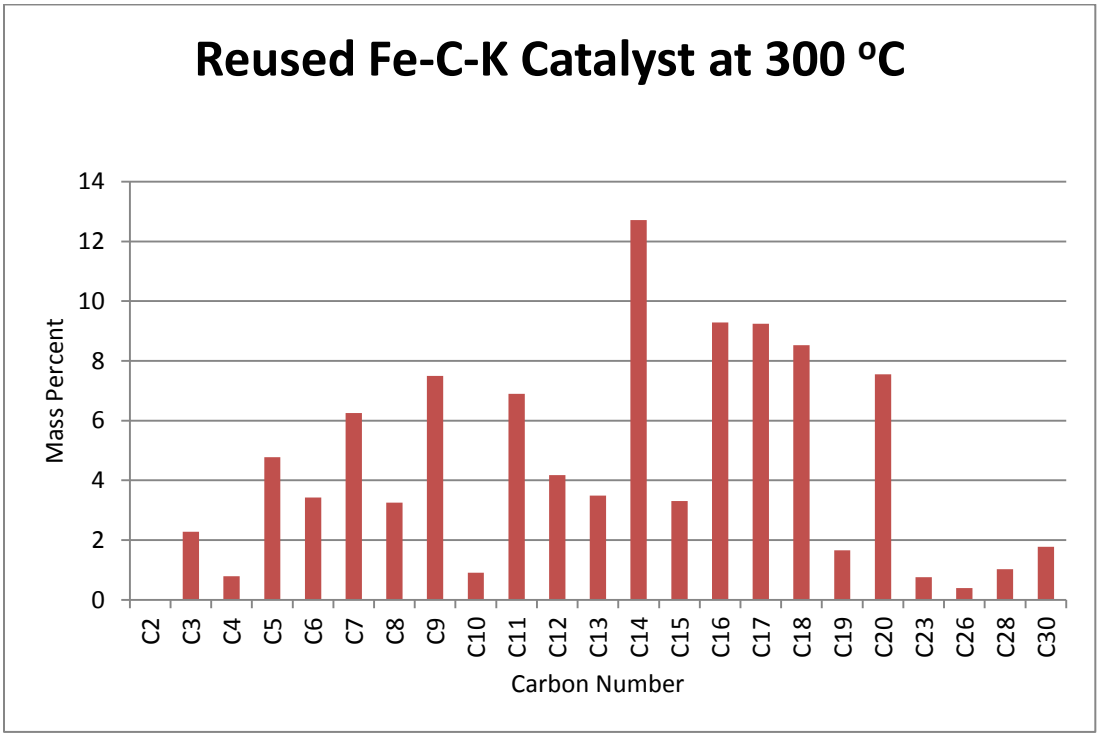

Figure 35: Chain Length Distribution of Reused Iron Carbon Potassium Catalyst at 300 °C

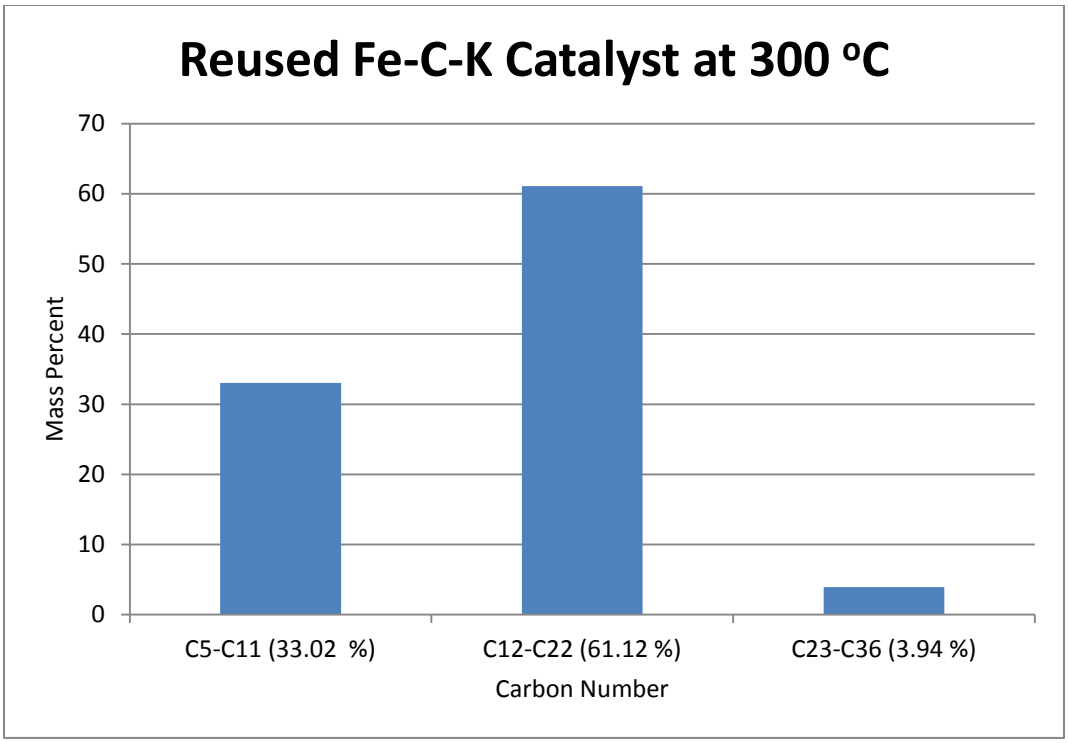

Figure 36: Chain Length Distribution of Iron Carbon Potassium Catalyst at 300 °C

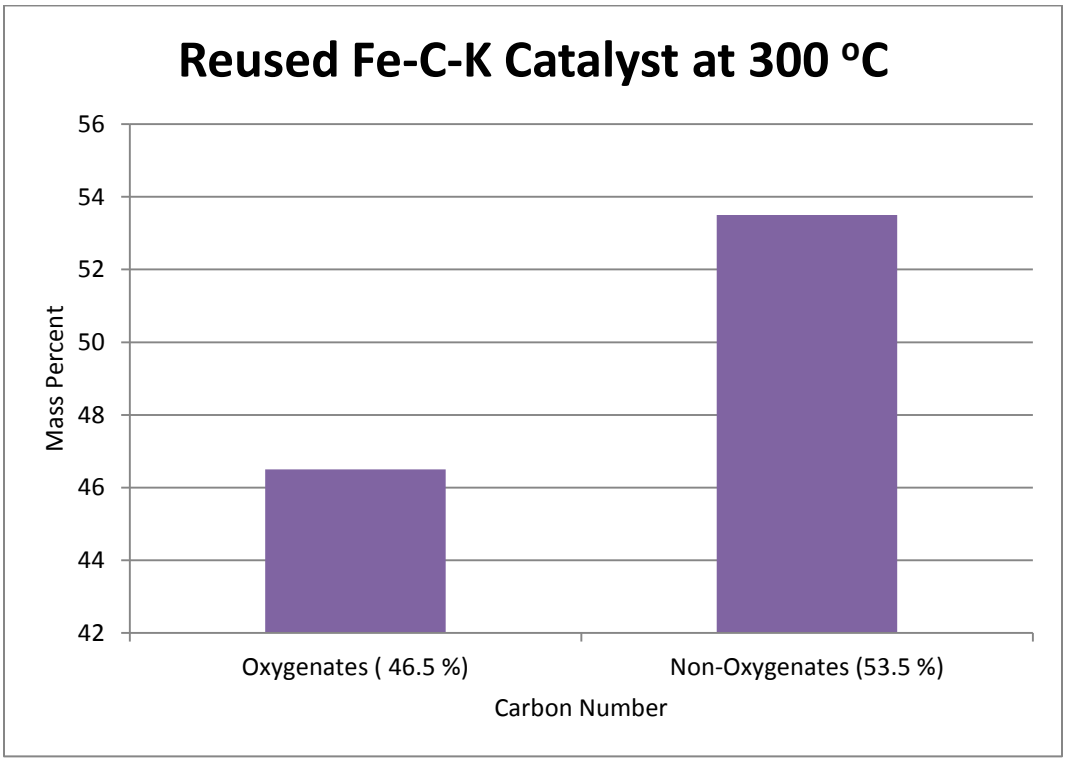

Figure 37: Comparison of Oxygenates and Non-Oxygenates at 300 °C

Table 7: List of compounds in the FT product by using iron carbide catalyst at 350 ^{o}C

Peak #	Name	Formula	Similarity	Mol. Wt	Area %	Height %
1	Octane	C8H18	88	114	0.3	0.48
2	Glycolaldehyde dimer	C5H8O4	66	120	0.19	0.12
3	Valeric acid hydrazide	C5H12N2O	58	116	0.21	0.22
4	Nonane	C9H20	88	128	0.44	0.71
5	4-Phenylsemicarbazide	C7H9N3O	59	151	0.22	0.17
6	N-Isopentyl-N-nitroso-pentylamine	C10H22N2O	58	186	0.19	0.16
7	Amphetamine	C9H13N	61	135	0.24	0.17
8	Phenol	C6H6O	84	94	0.21	0.26
9	Decane	C10H22	92	142	0.68	0.98
10	2-Decene, (E)-	C10H20	66	140	0.25	0.13
11	Decane, 3-methyl-	C11H24	81	156	0.3	0.29
12	2-Propen-1-amine, N,N-bis(1-met	C9H19N	81	141	0.81	0.81
13	Undecane	C11H24	97	156	1.16	1.74
14	4-Piperidinone, 2,2,6,6-tetramethy	C9H17NO	75	155	0.26	0.27
15	nor-Mephedrone	C10H13NO	57	163	0.22	0.14
16	3,3-Dimethylpiperidine	C7H15N	65	113	0.2	0.19
17	Nonane, 4,5-dimethyl-	C11H24	84	156	0.4	0.39
18	Octane, 6-ethyl-2-methyl-	C11H24	76	156	0.4	0.43
19	Decane, 3-methyl-	C11H24	86	156	0.42	0.37
20	Undecane, 3-methyl-	C12H26	91	170	0.51	0.46
21	4-Trifluoroacetoxytridecane	C15H27F3O2	66	296	0.33	0.35
22	Undecane	C11H24	95	156	2.13	2.87
23	3-Dodecene, (Z)-	C12H24	73	168	0.25	0.22
24	1-Hexene, 3,5,5-trimethyl-	C9H18	79	126	0.19	0.18
25	Decane	C10H22	59	142	0.19	0.14
26	nor-Mephedrone	C10H13NO	50	163	0.2	0.2
27	Decanohydrazide	C10H22N2O	60	186	0.23	0.16
28	Heptane, 3-ethyl-2-methyl-	C10H22	79	142	0.35	0.45

29	Octane, 6-ethyl-2-methyl-	C11H24	77	156	0.28	0.49
30	Dodecane, 4-methyl-	C13H28	89	184	0.3	0.39
31	Undecane, 3-methyl-	C12H26	84	170	0.35	0.5
32	Dodecane, 3-methyl-	C13H28	88	184	0.34	0.5
33	Tridecane	C13H28	96	184	2.65	3.73
34	3,3-Dimethylpiperidine	C7H15N	51	113	0.31	0.13
35	Nonane, 4,5-dimethyl-	C11H24	81	156	0.34	0.27
36	Tridecane, 6-methyl-	C14H30	90	198	0.5	0.58
37	2,4-Dimethyldodecane	C14H30	83	198	0.44	0.47
38	Decane, 3,7-dimethyl-	C12H26	86	170	0.35	0.42
39	Pentadecane	C15H32	87	212	0.62	0.59
40	2-Bromo dodecane	C12H25Br	86	248	0.48	0.48
41	3,3'-Iminobispropylamine	C6H17N3	60	131	0.21	0.17
42	3-(Dimethylcarbamoyl)-1-methyl-1H-pyrazole-5-carboxylic acid	C8H11N3O3	49	197	0.26	0.22
43	(S)-(+)-5-Methyl-1-heptanol	C8H18O	58	130	0.29	0.25
44	Dec-5-ene-3,7-diyne, 2,9-dimethy	C12H16	53	160	0.34	0.23
45	Tetradecane	C14H30	98	198	3.13	4.17
46	1-Decanol	C10H22O	77	158	0.32	0.33
47	Dichloroacetic acid, 2-octyl ester	C10H18Cl2O2	75	240	0.31	0.29
48	Valeric acid hydrazide	C5H12N2O	52	116	0.19	0.18
49	Nonane, 3-methyl-5-propyl-	C13H28	85	184	0.48	0.47
50	Tetradecane, 5-methyl-	C15H32	81	212	0.25	0.37
51	Dodecane, 2-methyl-	C13H28	84	184	0.39	0.42
52	2-Bromo dodecane	C12H25Br	90	248	0.45	0.49
53	Decane, 3,8-dimethyl-	C12H26	83	170	0.58	0.53
54	Heptane, 2,3-epoxy-	C7H14O	62	114	0.28	0.2
55	Pentadecane	C15H32	97	212	3.78	4.63
56	1-Dodecanol	C12H26O	70	186	0.27	0.25
57	l-Alanine, N-(1-oxopentyl)-, methyl ester	C9H17NO3	63	187	0.46	0.19
58	Undecane, 3,8-dimethyl-	C13H28	80	184	0.3	0.29
59	Octadecane, 1-chloro-	C18H37Cl	69	288	1.21	0.87
60	Undecane, 3,7-dimethyl-	C13H28	82	184	0.41	0.51
61	Dodecane, 4-methyl-	C13H28	83	184	0.41	0.42

62	Hexadecane	C16H34	87	226	0.38	0.45
63	Pentadecane, 3-methyl-	C16H34	87	226	0.37	0.41
64	Hexadecane	C16H34	96	226	3.97	4.57
65	Decanohydrazide	C10H22N2O	49	186	0.23	0.25
66	Benzeneethanamine, N-methyl-	C9H13N	63	135	0.24	0.18
67	2H-Azepin-2-one, hexahydro-1-m	C7H13NO	63	127	0.3	0.24
68	Nonane, 5-butyl-	C13H28	80	184	0.58	0.49
69	Tetradecane, 5-methyl-	C15H32	76	212	0.23	0.34
70	Nonane, 1-iodo-	C9H19I	81	254	0.35	0.29
71	2-Bromotetradecane	C14H29Br	82	276	0.35	0.33
72	Decane, 3,8-dimethyl-	C12H26	82	170	0.28	0.37
73	Heptadecane	C17H36	97	240	2.79	3.84
74	DL-Alanine, N-DL-alanyl-	C6H12N2O3	58	160	0.22	0.16
75	3-Ethyl-1,3-dimethyldiaziridine (trans)	C5H12N2	55	100	0.2	0.14
76	Hexadecane	C16H34	88	226	0.91	0.58
77	4,4-Dimethyl octane	C10H22	68	142	0.28	0.25
78	Tetradecane, 4-methyl-	C15H32	84	212	0.33	0.27
79	Heptadecane, 2-methyl-	C18H38	80	254	0.36	0.32
80	Pentadecane, 3-methyl-	C16H34	74	226	0.34	0.28
81	Epinephrine	C9H13NO3	59	183	0.34	0.12
82	Heptadecane	C17H36	96	240	2.38	3.15
83	1-Decanol, 2-hexyl-	C16H34O	73	242	0.46	0.39
84	2-Heptanamine, 5-methyl-	C8H19N	75	129	0.49	0.32
85	Undecane, 3,8-dimethyl-	C13H28	69	184	0.24	0.23
86	Dodecane, 2-methyl-	C13H28	73	184	0.23	0.22
87	Octane, 2-methyl-	C9H20	75	128	0.34	0.27
88	dl-Alanyl-l-alanine	C6H12N2O3	51	160	0.39	0.17
89	Heptadecane	C17H36	94	240	1.87	2.38
90	3,6-Dimethylpiperazine-2,5-dione	C6H10N2O2	64	142	0.3	0.22
91	4-Carboxy-2,2,5,5-tetramethyl-3-imidazoline[3-N]-1-oxyl	C8H14N2O3	54	186	0.38	0.18
92	dl-Alanyl-dl-leucine	C9H18N2	65	202	0.42	0.28

		O3				
93	Heptane, 3,4,5-trimethyl-	C10H22	62	142	0.19	0.23
94	Dodecane, 2-methyl-	C13H28	73	184	0.39	0.29
95	Dodecane, 1-iodo-	C12H25I	66	296	0.28	0.21
96	Octadecane, 2-methyl-	C19H40	75	268	0.4	0.28
97	D,L-3-Camphorcarboxylic acid	C11H16O3	43	196	0.28	0.12
98	1-(3-Oxobutyl)-3,3-pentamethylenediaziridine	C10H18N2O	51	182	0.32	0.18
99	Octadecane	C18H38	95	254	1.48	1.73
100	Thiophene, 2-(2-butenyl)-, (E)-	C8H10S	44	138	0.33	0.14
101	1,6-Hexanediamine, N,N'-dimethyl-	C8H20N2	51	144	0.23	0.19
102	dl-Phenylephrine	C9H13NO2	66	167	0.29	0.11
103	Heptadecane	C17H36	63	240	0.4	0.24
104	3-Ethyl-1,3-dimethyldiaziridine (t	C5H12N2	54	100	0.28	0.14
105	Octadecane, 2-methyl-	C19H40	67	268	0.3	0.19
106	trans-2,3-Epoxydecane	C10H20O	55	156	0.34	0.18
107	Piperazine, 2-methyl-	C5H12N2	48	100	0.27	0.17
108	Eicosane	C20H42	94	282	1.26	1.43
109	3-Fluoroamphetamine	C9H12FN	69	153	0.22	0.22
110	Phenol, 4-(2-aminopropoxy)-3,5-dimethyl-	C11H17NO2	44	195	0.24	0.15
111	6H-Pyrazolo[1,2-a][1,2,4,5]tetrazine, hexahydro-2,3-dimethyl-	C7H16N4	49	156	0.22	0.19
112	Dodecane, 2,6,10-trimethyl-	C15H32	56	212	0.2	0.26
113	Tridecane, 1-iodo-	C13H27I	63	310	0.29	0.28
114	Eicosane	C20H42	94	282	0.98	1.16
115	2-Acetamido-2-deoxy-d-mannolactone	C8H11NO6	49	217	0.21	0.12
116	Octadecane, 1-bromo-	C18H37Br	48	332	0.24	0.21
117	Dodecanoic acid, ethenyl ester	C14H26O2	59	226	0.49	0.22
118	2-(Methylamino)ethanol, N,O-diacetyl	C7H13NO3	54	159	0.31	0.25
119	p-Menthane-1,3-diol	C10H20O2	61	172	0.38	0.27

120	Heptadecane	C17H36	87	240	0.81	0.9
121	9H-Purine, 9-(trimethylsilyl)-	C8H12N4Si	42	192	0.19	0.24
122	N.omega.-Nitro-L-arginine	C6H13N5O4	54	219	0.29	0.22
123	Pentadecane, 3-methyl-	C16H34	56	226	0.64	0.38
124	N-(2-Methylbutylidene)-2-butylamine	C9H19N	44	141	0.22	0.31
125	Boron, (2-aminoethanolato-N,O)(1,5-cyclooctanediyl)-, Tt-4)-	C10H20BNO	53	181	0.22	0.27
126	Butyric acid hydrazide	C5H10N2O	53	102	0.19	0.23
127	3-Azabicyclo[3.2.2]nonane	C8H15N	49	125	0.28	0.25
128	dl-Alanyl-dl-leucine	C9H18N2O3	51	202	0.47	0.26
129	[4,4']Bipiperidinyl	C10H20N2	47	168	0.3	0.24
130	R-(-)-Cyclohexylethylamine	C8H17N	63	127	0.49	0.31
131	2-Bromotetradecane	C14H29Br	85	276	0.63	0.63
132	3-Azabicyclo[3.2.2]nonane	C8H15N	49	125	0.26	0.2
133	3-Azabicyclo[3.2.2]nonane	C8H15N	50	125	0.19	0.18
134	(S)-(+)-1-Cyclohexylethylamine	C8H17N	57	127	0.19	0.2
135	Asparagine, N-dl-alanyl-, l-	C7H13N3O4	57	203	0.22	0.29
136	4-Carboxy-2,2,5,5-tetramethyl-3-i	C8H14N2O3	50	186	0.2	0.29
137	2-Ethylbutyric acid, 3,7-dimethyloctyl ester	C16H32O2	49	256	0.38	0.22
138	Epinephrine	C9H13NO3	63	183	0.22	0.26
139	1-Octadecanamine, N-methyl-	C7H15N	59	113	0.24	0.21
140	2-Methylamino-N-phenyl-acetami	C9H12N2O	64	164	0.21	0.27
141	Cyano[(1H-tetrazol-5-yl)hydrazono]acetic acid, ethyl ester	C6H7N7O2	43	209	0.2	0.21
142	Eicosane	C20H42	82	282	0.59	0.59
143	D-erythro-Pentose, 2-deoxy-	C5H10O4	48	134	0.22	0.21
144	3-Fluoroamphetamine	C9H12FN	60	153	0.35	0.21

145	Imidazo[2,1-b][1,3]thiazol-6-ylmethanamine	C6H7N3S	32	153	0.52	0.44
146	Propanoic acid-3-oxo, 3-(2,4-dich	C11H10Cl2O3	47	260	0.35	0.31
147	4-Aminobutyramide, N-methyl-N-[4-(1-pyrrolidinyl)-2-butynyl]-N',N'-bis(trifluoroacetyl)-	C17H21F6N3O3	43	429	0.23	0.2
148	Tricyclo[4.3.1.1(3,8)]undecane-3-	C12H18O2	44	194	0.37	0.17
149	Spiro[4.4]nonane-1,6-dione	C9H12O2	45	152	0.33	0.23
150	Nonyl tetradecyl ether	C23H48O	73	340	0.62	0.54
151	3-Azabicyclo[3.2.2]nonane	C8H15N	57	125	0.2	0.24
152	1,6-Hexanediamine, N,N'-dimethy	C8H20N2	58	144	0.35	0.25
153	Azocine, octahydro-	C7H15N	51	113	0.22	0.29
154	Cyclohexane, 1-methyl-4-(1-methylethyl)-, trans-	C10H20	50	140	0.33	0.31
155	Acetamide, N-methyl-N-[methyl(isopropyl)phosphinatomethyl]-	C8H18NO3P	54	207	0.19	0.29
156	Pyrazole[4,5-b]imidazole, 1-formy	C12H16N4O5	57	296	0.23	0.28
157	Benzoic acid, 2,5-dichloro-3,6-di	C10H10Cl2O4	40	264	0.28	0.19
158	Boron, (2-aminoethanolato-N,O)(	C10H20BNO	48	181	0.24	0.29
159	Octadecane	C18H38	48	254	0.27	0.4
160	(S)-(+)-1-Cyclohexylethylamine	C8H17N	55	127	0.3	0.28
161	s-Triazine, 2,4-bis(ethylamino)-6-methyl-	C8H15N5	49	181	0.28	0.31
162	1,4-Benzenedicarboxylic acid, bis	C24H38O4	92	390	5.7	4.2
163	1H-Imidazole, 2-ethyl-4,5-dihydro	C6H12N2	48	112	1.01	0.86
164	3-Azabicyclo[3.2.2]nonane	C8H15N	58	125	0.26	0.52
165	Benzeneethanamine, 4-fluoro-.alpha.-methyl-	C9H12FN	50	153	0.3	0.35
166	1,2-Ethanediamine, N,N'-bis(2-am	C6H18N4	50	146	0.3	0.35
167	1,3-Cyclohexanediol	C6H12O2	44	116	0.25	0.42
168	1,2-Ethanediamine, N-(2-aminoet	C5H13N3	55	103	0.54	0.45
169	Carbromal	C7H13BrN2O2	49	236	0.69	0.35
170	Hexatriacontane	C36H74	57	506	0.46	0.39
171	5H-Thiazolo[3,2-a]pyrimidin-5-on	C7H6N2OS	46	166	1.13	0.48

172	3-Azabicyclo[3.2.2]nonane	C8H15N	40	125	0.37	0.34
173	Decanohydrazide	C10H22N2O	37	186	0.22	0.34
174	Ethyl isopropyl dimethylphosphor	C7H18NO3P	49	195	0.65	0.43
175	Benzeneethanamine, 4-fluoro-.beta.,3-dihydroxy-N-methyl-	C9H12FNO2	61	185	0.46	0.33
176	1,3-Dioxolane, 4-ethyl-5-octyl-2,2	C15H24F6O2	50	350	0.5	0.38
177	Cyclohexanone, 3-(4-hydroxybutyl)-2-methyl-	C11H20O2	46	184	0.21	0.3
178	Propan-1-one, 2-amino-1-piperidi	C8H16N2O	53	156	0.28	0.27
179	6H-Pyrazolo[1,2-a][1,2,4,5]tetrazine, hexahydro-2,3-dimethyl-	C7H16N4	51	156	0.56	0.48
180	[2,7]Naphthyridine-1,3,6,8-tetraol	C8H6N2O4	44	194	0.31	0.54
181	3-Bornanol, 2-(methylamino)-, en	C11H21NO	44	183	0.46	0.38
182	Sulfoxide, 2-hydroxyhexyl t-butyl (polar)	C10H22O2S	47	206	0.95	0.67
183	dl-Alanyl-l-alanine	C6H12N2O3	58	160	0.67	0.64
184	Asparagine, N-dl-alanyl-, l-	C7H13N3O4	47	203	0.43	0.41
185	3-Deoxyglucose	C6H12O5	44	164	0.33	0.32
186	1H-Purin-2-amine, 6-methoxy-N-methyl-	C7H9N5O	40	179	0.25	0.31
187	3-Bromo-2-ethyltetrahydropyran	C7H13BrO	46	192	0.24	0.32
188	Benzeneethanamine, 4-chloro-.alp	C9H12ClN	57	169	0.25	0.37
189	Cyclopentane-trans-1,3-dicarboxa	C7H12N2O2	46	156	0.2	0.27
190	Pterin-6-carboxylic acid	C7H5N5O3	51	207	0.32	0.27
191	N,N'-Bis(3-aminopropyl)ethylenediamine	C8H22N4	57	174	0.31	0.28
192	2,6R-Diethyl-3,5S-dimethyl-3,4-dihydro-2H-pyran	C11H20O	47	168	0.52	0.4

193	1,4-Bis(trimethylsilyl)benzene	C12H22Si2	49	222	0.28	0.31
194	1H-Purin-2-amine, 6-methoxy-N-	C7H9N5O	47	179	0.43	0.48
195	2,10,10-Trimethyl-6-methylene-1-oxaspiro[4.5]decan-7-one	C13H20O2	42	208	0.32	0.43
196	Cyclohexanemethanol, 5-t-butyl-2-hydroxy-	C11H22O2	44	186	0.63	0.41
197	Tricyclo[4.3.1.1(3,8)]undecan-1-amine	C11H19N	56	165	0.23	0.25
198	Iron, tris(.eta.3-2-propenyl)-	C9H15Fe	47	179	0.38	0.41
199	1,1,3,3-Tetraallyl-1,3-disilacyclobutane	C14H24Si2	48	248	0.44	0.36
200	1H-Pyrimidine-2,4-dione, 1-(2,5-d	C11H8FN5O3	42	277	0.52	0.35

Table 8: List of compounds in the FT product by using Fe-C-K catalyst at 300 ^{o}C

Peak#	Name	Formula	Similarity	Mol. Wt	Area%	Height%
1	1-Pentanol	C5H12O	95	88	0.58	1.1
2	1,3,5-Cycloheptatriene	C7H8	55	92	0.05	0.06
3	alpha.-D-Mannopyranoside, meth	C7H12O5	73	176	0.09	0.1
4	1-Hexanol	C6H14O	91	102	0.11	0.22
5	Hexane, 2,2,3,3-tetramethyl-	C10H22	82	142	0.08	0.12
6	1-Methyldecylamine	C11H25N	66	171	0.14	0.06
7	Valeric acid hydrazide	C5H12N2O	50	116	0.14	0.05
8	Phenol	C6H6O	92	94	0.22	0.34
9	Undecane	C11H24	91	156	0.2	0.3
10	Aziridine, 2-heptyl-3-methyl-	C10H21N	75	155	0.19	0.16
11	Phenol, 2-methyl-	C7H8O	54	108	0.11	0.1
12	Nonane, 4,5-dimethyl-	C11H24	74	156	0.24	0.11
13	3-Ethyl-3-methylheptane	C10H22	72	142	0.05	0.1
14	2-Bromononane	C9H19Br	72	206	0.13	0.14
15	2-Propen-1-amine, N,N-bis(1-methylethyl)-	C9H19N	83	141	1.5	1.41
16	Undecane	C11H24	96	156	0.87	1.14
17	2-Propanone, 2-propenylhydrazon	C6H12N2	66	112	0.13	0.07
18	4-Piperidinone, 2,2,6,6-tetramethy	C9H17NO	81	155	0.16	0.16
19	N-Isopentylidene-2-butylamine	C9H19N	70	141	0.16	0.09
20	Heptanal	C7H14O	53	114	0.18	0.05
21	Octane, 2-methyl-	C9H20	89	128	0.31	0.24
22	2,3-Dimethyldecane	C12H26	84	170	0.3	0.28
23	Undecane, 2-methyl-	C12H26	92	170	0.22	0.29
24	Aziridine, 1,2-diisopropyl-3-meth	C9H19N	69	141	0.23	0.28
25	Decane, 3-methyl-	C11H24	84	156	0.23	0.33
26	1-Undecanol	C11H24O	75	172	0.12	0.13
27	1-Octanol	C8H18O	71	130	0.1	0.12
28	Dodecane	C12H26	97	170	2.37	2.98
29	Cyclopropane, octyl-	C11H22	72	154	0.18	0.12
30	Heptane, 2,3-epoxy-	C7H14O	66	114	0.11	0.12
31	Decane, 2,6,7-trimethyl-	C13H28	83	184	0.21	0.2
32	Octane, 2-methyl-	C9H20	75	128	0.22	0.12

33	Undecane, 2,5-dimethyl-	C13H28	85	184	0.34	0.4
34	Nonane, 5-methyl-	C10H22	80	142	0.41	0.5
35	Dodecane, 4-methyl-	C13H28	92	184	0.35	0.4
36	Benzene, hexyl-	C12H18	70	162	0.18	0.15
37	Dodecane, 2-methyl-6-propyl-	C16H34	90	226	0.38	0.47
38	Dodecane, 3-methyl-	C13H28	92	184	0.58	0.56
39	Undecane, 3,8-dimethyl-	C13H28	86	184	0.24	0.26
40	3,3-Dimethylpiperidine	C7H15N	50	113	0.05	0.06
41	Cetene	C16H32	79	224	0.2	0.16
42	Pentadecane	C15H32	97	212	3.6	4.08
43	1-Undecanol	C11H24O	79	172	0.11	0.16
44	Dichloroacetic acid, nonyl ester	C11H20Cl2O2	78	254	0.19	0.14
45	3-Ethyl-3-methylheptane	C10H22	85	142	0.26	0.28
46	Tridecane, 4-methyl-	C14H30	69	198	0.1	0.13
47	Diglycolic acid, isohexyl 3-methyl	C15H28O5	52	288	0.07	0.06
48	Eicosane, 7-hexyl-	C21H44	72	296	0.45	0.16
49	Octane, 2-methyl-	C9H20	66	128	0.1	0.13
50	Dodecane, 2,6,10-trimethyl-	C15H32	91	212	0.65	0.63
51	Tridecane, 5-methyl-	C14H30	86	198	0.56	0.5
52	Tridecane, 4-methyl-	C14H30	91	198	0.42	0.49
53	Tridecane, 2-methyl-	C14H30	90	198	0.71	0.61
54	Tetradecane, 2-methyl-	C15H32	89	212	0.65	0.59
55	3,5-Dimethylamphetamine	C11H17N	50	163	0.1	0.09
56	1-Decanol	C10H22O	76	158	0.07	0.11
57	cis-5-Methyl-2-isopropyl-2-hexen-1-al	C10H18O	49	154	0.13	0.13
58	Tetradecane	C14H30	98	198	4.32	5.31
59	Cyclododecane	C12H24	80	168	0.19	0.22
60	Dodecane, 2,6,10-trimethyl-	C15H32	76	212	0.21	0.2
61	1-Hexanol, 5-methyl-2-(1-methylethyl)-	C10H22O	75	158	0.42	0.23
62	Hexadecane, 1-chloro-	C16H33Cl	70	260	0.21	0.2
63	1-.beta.-d-Ribofuranosyl-1,2,4-tri	C8H11N3O6	60	245	0.07	0.06
64	Nonane, 1-iodo-	C9H19I	57	254	0.09	0.12
65	7,10-Epoxytricyclo[4.2.1.1(2,5)]decane, 1-trimethylsilyl-	C13H22OSi	64	222	0.08	0.15

66	1,7,7-Trimethyl-2-vinylbicyclo[2.2.1]hept-2-ene	C12H18	50	162	0.08	0.07
67	Decane, 5-propyl-	C13H28	88	184	0.98	0.67
68	Tetradecane, 5-methyl-	C15H32	92	212	0.51	0.57
69	Decane, 2,3,4-trimethyl-	C13H28	84	184	0.82	0.67
70	Hexadecane	C16H34	93	226	0.69	0.65
71	2-Azetidinone, 1-phenyl-	C9H9NO	56	147	0.16	0.16
72	Tetradecane, 3-methyl-	C15H32	91	212	0.7	0.67
73	3,5-Disilaheptane, 3,3,5,5-tetramethyl-	C9H24Si2	59	188	0.16	0.11
74	Dodecane, 4,6-dimethyl-	C14H30	83	198	0.3	0.28
75	Ethanal, 2-(3-ethyl-2,2-dimethylcy	C11H21N3O	52	211	0.31	0.15
76	Pentadecane	C15H32	97	212	4.98	6.23
77	Trichloroacetic acid, tridecyl ester	C15H27Cl3O2	79	344	0.09	0.16
78	1,1,1,3,5,7,7,7-Octamethyl-3,5-bis(trimethylsiloxy)tetrasiloxane	C14H42O5Si6	67	458	0.37	0.24
79	Octadecane, 5-methyl-	C19H40	65	268	0.1	0.12
80	Hexadecane	C16H34	89	226	0.25	0.31
81	Chloroacetylamine, N-[2-n-octyl]-	C10H20ClNO	55	205	0.07	0.11
82	N-Isovaleroylglycine, TMS derivative	C10H21NO3Si	62	231	1.8	1.27
83	Tetradecane, 2-methyl-	C15H32	85	212	0.37	0.44
84	Pentadecane, 4-methyl-	C16H34	90	226	0.58	0.55
85	2-Methylaminomethyl-1,3-dioxolane	C5H11NO2	49	117	0.18	0.27
86	Hexadecane	C16H34	92	226	0.7	0.63
87	Pentadecane, 3-methyl-	C16H34	89	226	0.5	0.61
88	Benzenesulfonic acid, 4-methyl-, dodecyl ester	C19H32O3S	60	340	0.24	0.14
89	Hexadecane	C16H34	96	226	4.86	6.01
90	Methanol, [3-(1,1-dimethylethyl)-5-nitro-1,3-oxazinan-5-yl]-	C9H18N2O4	55	218	0.44	0.35
91	Tetradecanenitrile	C14H27N	58	209	0.13	0.1
92	Decane, 3-methyl-	C11H24	49	156	0.22	0.15
93	1-Hexanol, 5-methyl-2-(1-methylethyl)-	C10H22O	66	158	0.24	0.24
94	Tridecane, 2-methyl-	C14H30	68	198	0.13	0.11

95	Hexadecane	C16H34	88	226	1.01	0.73
96	3,5-Dimethyldodecane	C14H30	80	198	0.32	0.43
97	Tetradecane, 5-methyl-	C15H32	86	212	0.43	0.41
98	Tetradecane, 4-methyl-	C15H32	87	212	0.52	0.38
99	Hexadecane, 2-methyl-	C17H36	85	240	0.44	0.42
100	Tetradecane, 3-methyl-	C15H32	88	212	0.39	0.45
101	Decanohydrazide	C10H22N2O	67	186	0.07	0.08
102	Heptadecane	C17H36	97	240	4.36	4.99
103	Heptadecane, 8-methyl-	C18H38	60	254	0.07	0.11
104	1,4-di-iso-propylnaphthalene	C16H20	70	212	0.2	0.17
105	1,7-di-iso-propylnaphthalene	C16H20	68	212	0.18	0.16
106	Heptadecane	C17H36	90	240	1.12	0.65
107	Tetradecane, 4-ethyl-	C16H34	75	226	0.36	0.32
108	Tetradecane, 4-methyl-	C15H32	87	212	0.2	0.25
109	Heptadecane, 2-methyl-	C18H38	87	254	0.31	0.36
110	1,1,1,5,7,7,7-Heptamethyl-3,3-bis(trimethylsiloxy)tetrasiloxane	C13H40O5Si6	66	444	0.49	0.47
111	Hexadecane, 1-iodo-	C16H33I	81	352	0.7	0.55
112	Propyl undecyl carbonate	C15H30O3	56	258	0.1	0.08
113	Hexadecane	C16H34	95	226	3.14	3.78
114	Hexadecane	C16H34	83	226	0.5	0.33
115	Octane, 2,5,6-trimethyl-	C11H24	65	156	0.23	0.27
116	Tetradecane, 5-methyl-	C15H32	78	212	0.2	0.2
117	Undecane, 3,8-dimethyl-	C13H28	85	184	0.2	0.21
118	Octadecane, 2-methyl-	C19H40	79	268	0.2	0.2
119	Meglumine	C7H17NO5	61	195	0.04	0.06
120	Heptadecane, 2-methyl-	C18H38	82	254	0.21	0.23
121	9-Hexadecenoic acid, methyl ester	C17H32O2	72	268	0.17	0.17
122	Nonadecane	C19H40	95	268	2.36	2.77
123	Hexadecanoic acid, methyl ester	C17H34O2	88	270	0.45	0.38
124	2,6,10-Trimethyltridecane	C16H34	80	226	0.27	0.23
125	Octasiloxane, 1,1,3,3,5,5,7,7,9,9,1	C14H42O	75	518	1.29	0.71

		7Si7				
126	Hexadecane	C16H34	87	226	0.76	0.24
127	2,6,10-Trimethyltridecane	C16H34	83	226	0.45	0.36
128	Dodecane, 2,6,10-trimethyl-	C15H32	77	212	0.27	0.2
129	2,6,10-Trimethyltridecane	C16H34	81	226	0.33	0.26
130	1-(4-Methyl-1,3-thiazol-2-yl)piper	C8H13N3S	57	183	0.32	0.11
131	Methylpent-4-enylamine	C6H13N	67	99	0.08	0.1
132	Nonadecane	C19H40	94	268	1.82	2.01
133	3,3-Dimethylpiperidine	C7H15N	60	113	0.11	0.12
134	2,6,10-Trimethyltridecane	C16H34	82	226	0.41	0.18
135	Tetradecane, 5-methyl-	C15H32	72	212	0.08	0.09
136	Pentadecane, 4-methyl-	C16H34	67	226	0.12	0.08
137	Cyclooctasiloxane, hexadecameth	C16H48O8Si8	77	592	0.76	0.53
138	2-Carbomethoxy-5,5-dimethoxy q	C11H19NO4	55	229	0.13	0.09
139	Bicyclo[3.1.0]hexan-3-one, 4-methyl-1-(1-methylethyl)-	C10H16O	61	152	0.11	0.12
140	9-Octadecenoic acid (Z)-, methyl	C19H36O2	82	296	0.22	0.21
141	Nonadecane	C19H40	95	268	1.31	1.47
142	Hexadecane, 2,6,11,15-tetramethyl-	C20H42	71	282	0.19	0.14
143	Eicosane	C20H42	78	282	0.34	0.14
144	Eicosane	C20H42	81	282	0.26	0.17
145	Hexadecane, 1-iodo-	C16H33I	77	352	0.08	0.1
146	Eicosane	C20H42	94	282	1.05	1.11
147	1,1,1,5,7,7,7-Heptamethyl-3,3-bis(trimethylsiloxy)tetrasiloxane	C13H40O5Si6	72	444	0.5	0.5
148	Piperazine, 2,6-dimethyl-	C6H14N2	51	114	0.07	0.07
149	13-Methylheptacosane	C28H58	78	394	0.33	0.15
150	1-Hexanol, 5-methyl-2-(1-methylethyl)-	C10H22O	48	158	0.09	0.08
151	3,3-Dimethylpiperidine	C7H15N	65	113	0.13	0.12
152	3,3'-Iminobispropylamine	C6H17N3	52	131	0.14	0.08
153	Heneicosane	C21H44	93	296	0.79	0.81
154	Cyclononasiloxane, octadecameth	C18H54O9Si9	70	666	0.42	0.32
155	Heptanamide, N-(1-cyclohexyleth	C16H31N	53	253	0.18	0.08

		O				
156	dl-Alanylglycylglycine	C7H13N3O4	65	203	0.11	0.12
157	Eicosane	C20H42	90	282	0.55	0.55
158	dl-Alanyl-dl-valine	C8H16N2O3	65	188	0.16	0.08
159	Stearic acid hydrazide	C18H38N2O	61	298	0.27	0.08
160	Benzenemethanamine, N-(phenylmethylene)-	C14H13N	77	195	9.43	9.46
161	Cyclooctasiloxane, hexadecamethyl-	C16H48O8Si8	64	592	0.41	0.27
162	Eicosane	C20H42	89	282	0.46	0.45
163	Triphenylphosphine oxide	C18H15OP	91	278	0.88	0.83
164	Ethylamine, 2-(adamantan-1-yl)-1-methyl-	C13H23N	52	193	0.13	0.07
165	Eicosyl isopropyl ether	C23H48O	72	340	0.72	0.63
166	3-Azabicyclo[3.2.2]nonane	C8H15N	50	125	0.21	0.1
167	dl-Alanyl-l-alanine	C6H12N2O3	62	160	0.06	0.06
168	Eicosane	C20H42	82	282	0.23	0.27
169	Heptasiloxane, hexadecamethyl-	C16H48O6Si7	63	532	0.18	0.22
170	[2,7]Naphthyridine-1,3,6,8-tetraol	C8H6N2O4	53	194	0.14	0.12
171	Tetrakis(dimethylamino)vanadium	C8H24N4V	43	227	0.1	0.07
172	N,N'-Bis(3-aminopropyl)ethylenediamine	C8H22N4	49	174	0.07	0.09
173	Meglumine	C7H17NO5	57	195	0.06	0.08
174	2-Isopropyl-5-methyl-1-heptanol	C11H24O	75	172	0.28	0.3
175	Squalene	C30H50	93	410	1.13	1.05
176	1-Octadecanamine, N-methyl-	C19H41N	46	283	0.09	0.1
177	Heptasiloxane, hexadecamethyl-	C16H48O6Si7	62	532	0.52	0.32
178	Purine, 2,6-diamino-9-[.beta.-d-ribofuranosyl]-1-oxide	C10H14N6O5	44	298	0.24	0.19
179	3-Azabicyclo[3.2.2]nonane	C8H15N	50	125	0.17	0.21

180	2-Aminononadecane	C9H12FNO2	59	185	0.12	0.14
181	4H-1,2,4-triazole-3,5-diamine, N3-(4-fluorophenyl)-N5-methyl-	C9H10FN5	46	207	0.26	0.15
182	1,4-Naphthalenediol, decahydro-, (1.alpha.,4.alpha.,4a.alpha.,8a.alpha.)-	C10H18O2	39	170	0.09	0.07
183	Eicosane	C20H42	71	282	0.4	0.26
184	4-Allyloxy-6-methoxy-N,N-dimet	C9H14N4O2	43	210	0.19	0.09
185	1H-imidazole-2-methanol, 1-decyl-	C14H26N2O	40	238	0.13	0.07
186	1H-Pyrazole, 1-methyl-4-methyla	C6H11N3	44	125	0.24	0.17
187	Boron, (2-aminoethanolato-N,O)(	C10H20BNO	44	181	0.15	0.1
188	3-Fluoroamphetamine	C9H12FN	53	153	0.14	0.12
189	dl-Alanyl-l-alanine	C6H12N2O3	56	160	0.08	0.12
190	Heptasiloxane, hexadecamethyl-	C16H48O6Si7	61	532	0.49	0.38
191	3-Methyl-7-(4-methyl-piperazin-1-yl)-3H-thiazolo[4,5-d]pyrimidine-2-thione	C11H15N5S2	40	281	0.16	0.09
192	Eicosane, 10-methyl-	C21H44	56	296	0.21	0.16
193	4-Quinolinamine, decahydro-1-methyl-	C10H20N2	49	168	0.21	0.15
194	1,3,5-Trimethyl-3,7-diazabicyclo[3.3.1]nonan-9-ol	C10H20N2O	49	184	0.11	0.15
195	8-[N-Aziridylethylamino]-2,6-dimethyloctene-2	C14H28N2	52	224	0.07	0.1
196	l-Alanine, N-(3-cyclopentylpropionyl)-, methyl ester	C12H21NO3	52	227	0.23	0.08
197	Methyl[2-(1-methylpyrazol-4-yl)e	C7H13N3	52	139	0.07	0.09
198	6-Methyl-6-[(trimethylsilyl)oxy]h	C11H27NOSi	46	217	0.04	0.08
199	Benzeneethanamine, 2-fluoro-.beta.,5-dihydroxy-N-methyl-	C9H12FNO2	54	185	0.16	0.11
200	4-MTA	C10H15NS	46	181	0.05	0.07

Table 9: List of compounds in the FT product with reuse of Fe-C-K catalyst at 300 °C

Peak #	Name	Formula	Similarity	Mol.Wt	Area %	Height %
1	4-Phenylsemicarbazide	C7H9N3O	57	151	0.17	0.07
2	4-Methyl-3,4-dihydro-[1,2,3]triazolo[4,5-d]pyrimidine-5,7-dione	C5H5N5O2	51	167	0.17	0.16
3	4-Methyl-3,4-dihydro-[1,2,3]triazolo[4,5-d]pyrimidine-5,7-dione	C5H5N5O2	49	167	0.19	0.15
4	Ethanamine, 2-(2,6-dimethylphenoxy)-N-methyl-	C11H17NO	58	179	0.21	0.11
5	3,4-Furandiol, tetrahydro-, cis-	C4H8O3	54	104	0.18	0.08
6	2-Propen-1-amine, N,N-bis(1-methylethyl)-	C9H19N	79	141	1.08	0.97
7	2-Pentanamine	C5H13N	63	87	0.17	0.19
8	L-Alanine, N-(N-acetylglycyl)-, butyl ester	C11H20N2O4	62	244	0.17	0.17
9	Valeric acid hydrazide	C5H12N2O	59	116	0.23	0.16
10	Nonane, 2,3-dimethyl-	C11H24	81	156	0.25	0.31
11	3-Methyl -6-(3-methylthiophen-2-	C9H8N4S2	49	236	0.19	0.15
12	n-decyl methyl imine	C11H23N	66	169	0.22	0.23
13	Dodecane	C12H26	87	170	0.3	0.5
14	1-Undecene, 4-methyl-	C12H24	72	168	0.24	0.15
15	Decane, 1-iodo-	C10H21I	64	268	0.19	0.18
16	Octane, 2,3,3-trimethyl-	C11H24	70	156	0.25	0.23
17	Pentadecane, 6-methyl-	C16H34	69	226	0.2	0.2
18	Dodecane, 2,6,10-trimethyl-	C15H32	80	212	0.26	0.37
19	Phosphonoacetic Acid, 3TMS derivative	C11H29O5PSi3	59	356	2.31	0.8
20	Cyclohexasiloxane, dodecamethyl	C12H36O6Si6	53	444	1.62	0.74
21	Cyclohexasiloxane, dodecamethyl	C12H36O6Si6	69	444	0.59	0.63
22	Tridecane	C13H28	93	184	0.77	1.04
23	1-Sec-butyldiaziridine	C5H12N2	67	100	0.22	0.15
24	Nonane, 5-(2-methylpropyl)-	C13H28	86	184	0.18	0.23
25	Propanoic acid, 3-hydroxy-, hydra	C3H8N2O2	58	104	0.16	0.11
26	Nonane, 3,7-dimethyl-	C11H24	77	156	0.19	0.24
27	Piperazine, 2-methyl-	C5H12N2	63	100	0.2	0.19
28	Undecane, 3,8-dimethyl-	C13H28	71	184	0.17	0.2
29	Tetradecane	C14H30	94	198	0.96	1.33
30	Octane, 6-ethyl-2-methyl-	C11H24	66	156	0.24	0.25
31	Piperazine, 2-methyl-	C5H12N2	72	100	0.15	0.17
32	2-(Methylamino)ethanol, tert-buty	C9H23NOSi	60	189	0.15	0.23
33	Dodecane, 4-methyl-	C13H28	68	184	0.15	0.27
34	Cycloheptasiloxane, tetradecamet	C14H42O7Si7	90	518	2.46	2.01
35	5,5-Dibutylnonane	C17H36	77	240	0.21	0.24
36	Azetidin-2-one 3,3-dimethyl-4-(1-	C7H14N2O	62	142	0.17	0.23
37	Hexadecane, 1-iodo-	C16H33I	84	352	0.32	0.38
38	1,4-Diaza-9-oxaspiro[5.5]undecan	C11H22N2O	47	198	0.28	0.2

39	Pentadecane	C15H32	95	212	1.41	1.87
40	Methylpent-4-enylamine	C6H13N	63	99	0.39	0.22
41	2-Propenamide	C3H5NO	50	71	0.23	0.19
42	4-Methyl-3,4-dihydro-[1,2,3]triazolo[4,5-d]pyrimidine-5,7-dione	C5H5N5O2	55	167	0.34	0.18
43	1-(5-Bicyclo[2.2.1]heptyl)ethylamine	C9H17N	59	139	0.24	0.15
44	Dodecane, 2,6,10-trimethyl-	C15H32	83	212	0.38	0.47
45	2-Guanidino-5-methylbenzimidazole	C9H11N5	65	189	1.2	1.12
46	Sulfurous acid, dodecyl hexyl este	C18H38O3S	74	334	0.22	0.25
47	Sulfurous acid, pentyl undecyl ester	C16H34O3S	76	306	0.38	0.32
48	Undecane, 3,8-dimethyl-	C13H28	77	184	0.4	0.33
49	Eicosane	C20H42	84	282	0.41	0.34
50	dl-Alanyl-dl-leucine	C9H18N2O3	62	202	0.27	0.17
51	dl-Alanyl-dl-leucine	C9H18N2O3	71	202	0.17	0.16
52	(S)-(+)-1-Cyclohexylethylamine	C8H17N	67	127	0.26	0.18
53	Hexadecane	C16H34	96	226	3.04	4.23
54	4-(Phenylthio)pyridine 1-oxide	C11H9NOS	52	203	0.38	0.43
55	1,4-Bis(3-aminopropyl)piperazine	C10H24N4	52	200	0.23	0.18
56	Ethanedial, bis(dimethylhydrazon	C6H14N4	63	142	0.21	0.18
57	Cyclooctasiloxane, hexadecameth	C16H48O8Si8	82	592	0.66	0.75
58	2,6,10-Trimethyltridecane	C16H34	79	226	0.51	0.52
59	2-Propyl-1-pentanol	C8H18O	66	130	0.16	0.3
60	Tetradecane, 5-methyl-	C15H32	78	212	0.25	0.36
61	Nonane, 5-methyl-5-propyl-	C13H28	79	184	0.28	0.33
62	Hexadecane	C16H34	81	226	0.25	0.44
63	Heptadecane, 2-methyl-	C18H38	80	254	0.54	0.55
64	Hydrazinecarbothioamide, N-ethyl-	C3H9N3S	44	119	0.27	0.19
65	Heptadecane	C17H36	96	240	4.31	6.32
66	Eicosane	C20H42	85	282	1.59	1.05
67	Octadecane, 5-methyl-	C19H40	81	268	0.3	0.38
68	Pentadecane, 4-methyl-	C16H34	82	226	0.36	0.45
69	Dodecane, 2-methyl-	C13H28	83	184	0.57	0.61
70	Heptadecane, 3-methyl-	C18H38	79	254	0.41	0.5
71	Cyclononasiloxane, octadecameth	C18H54O9Si9	61	666	0.41	0.35
72	1,3-Cyclohexanediol	C6H12O2	54	116	0.16	0.2
73	cis-5-Methyl-2-isopropyl-2-hexen	C10H18O	49	154	0.18	0.17
74	Thiophene, 2-propyl-	C7H10S	44	126	0.15	0.22
75	Heptadecane	C17H36	95	240	4.04	5.43
76	2-(Methylamino)ethanol, N,O-dia	C7H13NO3	68	159	0.33	0.3
77	dl-Alanylglycylglycine	C7H13N3O4	60	203	0.25	0.28
78	(+)-2-Aminoheptane	C7H17N	56	115	0.21	0.22
79	Glycine, N-(N-L-alanylglycyl)-	C7H13N3O4	62	203	0.22	0.18
80	Azetidin-2-one 3,3-dimethyl-4-(1-	C7H14N2O	63	142	0.23	0.14

81	Hexadecane	C16H34	81	226	0.62	0.49
82	Piperazine, 2-methyl-	C5H12N2	67	100	0.17	0.3
83	Tetradecane, 5-methyl-	C15H32	74	212	0.17	0.25
84	Dodecane, 4-methyl-	C13H28	77	184	0.25	0.27
85	Octadecane	C18H38	76	254	0.32	0.29
86	5,5,7,7-Tetraethylundecane	C19H40	82	268	0.27	0.35
87	Octadecane	C18H38	95	254	2.77	3.83
88	dl-Alanyl-dl-.alpha.-amino-n-buty	C7H14N2O3	66	174	0.29	0.32
89	1-(5-Bicyclo[2.2.1]heptyl)ethylam	C9H17N	65	139	0.26	0.16
90	1,2-Ethanediamine, N-(2-aminoet	C4H13N3	60	103	0.21	0.26
91	Piperazine, 2-methyl-	C5H12N2	65	100	0.27	0.34
92	Uramil-N,N-diacetic acid	C8H9N3O7	46	259	0.17	0.33
93	Valeric acid hydrazide	C5H12N2O	54	116	0.19	0.24
94	Octane, 2-methyl-	C9H20	64	128	0.18	0.26
95	Eicosane	C20H42	85	282	0.54	0.43
96	Heptadecane, 2-methyl-	C18H38	74	254	0.33	0.3
97	2-Methylpentacosane	C26H54	76	366	0.39	0.37
98	2-Butene ozonide	C4H8O3	49	104	0.4	0.31
99	Meglumine	C7H17NO5	65	195	0.19	0.2
100	N-dl-Alanylglycine	C5H10N2O3	65	146	0.19	0.23
101	3-Deoxyglucose	C6H12O5	51	164	0.31	0.25
102	Eicosane	C20H42	96	282	2.43	2.76
103	L-Alanine, N-(N-acetylglycyl)-, butyl ester	C11H20N2O4	62	244	0.26	0.24
104	2-Methylamino-N-phenyl-acetami	C9H12N2O	74	164	0.17	0.24
105	1-(5-Bicyclo[2.2.1]heptyl)ethylam	C9H17N	61	139	0.43	0.21
106	Dodecane, 2,6,10-trimethyl-	C15H32	50	212	0.21	0.28
107	Acetamide, 2-cyano-N-[(ethylamino)carbonyl]-2-(methoxyimino)-	C7H10N4O3	47	198	0.17	0.22
108	Methylpent-4-enylamine	C6H13N	62	99	0.16	0.24
109	Azetidin-2-one 3,3-dimethyl-4-(1-	C7H14N2O	66	142	0.17	0.2
110	3,6-Dimethylpiperazine-2,5-dione	C6H10N2O2	70	142	0.29	0.25
111	Norephedrine, (.+/-.)-	C9H13NO	56	151	0.22	0.2
112	Piperazine, 2-methyl-	C5H12N2	60	100	0.2	0.3
113	(7R,8RS)-7-hydroxymethyl-8-ethoxy-trans-bicyclo[4.3.0]-3-nonene	C12H20O2	39	196	0.4	0.12
114	Eicosane	C20H42	94	282	1.47	1.91
115	Ethyl isopropyl dimethylphosphoramidate	C7H18NO3P	60	195	0.16	0.16
116	N-[2,2,2-Trifluoro-1-(isopropylamino)-1-(trifluoromethyl)ethyl]isovaleramide	C11H18F6N2O	54	308	0.28	0.24
117	Azetidin-2-one 3,3-dimethyl-4-(1-aminoethyl)-	C7H14N2O	66	142	0.36	0.31
118	6,8-Doixatetradecane	C12H26O2	53	202	0.29	0.2
119	1,3,5-Triazine, hexahydro-1,3,5-trimethyl-	C6H15N3	44	129	0.27	0.18
120	2H-Azepin-2-one, hexahydro-1-m	C7H13NO	66	127	0.21	0.2
121	5,5-Diethyltridecane	C17H36	66	240	0.44	0.28

122	1-Octanamine, N-methyl-	C9H21N	62	143	0.32	0.24
123	Azocine, octahydro-	C7H15N	51	113	0.31	0.18
124	Eicosane	C20H42	91	282	1.67	1.42
125	Benzeneethanamine, 2,5-dimethox	C11H17NO2	53	195	0.23	0.18
126	(S)-(+)-1-Cyclohexylethylamine	C8H17N	71	127	0.25	0.25
127	10-Methylnonadecane	C20H42	60	282	0.4	0.25
128	Benzeneethanamine, 2,5-difluoro-	C9H11F2NO3	61	219	0.34	0.24
129	dl-Alanyl-l-alanine	C6H12N2O3	70	160	0.25	0.22
130	Glycine, N-(N-L-alanylglycyl)-	C7H13N3O4	75	203	0.25	0.2
131	Tetrahydro-4H-pyran-4-ol	C5H10O2	57	102	0.2	0.17
132	Docosane	C22H46	88	310	1.03	0.99
133	(S)-(+)-1-Cyclohexylethylamine	C8H17N	72	127	0.19	0.2
134	Benzenemethanamine, N-hydroxy	C14H15NO	76	213	9.3	7.76
135	Semioxamazide	C2H5N3O2	58	103	0.15	0.27
136	dl-Alanyl-dl-.alpha.-amino-n-buty	C7H14N2O3	60	174	0.28	0.33
137	dl-Alanyl-dl-leucine	C9H18N2O3	62	202	0.36	0.26
138	(S)-(+)-1-Cyclohexylethylamine	C8H17N	65	127	0.43	0.15
139	Cyclohexanol, 2-(methylaminome	C8H17NO	59	143	0.19	0.3
140	Heptasiloxane, hexadecamethyl-	C16H48O6Si7	51	532	0.41	0.43
141	Boron, (2-aminoethanolato-N,O)(	C10H20BNO	51	181	0.31	0.26
142	propanamide, N-(2-hydroxyethyl)-	C8H17NO2	50	159	0.2	0.22
143	Tetracosane	C24H50	85	338	0.76	0.71
144	(S)?-??N-?Desmethylcitalopram	C19H19FN2O	53	310	0.16	0.26
145	Butylsemithiocarbazide	C5H13N3S	54	147	0.27	0.39
146	Triphenylphosphine oxide	C18H15OP	86	278	1.93	1.79
147	4-Oxononanal	C9H16O2	43	156	0.39	0.25
148	Glutaraldehyde	C5H8O2	58	100	0.68	0.32
149	(S)-(+)-1-Cyclohexylethylamine	C8H17N	61	127	0.16	0.29
150	Amphetamine	C9H13N	58	135	0.39	0.46
151	1-Octanamine, N-methyl-	C9H21N	56	143	0.19	0.18
152	dl-Alanyl-l-alanine	C6H12N2O3	63	160	0.41	0.26
153	(S)-(+)-1-Cyclohexylethylamine	C8H17N	65	127	0.32	0.23
154	Ethyl 2-acetamido-3,3,3-trifluoro-2-(2-fluoroanilino)propionate	C13H14F4N2O3	47	322	0.24	0.2
155	Eicosane	C20H42	73	282	0.51	0.56
156	Acetamide, 2-cyano-N-[(ethylamin	C7H10N4O3	47	198	0.18	0.31
157	Heptasiloxane, hexadecamethyl-	C16H48O6Si7	61	532	0.79	0.61
158	3,3-Dimethylpiperidine	C7H15N	66	113	0.44	0.48
159	Cyclononasiloxane, octadecamethyl-	C18H54O9Si9	61	666	0.43	0.38
160	1,3-Pentanediamine	C5H14N2	50	102	0.2	0.16
161	1-Octadecanamine, N-methyl-	C19H41N	49	283	0.23	0.18
162	Dodecane, 2,6,11-trimethyl-	C15H32	71	212	0.63	0.51
163	Glucopyranuronamide, 1-(4-amino	C16H25N7O8	55	443	0.28	0.24

164	Epinephrine	C9H13NO3	52	183	0.2	0.26
165	1,2-Propanediamine, N,N'-dimeth	C11H18N2	46	178	0.68	0.23
166	N-dl-Alanylglycine	C5H10N2O3	63	146	0.19	0.23
167	1-(2-Cyano-2-ethyl-butyryl)-3-iso	C11H19N3O2	51	225	0.18	0.2
168	Heptasiloxane, hexadecamethyl-	C16H48O6Si7	57	532	0.46	0.42
169	7-Methyl-octadecane	C19H40	66	268	0.53	0.41
170	dl-Alanyl-l-alanine	C6H12N2O3	57	160	0.25	0.18
171	Hydrastininic acid	C11H9NO6	57	251	0.16	0.21
172	9,9-Dimethoxybicyclo[3.3.1]nona-2,4-dione	C11H16O4	50	212	0.25	0.23
173	1,3-Propanediamine, N-(2-aminoethyl)-	C5H15N3	56	117	0.16	0.24
174	Squalene	C30H50	86	410	1.77	1.71
175	Diethyl 4,4'-methylenediallophana	C9H16N4O6	63	276	0.24	0.32
176	Piperazine, 2-methyl-	C5H12N2	61	100	0.39	0.41
177	Hydrastininic acid	C11H9NO6	61	251	0.17	0.27
178	Undec-10-ynoic acid, heptyl ester	C18H32O2	50	280	0.17	0.19
179	Meglumine	C7H17NO5	44	195	0.34	0.41
180	1,1,1,5,7,7,7-Heptamethyl-3,3-bis(trimethylsiloxy)tetrasiloxane	C13H40O5Si6	49	444	0.48	0.53
181	dl-Alanyl-dl-.alpha.-amino-n-butyric acid	C7H14N2O3	55	174	0.22	0.31
182	p-Hydroxynorephedrine	C9H13NO2	61	167	0.26	0.18
183	2-Amino-4-dimethylaminomethylenepentanedinitrile	C8H12N4	52	164	0.26	0.27
184	Silane, dimethylisobutoxydocosyloxy-	C28H60O2Si	54	456	1.02	0.71
185	Cyclotetrasiloxane, octamethyl-	C8H24O4Si4	41	296	0.36	0.33
186	p-Butyrophenetidide	C12H17NO2	43	207	0.38	0.39
187	1,3-Propanediamine, N,N',2,2-tetr	C7H18N2	52	130	0.38	0.37
189	Ethylamine, 1-methyl-2-(5-methyl	C7H13N3	50	139	0.21	0.23
190	Heptasiloxane, hexadecamethyl-	C16H48O6Si7	60	532	0.53	0.61
191	3-Ethoxy-1,4,4a,5,6,7,8,8a-octahydroisoquinoline	C11H19NO	41	181	0.19	0.18
192	Vinyl decanoate	C12H22O2	50	198	0.33	0.23
193	1,2,4-Triazol-3-amine, 5-(1,3,5-trimethyl-4-pyrazolyl)amino-	C8H13N7	51	207	0.3	0.37
194	silane, [2-(ethenylsulfonyl)ethoxy	C7H16O3SSi	46	208	0.17	0.28
195	1-(9-Allyl-9-azabicyclo[3.3.1]non-3-yl)-3-m-tolylurea	C19H27N3O	41	313	0.17	0.16
196	3,3'-Iminobispropylamine	C6H17N3	43	131	0.2	0.25
197	l-Alanine, N-(cyclohexylcarbonyl)-, heptyl ester	C17H31NO3	44	297	0.24	0.29
198	2-Oxo-3-methyl-cis-perhydro-1,3-	C9H15NO2	57	169	0.25	0.33
199	6H-Pyrazolo[1,2-a][1,2,4,5]tetrazine, hexahydro-2,3-dimethyl-	C7H16N4	45	156	0.19	0.08
200	Heptasiloxane, hexadecamethyl-	C16H48O6Si7	36	532	0.48	0.42

5.3 Summary

The characterization results as well as FTS product analysis is given in this chapter. Developed an inexpensive carbon supported Fe based catalyst without promoter for FTS which shows catalytic activity and selectivity toward the desire hydrocarbons. In carbon iron supported catalyst (without promoter) the amount of oxygen are the confirmation of the oxide formation and these oxygen group are removed during the reduction process. The total percentage of different hydrocarbons (C_5-C_{11}) in the mixture is 45 % and (C_{12}-C_{22}) is 47 %. Total amount of Oxygenates are 36.5 % and Non-Oxygenates are 63.5 %. In second experiment the Iron Carbide with Potassium promoter catalyst is used at 300 ^{o}C with 20 bars. The total percentage of different hydrocarbons (C_5-C_{11}) in the mixture is 17.60 % and (C_{12}-C_{22}) is 80.22 %. Total amount of Oxygenates are 29.5 % and Non-Oxygenates are 70.5 %. In third experiment the Iron Carbide with Potassium promoter are reused on 300 ^{o}C with 20 bars. The total percentage of different hydrocarbons (C_5-C_{11}) in the mixture is 33.02 % and (C_{12}-C_{22}) is 61.12 %. Total amount of Oxygenates are 46.5 % and Non-Oxygenates are 53.5 %.

5.4 Conclusion and Recommendations

Activated carbon with a highly porous structure or surface area is mainly used as an industrial adsorbent (dyes) and also wastewater treatment purposes. Phosphoric acid (H_3PO_4) is generally used as activator agent that increases the number of defects present in hemicelluloses, which also increase the surface area. Phosphoric acid used as a catalyst in order to promote the bond cleavage reaction and that enhanced the cross linking during the reaction through the condensation process. Highly porous activated carbon is used for the gas adsorption in order to make an environment friendly. XRD result shows that, peak at angle 23^o which revealed the presence of crystalline carbonaceous structure. Prepared activated carbon is used for the preparation of carbon supported iron based catalyst by wet impregnation method. Then prepared catalyst is tested into Fischer Tropsch synthesis reactor to find out the production of gasoline. The carbon supported iron catalyst with potassium promoter increase the catalyst activity and selectivity toward the desire hydrocarbons. In carbon iron supported catalyst (without promoter) the amount of oxygen are the confirmation of the oxide formation and these oxygen group are removed during the reduction process. The total percentage of different hydrocarbons (C_5-C_{11}) in the mixture is 45 % and (C_{12}-C_{22}) is 47 %. Total amount of Oxygenates are 36.5 % and Non-Oxygenates are 63.5 %. In second experiment the Iron Carbide with Potassium promoter catalyst is used at 300 ^oC with 20 bars. The total percentage of different hydrocarbons (C_5-C_{11}) in the mixture is 17.60 % and (C_{12}-C_{22}) is 80.22 %. Total amount of Oxygenates are 29.5 % and Non-Oxygenates are 70.5 %. In third experiment the Iron Carbide with Potassium promoter are reused on 300 ^oC with 20 bars. The total percentage of different hydrocarbons (C_5-C_{11}) in the mixture is 33.02 % and (C_{12}-C_{22}) is 61.12 %. Total amount of Oxygenates are 46.5 % and Non-Oxygenates are 53.5 %. Different types of promoter can be used in FTS for increasing the C5+ selectivity and to minimize the Oxygenates.

Acknowledgements

Most of all I am thankful to Almighty Allah who gave me the will and determination to accomplish task in this manner.

I owe my sincere gratitude to Dr. Zuhair S. Khan (Principal/Dean USPCAS-E), Dr.Naseem Iqbal (HoD, ESE) and USPCAS-E Administration for their inspiration, guidance and support.

Writing this thesis and accomplishing this task so appreciably is only due to the unrelenting support and critical comments of my supervisor Dr. Naseem Iqbal and other GEC members for guidance and profitable knowledge whenever i needed it.

I would also like to offer my gratitude to Mr. Saeed Iqbal (In-charge FT apparatus) , Mr. Amin Durrani (FT Lab. Engineer), Mr. Haider Ejaz (Fossil Fuel Lab.) , Mr. Naveed Ahmed (Synthesis Lab.), Mr. Qamaruddin (Lab. Technician), Mr. Abdul Kashif Janjua (Smart grid Lab.) and Miss Anam Qadir (Biofuel Lab.) for their sincere support and technical assistance.

Sincerely,

Saleem Munir

Annex I

2nd International conference on "Impact of Nano Science on Energy Technologies (NanoSET-2017)" 25-27 Oct. 2017 CIIT Lahore. (Presented)

Synthesis and characterization of activated carbon from *Pongamia pinnata* (Sukh Chen) tree by H_3PO_4 chemical activation

[a]Saleem Munir; [a*]Naseem Iqbal; [b]Jamil Ahmad

[a]US-Pakistan Centre for Advanced Studies in Energy, USPCAS-E, National University of Sciences and Technology (NUST), Islamabad, Pakistan

[b] University of Management and Technology (UMT), Lahore, Pakistan

---

Abstract

Pongamia pinnata (Sukh Chen) is an agriculture biomass used to produce inexpensive activated carbon. Activated carbon, with a highly porous structure, is mainly used as an industrial adsorbent which makes it practically suitable for support material in development of catalyst for Fischer Tropsch process. It is further used in wastewater treatment process. It mainly removes chlorine, sediments, volatile organics, taste and odor from water. Activated carbon is impregnated by chemical activating agent. Phosphoric acid (H_3PO_4) is used as activating agent who increases the number of defects present in the hemicelluloses and act as a catalyst to promote the bond cleavage reaction. Phosphoric acid thermally degrades the hemicelluloses structure present in *Pongamia pinnata* (Sukh Chen) tree and creates porous formation. XRD (X-ray Diffraction) result showed the peak at angle 23^o, which revealed the existence of crystalline carbonaceous structure. EDX (Energy Dispersive X-ray Spectroscopy) analysis showed that more than 80 % of Activated carbon is present with little amount of Oxygen and Phosphorus. SEM (Scanning Electron Microscope) result showed that amorphous units formed after the activation with Phosphoric acid. TGA (Thermal gravimetric analysis) showed that the prepared activated carbon started degrading at 60 ^oC and fully degraded at above 600 ^oC. The main

purpose of this study is to find out the change in *Pongamia pinnata* (Sukh Chen) through activation with Phosphoric acid (H_3PO_4).

Keywords: Activated Carbon; *Pongamia Pinnata* (Sukh Chen); Chemical Activation; Phosphoric Acid (H_3PO_4).

Introduction

Activated carbon is prepared from such material which is rich in Carbon through carbonization and activation. Activated carbon with a high surface area are used for wastewater treatment, support for catalyst and gas adsorption. A porous structure and its adsorption properties can be obtained in carbonaceous materials via chemical or physical1 activation. Activated carbon produces from *Pongamia Pinnata* (Sukh Chen) shows micro-pores structures. Potassium hydroxide (KOH), Phosphoric acid (H_3PO_4), zinc chloride ($ZnCl_2$) and potassium carbonate (K_2CO_3) are generally used as activating agent. By using Phosphoric acid (H_3PO_4) as an activating agent then pore structure are formed in activated carbon. This study shows that the Activated carbon content is increased up to 80 % due to destroying the cellulose crystalline structure. Phosphoric acid (H_3PO_4) is used as activated agent that changed the thermal degradation of *Pongamia Pinnata* (Sukh Chen) tree leaves. Phosphoric acid (H_3PO_4) has increased the number of defects in material and also increased surface area. Phosphoric acid (H_3PO_4), act as a catalyst promoting the bond cleavage reaction and promoting the cross linking through cyclization and condensation.

Experimental Work

Fallen or wasted dead tree leaves of "*Pongamia Pinnata* (Sukh Chen)" are collected and washed with hot water to remove physical contamination and dried in presence of sunlight atmosphere about 70 to 80 % moisture is removed. After that to put into oven for drying the remaining moisture at 105 ^oC for 5 hrs. Dried leaves are crushed and passed through a sieve of 250 µm and a very fine powder in green color is obtained. Phosphoric acid (H_3PO_4) is used as an activated agent that changed the thermal degradation of *Pongamia Pinnata* (Sukh Chen) tree leaves. In activation process the Phosphoric acid is used as activating agent with 50 % wt. into leaves powder for 16 hours at room temperature with 1:1 ratio. Then the absorption material is calcined in a box resistance furnace at 500-600 ^oC for 2 hrs. After collecting char (activated

carbon) to wash with distilled water for maintaining 6 to 7 Ph. Then dried in an oven at 105 ^{o}C for 1 hour in order to obtain an activated carbon.

Characterization Techniques

Surface morphology of the activated carbon is analyzed by scanning electron microscopy (SEM), crystal structure through X-ray diffraction (XRD), elemental composition is find out through Energy dispersive spectroscopy (EDS) and thermal degradation through TGA (Thermal gravimetric analysis).

Scanning Electron Microscopy (SEM)

Scanning Electron Microscopy (SEM) result shows that amorphous units have formed after activation. The pore structure of activated carbon has developed when phosphoric acid is used as an activator agent. The amount of fixed carbon is produced when volatiles matters are removed due to carbonization and activation. The amorphous porous carbon structure shows that material can be used for gas adsorption, waste water treatment and provide support for catalyst.

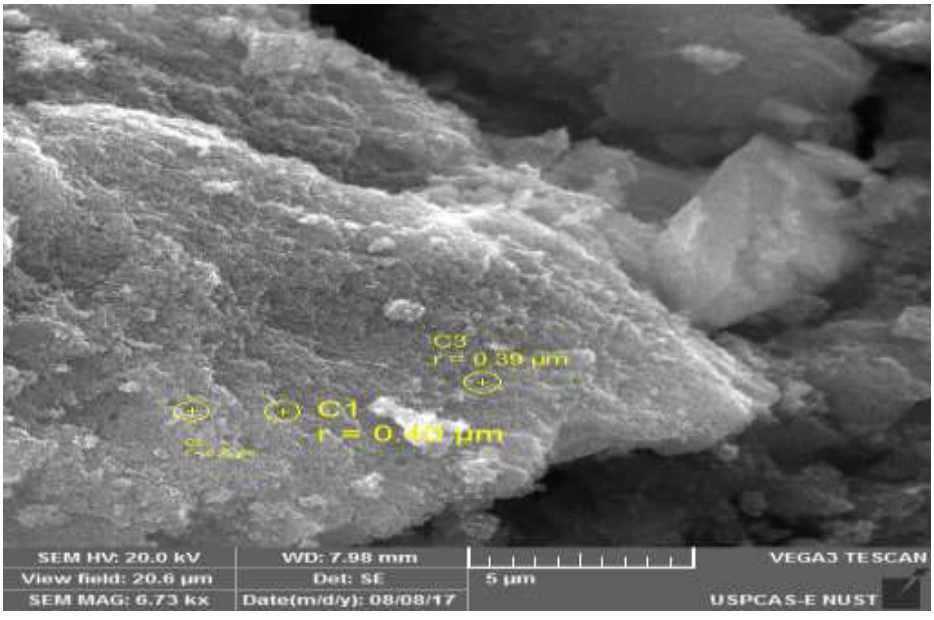

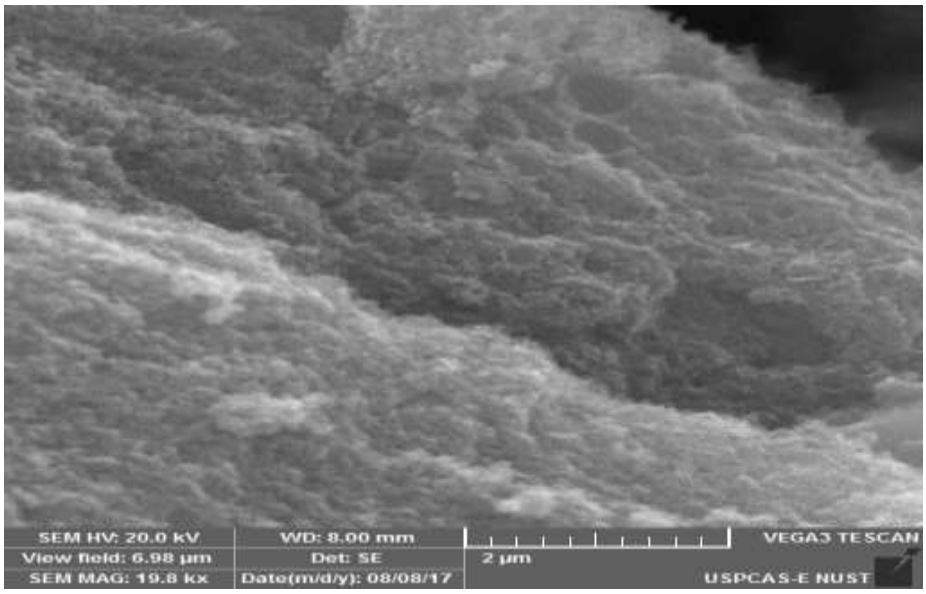

Figure 1: Scanning Electron Microscopy of activated carbon

X-ray Diffraction (XRD)

XRD results show that the peak at angle 23^{o} with mirror indices (012) is Calcite reference card is PDF # 05-0586. Angle 26^{o} with mirror indices (003) is Graphite (C) reference card is PDF # 26-1079, which reveals the presence of carbonaceous structure if layer alignment is better than sharp peak is produced and that shows crystalline structure is produced. Stacked layer of activated carbon is produced due to the exothermic reaction of water and acid.

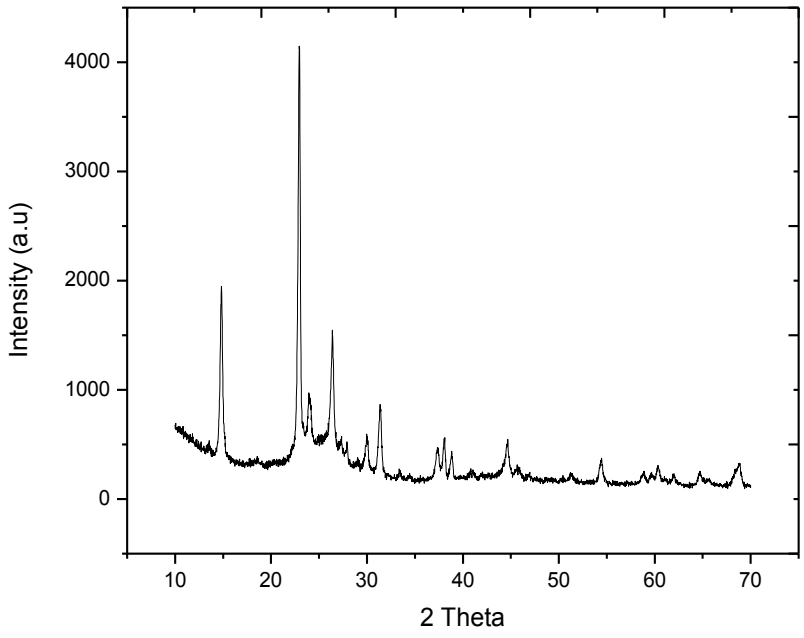

Thermo- gravimetric Analysis (TGA)

Thermal gravimetric analysis shows that the prepared activated carbon starts their degradation from 60 ^{o}C and fully degraded at above 600 ^{o}C.

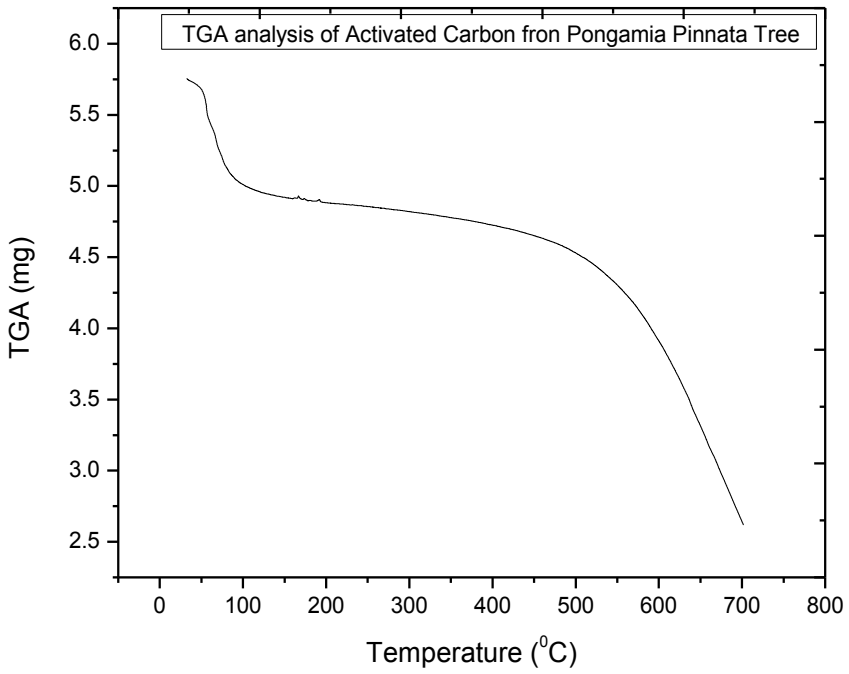

Figure 2: Thermo gravimetric Analysis (TGA) of *Pongamia Pinnata* (Sukh chen)

Elemental Analysis

Energy dispersive X-ray (EDX) analysis shows that the presence of carbon in a prepared sample is greater than 80 % which reveal that the part of cellulose crystalline structure was destroyed during process and resulting activation. A little amount of Phosphoric is also present.

Table 1: Elemental Analysis from EDX

Sample ID	Carbon (%)	Oxygen (%)	Phosphorus (%)
Activated Carbon	80.48	17.83	1.69

Conclusion

This study discussed the preparation of activated carbon using Phosphoric acid (H_3PO_4) as activator that increases number of defects present in hemicelluloses and as well as increase the surface area. Phosphoric acid act as a catalyst to promote bond cleavage reaction and enhance the cross linking during the reaction through the condensation process. Highly porous activated carbon is used for the gas adsorption and waste water treatment which is an environment friendly. Further, many activator agents like Potassium hydroxide (KOH), Zinc chloride ($ZnCl_2$) and potassium carbonate (K_2CO_3) etc. are used to studies the effect of activation on *Pongamia Pinnata* (Sukh Chen) tree is recommended.

References

[1] Chong Qin, Yao Chon, Jino-min Gao Material letters, **2014**,135,123-126 , Manufacture and characterization of activated carbon from marigold straw by H_3PO_4 chemical activation.

[2] Chao pang, Xing-bin Yan, Ru-tao wang, Jun-wei Lang, Yu-jing Ou, Qun-ji Xue Electochimica Acta **2013**,87,401-408, Promising activated carbon derived from waste tea-leaves and their applications in high performance supercapacitor's electrodes.

[3] Jadhav A, Mohanraj G , Chemical Technology 10,0-2,**2016**, Synthesis of activated carbon from Cocos Nucifera leaves Agrowaste by chemical activation method.

[4] Elisabelth Schroder, Klaus Thomanske, Christine Weber, Andreas Hornung, Vander Turniatti, **2007**,79,106-111, Experiment on the generation of activated carbon from biomass.

[5] Jianzhong Xu, Lingzhi Chan, Hongqiang Qu, Yunhong Jiao, Jixing Xic, Preparation and characterization of activated carbon from reedy grass leaves by chemical activation with H_3PO_4.

[6] O.A.Ekpete, A.C.Marcus and V.Osi, **2017**, 3:6, Preparation and Characterization of activated carbon obtained from plantain (Musa,paradisiacal) Fruit, stem

[7] Dipa Das, Debi Prasad Samal, Meikap BC,**2015**,6:5, Preparation of Activated Carbon from Green Coconut Shell and its Characterization.

Annex II

International Conference on Recent Innovations in Science, Engineering, Technology and Management (ASAR-ICRISETM-2017) 15th July Bengaluru India. (Presented)

Development of MOF derived iron catalyst for a Fischer Tropsch synthesis

[a]Muhammad Amin, [a]Saleem Munir, [a *]Naseem Iqbal

[a]*US-Pakistan Centre for Advanced Studies in Energy, USPCAS-E NUST Islamabad (44000), Pakistan*

Abstract

Metal organic frameworks (MOFs) are generally used for a gas storage and catalysis applications due to their porous structure formulation. Catalysts are extensively used in different process industries in order to increase the rate of reaction. Iron based catalyst is prepared by a solvo-thermal method and were annealed in a tube furnace at 550 ^{o}C for 3 hrs. SEM morphology of metal organic framework is linear in shape and they will be deforming into an oval shape when they were calcined in a tube furnace and become porous structure. TGA analysis of MOF shows that thermally degradation start at 200 ^{o}C and fully degraded at 450 ^{o}C. BET surface area and pore volume are 11.1701 m²/g & 0.007767 cm³/g respectively. XRD peaks at 38^{o} shows that the formation of the Fe_3O_4 and that kind of catalyst will enhance the C_{5+} selectivity for hydrocarbons in Fischer-Tropsch process.

Keyword: Metal Organic Framework; Fischer Tropsch Synthesis; Solvothermal Method.

*Corresponding Author; Tel: +92-51-9085-5281, Email: naseem@casen.nust.edu.pk

Introduction

MOFs are basically evaluated in heterogeneous catalyst applications due to the reaction applications in liquid as well as in gases phase. They consist of metal ions and organic linkers and they will exhibit a several key advantages with respect to zeolite sand cobalt due to their easy tune able composition [1]. Their huge porosity and storage ability of different unfriendly gases makes them MOF are important. MOFs are prepared through hydrothermal or solvo-thermal crystallization. Now a days new methods are established in which high temperature by using conventional electrical (CE) heating system in order to decrease the reaction time and a temperature [2]. Metal organic frameworks (MOFs) are called with a different names such as porous coordination polymers or networks (PCPs) (PCNs) [3]. Water gas shift activity in iron based catalyst is highly significant and they received a highly attention of research as well as easy availability and low cost [4].

Experimental Work

Metal organic framework was prepared by literature reported method [5]. In typical method, solution of iron nitrate Fe $(NO_3)_3.9H_2O$ 1mmol solution in 5 ml DMF was added to Terephthalic1mmol in 5 ml Dimethyl Formamide. The mixture was stirred in flask for 30 minutes and then it was reacted in autoclave at a temperature of 150 °C for 2 hrs. After reaction, the sample was cool down to room temperature. The obtained yellow precipitate of MOF was separate by centrifugation method at 4000 rpm for a time of 15 minutes. Washing was performed with Dimethyl Formamide. It was then centrifuged in water and dried in oven at 105 °C for 6 hrs. For catalyst preparation the MOF was annealed at 550 ^oC for a 3 hrs in a tube furnace under nitrogen atmosphere in order to obtain the Fe_3O_4 and carbon composite.

Results and Discussion

Results and discussion are carried out with the help of scanning electron microscopy, x-ray diffraction, thermal gravimetric analysis and BET analysis.

Scanning Electron Microscopy

SEM morphology of metal organic framework shows linear in shape and the entire iron particles were distributed with a uniform formation. The calcined metal organic framework is

deforming into an oval shape due to the removal of all the undesired compounds and become a porous in structure. The distribution made of Fe_2O_4 carbon composite is aliened.

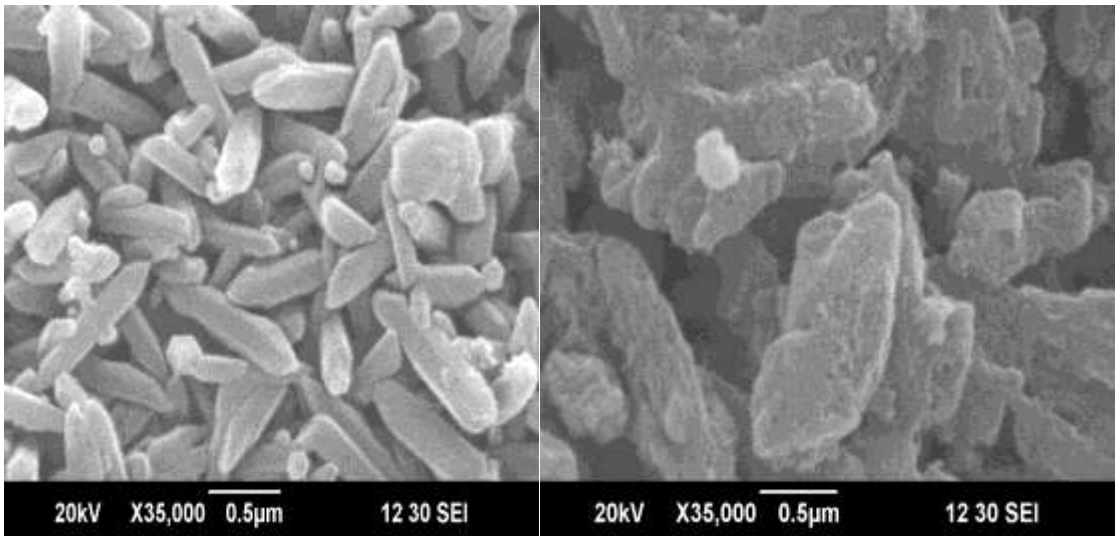

Figure 1: Scanning Electron Microscopy of Fe-MOF

X-Ray Diffraction

The XRD spectrum of prepared MOF shows that the peak at angle 9.69^o is formation of the metal organic framework as similar as MIL-53 and the second XRD peak at angle 17^o corresponds to a similar peak of MIL-90. Both shows a formation of the iron based MOF.

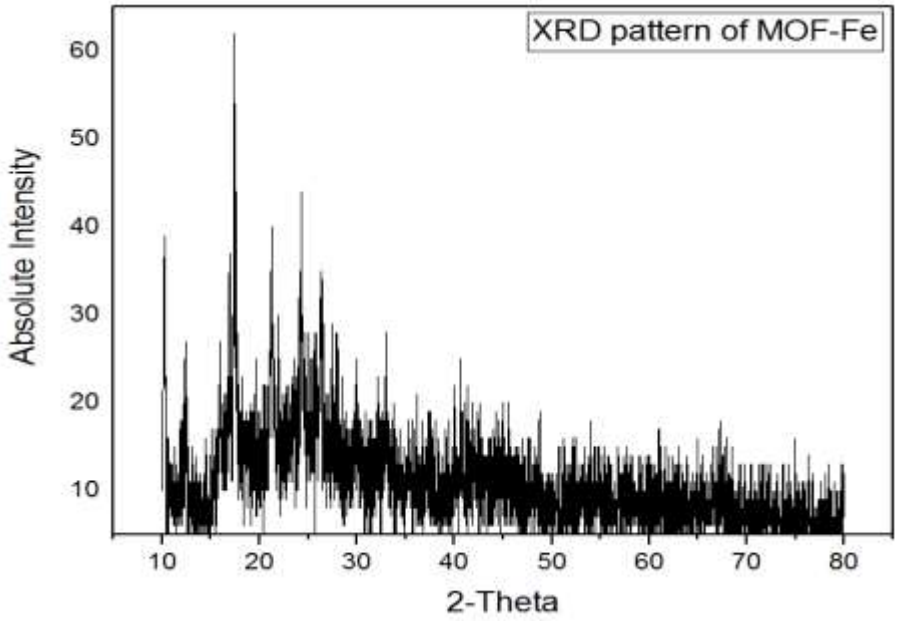

Figure 2: XRD analysis of Fe-MOF

XRD spectrum of calcined catalyst shows that the peak at angle 38^{o} is formation of the Fe_3O_4 structure. The broad spectrum in metal organic framework is due to the stack layer formation.

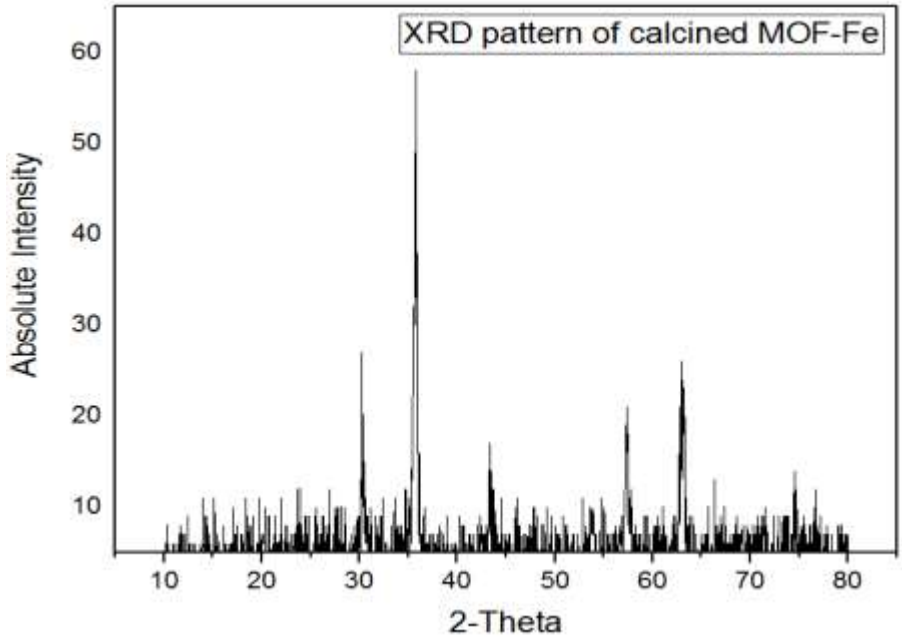

Figure 3: XRD analysis of Fe-Catalyst

Thermo-gravimetric analysis (TGA)

The results shows that metal organic framework will start their thermal degradation at 250 ^{o}C and full degraded at 450 ^{o}C. So calcinations were performing at above 450 ^{o}C for 3 hrs.

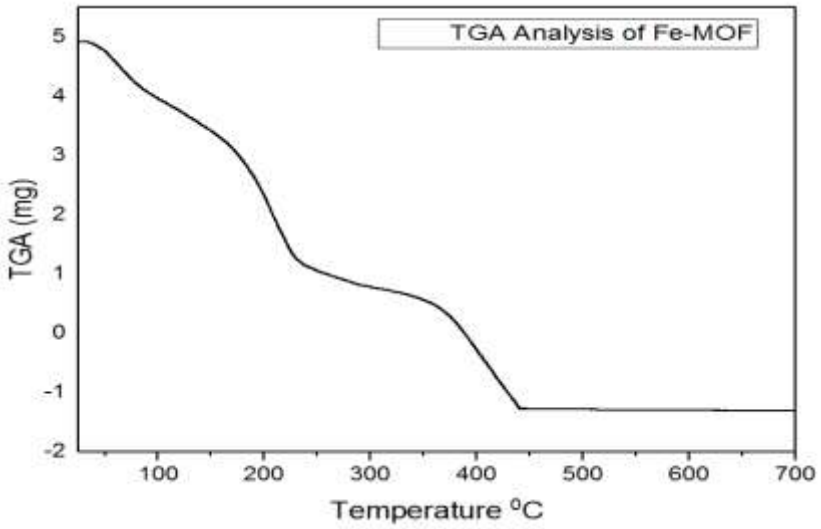

Figure 4: TGA analysis of Fe-MOF

TGA analysis of a calcined MOF shows their gradual degradation at 300 ^{o}C and then sharply degrading due to the formation of the Fe_2O_4 carbon composite.

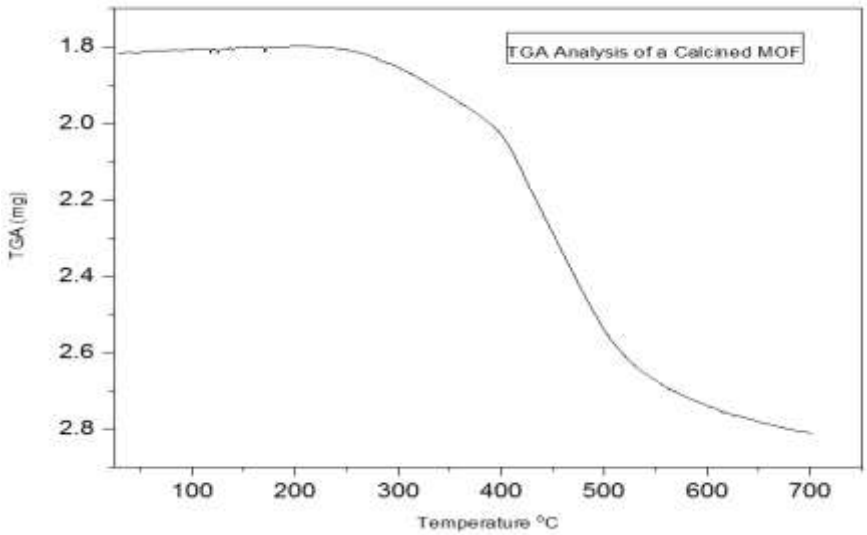

Figure 5: TGA analysis of Fe-Catalyst

BET Analysis

BET analysis of calcined metal organic framework were done through Micromeritics Instrument Corp machine with degassing time 3 to 4 hrs at 350 ^{o}C. BET surface area and pore volume are 11.1701 m^2/g & 0.007767 cm^3/g respectively.

Discussion

Catalyst with a highly porous structure can be used for gas adsorption and catalysis application. Iron (Fe) catalyst is generally used for a high temperature FT reaction and the above prepared catalyst are will be suitable for HTFT process to get better yield of C5+ hydrocarbons. The addition of different promoters like potassium will provide betters results in FT process.

References

[1] Mercedes Alvaro, Hubert Chevreau, Patricia Horcajada, Thomas Devic, Christian Serreb and Hermenegildo Garcia AmarajothiDhakshinamoorthy, "Iron(III) metal–organic frameworks as solid Lewis acids for the isomerization of a-pinene oxide",Catalysis Science & Technology, vol 2, pp.324–330,**2012**

[2] Imteaz Ahmed, JaewooJeon, Nazmul Abedin Khan, and Sung Hwa Jhung, "Synthesis of a Metal−Organic Framework, Iron- Benzene tri carboxyl ate, from Dry Gels in the Absence of Acid and Salt", American Chemical Society, vol.12, pp.5878−5881, **2012**

[3] Yujia Sun and Hong-Cai Zhou, "Recent progress in the synthesis of metal organic frameworks", Science and Technology of Advanced Materials, vol.16, pp.11, **2015**

[4] Abhik Banerjee, RohanGokhale, Sumit Bhatnagar, Jyoti Joga, Monika Bhardwaj, Benoit Lefez, Beatrice Hannoyer and Satishchandra Ogale, "MOF derived porous carbon-Fe_3O_4 nanocomposite as a high performance, recyclable environmental super adsorbent", The Royal Society of Chemistry 2012, Vol. 12, pp. 76801,**2012**

[5] Hanif A. Choudhury, Vijayanand S. Moholkar, "Synthesis of liquid hydrocarbons by Fischer-Tropsch process using industrial iron catalyst", International Journal of Innovative Research in Science, Engineering and Technology, Vol. 2, 8, August **2013.**

Annex III

2nd International Conference on Phosphorous, Boron and Silicon PBSi-2017 03-05 July, Paris France. (Presented)

Synthesis and characterization of activated carbon from *olive* tree by H_3PO_4 chemical activation

[a]Muhammad Amin , [a]Saleem Munir, [a*]Naseem Iqbal

[a]*US-Pakistan Centre for Advanced Studies in Energy, USPCAS-E, National University of Sciences and Technology, Islamabad, Pakistan*

Abstract

Activated carbon with a highly porous structure or surface area is mainly used as an industrial adsorbent and also wastewater treatment purposes. Phosphoric acid (H_3PO_4) is generally used as activator agent that increases the number of defects present in a hemicelluloses and act as a catalyst to promoting the bond cleavage reaction. They enhance the cross linking during the reaction through condensation. Phosphoric acid was thermally degrading the hemicelluloses structure present in an olive tree and creates the porous formation [1, 2]. XRD result shows that, peak a tangle 23^o which revealed the presence of crystalline carbonaceous structure. In SEM result shows that cylindrical units has deformed after the activation. Brunauer-Emmett-Teller (BET), surface area analysis has done through Micromeritics Instrument Corp machine, the total surface area are corresponding to 167.4715 m^2/g and adsorption average pore width are 27.3125 Å. Thermal gravimetric analysis shows that the prepared activated carbon starts their degradation from 200 ^oC and fully degraded at above 500 ^oC.

Keywords: Activated Carbon; Catalyst; Phosphoric Acid (H_3PO_4).

*Corresponding Author: Dr. Naseem Iqbal , Email: naseem@casen.edu.pk

Introduction

Activated carbon with a high surface area is used for wastewater treatment and gas adsorption. Preparation of activated carbon is carried out into two steps carbonization and activation. Activation is further divided into chemical and physical. When raw material is wood then chemical activation method is used and that is a single step process. Activated carbon produces from olive leaves shows micro-pores structures. Activators are KOH, H_3PO_4, zinc chloride and potassium carbonate etc. is generally used [3]. By using H_3PO_4 as an activator the porous structure of activated carbon is obtained. Results shows preferable carbon content through microstructure morphology, finding shows that carbon content is increased from 46 % to 74 % due to the cellulose crystalline structure was destroyed [4,5]. H_3PO_4 is used as activated agent that changed the thermal degradation of the olive tree leaves. H_3PO_4 are increase the number of defects which anchoring site for metal particles and also increase the surface area.H_3PO_4 act as a catalyst promoting the bond cleavage reaction and promoting the cross linking through cyclization and condensation.

Experimental Work

Wasted tree leaves of "olive" are collected and then dried in the presence of sunlight atmosphere for 3-4 days and then put into an oven dried to remove the remaining moisture content at 105 ^{o}C for 5hr. Dried leaves are crushed and passed through a sieve of 250 µm. A very fine powder in greenish color is obtained [6]. Then H_3PO_4 is used as a activated agent that changed the thermal degradation of the olive tree leaves. H_3PO_4 are increasing the number of defects which anchoring site for metal particles and also increase the surface area. Absorption time of H_3PO_4 (wt. 50%) into powder that is collected from dried leaves is 16 hrs. at room temperature with 1:1 ratio. Then the absorption material is calcined in a box resistance furnace at 500-600 ^{o}C for 2 hrs. We collect a char and convert into activated carbon with the help of washing (distilled water) and maintain the neutral ph. Then dried in an oven at 105 ^{o}C for 1 hr. in order to obtain the activated carbon [7].

Characterization Techniques

Morphology of the activated carbon is analyzed by scanning electron microscopy and crystal structure through XRD. The elemental composition is found out through EDS.

SEM (Scanning Electron Microscopy)

In SEM, result shows that cylindrical units has deformed after the activation. The pore structure of activated carbon is expanding when phosphoric acid is used as an activator agent. The amount of fixed carbon is produced when volatiles matters are removed due to carbonization and activation. The microspore presences are present which contributes towards the gas adsorption in future.

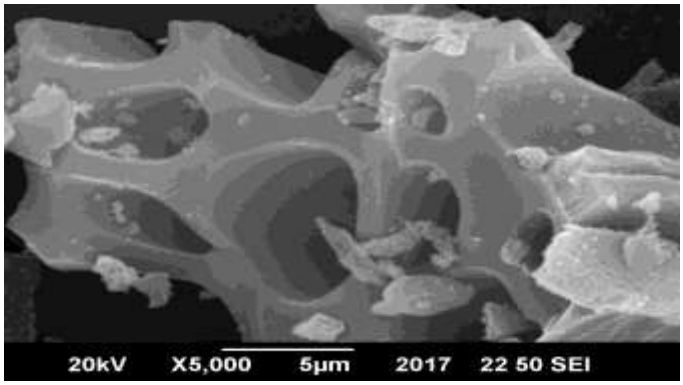

Figure 1: Scanning Electron Microscopy of olive activated carbon

X-ray Diffraction (XRD)

XRD result shows that, peak at angle 23^{o} which revealed the presence of crystalline carbonaceous structure. If layer alignment is better than sharp peak is produced and that shows crystalline structure is produced. Stacked layer of activated carbon is produced due to the exothermic reaction of water and acid.

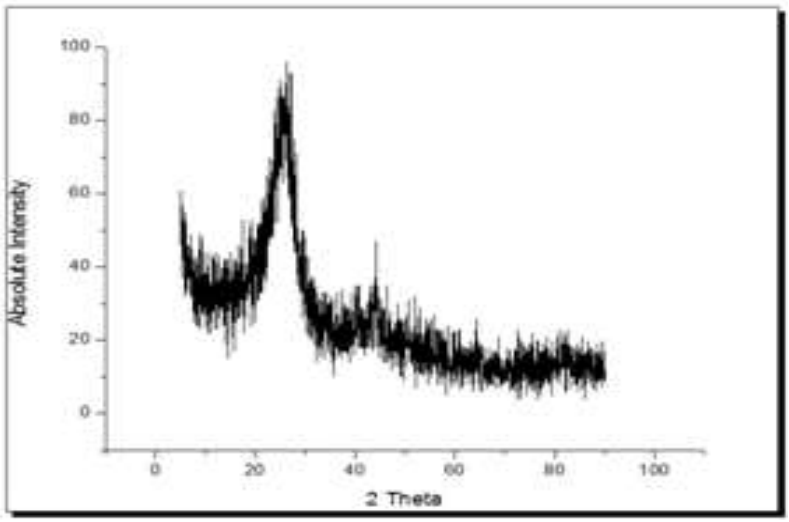

Fig.2: X-ray Diffraction (XRD) of *Olive* tree

Thermo gravimetric Analysis (TGA)

Thermal gravimetric analysis shows that the prepared activated carbon starts their degradation from 200 ^{o}C and fully degraded at above 550 ^{o}C.

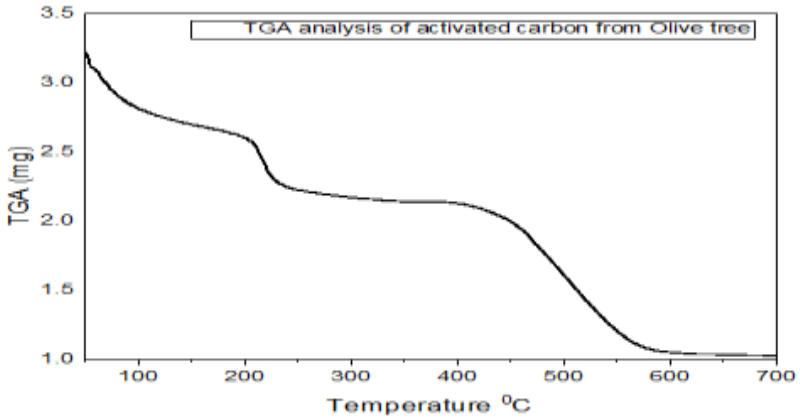

Figure 3: Thermo gravimetric Analysis (TGA) of Olive tree

Elemental Analysis

EDX analysis shows that the presence of carbon in a prepared sample is greater than 75% which reveal that the part of cellulose crystalline structure was destroyed during process and resulting activation. A little amount of Phosphoric is also present.

Table 1: Elemental Analysis Obtained from EDS

Sample ID	Carbon (%)	Oxygen (%)	Phosphorus (%)
Olive (AC)	77.51	17.85	4.64

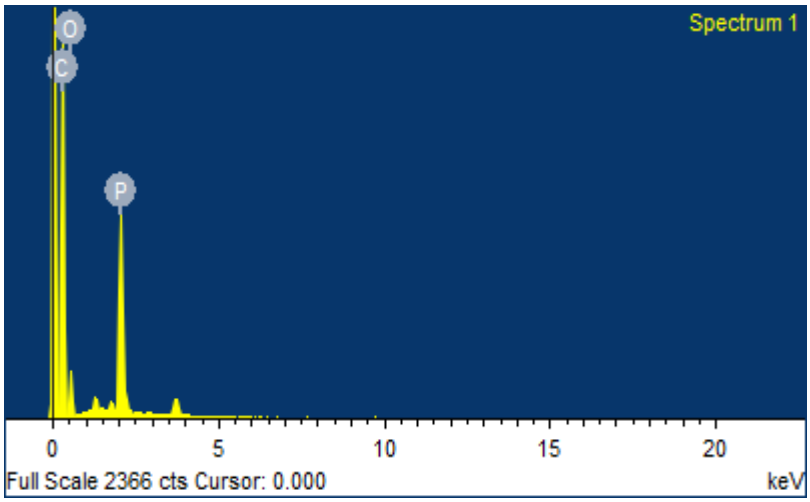

Figure 4: Elemental Analysis of activated carbon obtained from Olive tree

Conclusion

Phosphoric acid (H_3PO_4) is generally used as activator agent that increases the number of defects present in hemicelluloses, which also increase the surface area. H_3PO_4 act as a catalyst in order to promote the bond cleavage reaction and they enhance the cross linking during the reaction through the condensation process. Highly porous activated carbon is used for the gas adsorption in order to make an environment friendly. KOH, zinc chloride and potassium carbonate are also used as an activator agent but Phosphoric acid will produced better results. Thermal gravimetric analysis shows that prepared activated carbon starts their degradation from 200 ^{o}C and fully degraded at above 500 ^{o}C. Activated carbon made from olive tree has a significant porous structure and will start their thermally degradation at 200 ^{o}C and loss their major weight at 400 ^{o}C which is economical good for the formation of the activated carbon. Further, different activator agents like KOH, zinc chloride and potassium carbonate etc. are used to studies the effect of activation on olive tree is recommended in future.

References

[1] Chong Qin, Yao Chon, Jino-min Gao Material letters, **2014**,135,123-126 , Manufacture and characterization of activated carbon from marigold straw by H_3PO_4 chemical activation.

[2] Chao pang, Xing-bin Yan, Ru-tao wang, Jun-wei Lang, Yu-jing Ou, Qun-ji Xue Electochimica Acta **2013**,87,401-408, Promising activated carbon derived from waste tea-leaves and their applications in high performance supercapacitor's electrodes.

[3] Jadhav A, Mohanraj G , Chemical Technology 10,0-2,**2016**, Synthesis of activated carbon from Cocos Nucifera leaves Agrowaste by chemical activation method.

[4] Elisabelth Schroder, Klaus Thomanske, Christine Weber, Andreas Hornung, Vander Turniatti, **2007**,79,106-111, Experiment on the generation of activated carbon from biomass.

[5] Jianzhong Xu, Lingzhi Chan, Hongqiang Qu, Yunhong Jiao, Jixing Xic, Preparation and characterization of activated carbon from reedy grass leaves by chemical activation with H_3PO_4.

[6] O.A.Ekpete, A.C.Marcus and V.Osi, **2017**, 3: 6, Preparation and Characterization of activated carbon obtained from plantain (Musa,paradisiacal) Fruit, stem.

[7] Dipa Das, Debi Prasad Samal, Meikap BC,**2015**,6:5, Preparation of Activated Carbon from Green Coconut Shell and its Characterization.